THE ECOLOGY AND FEEDING BIOLOGY OF THECATE HETEROTROPHIC DINOFLAGELLATES

by

Dean Martin Jacobson

A.B., Occidental College 1979

SUBMITTED IN PARTIAL FULFILLMENT
OF THE REQUIREMENTS FOR THE DEGREE OF
DOCTOR OF PHILOSOPHY

at the
Massachusetts Institute of Technology
and the
Woods Hole Oceanographic Institution

February, 1987

Signature of Author _____
Department of Biology, Massachusetts Institute of Technology and the Joint Program in Oceanography, Massachusetts Institute of Technology/Woods Hole Oceanographic Institution, February, 1986.

Certified by _____
Donald M. Anderson, Thesis Supervisor

Accepted by _____
Sallie W. Chisholm, Chairman, Joint Committee for Biological Oceanography, Massachusetts Institute of Technology/Woods Hole Oceanographic Institution.

Table of Contents

Contents, cont'd.

List of Figures and Tables

Figures and Tables, cont'd,

ECOLOGY AND FEEDING BIOLOGY OF THECATE HETEROTROPHIC DINOFLAGELLATES

by

Dean Martin Jacobson

Submitted to the Massachusetts Institute of Technology/
Woods Hole Oceanographic Institution Joint Program
in Biological Oceanography in February 1987
in partial fulfillment of the requirements for
the degree of Doctor of Philosophy

ABSTRACT

A group of thecate heterotrophic dinoflagellates (THDs), principally in the diverse and ubiquitous genus Protoperidinium, was investigated both from an ecological and an organismal perspective. When this study was initiated, nothing was known about their feeding mechanisms, rates or food preferences. The population dynamics of these microheterotrophs were studied in a temperate estuary over a 13 month period, along with co-occurring diatoms, ciliates and pigmented (photosynthetic) dinoflagellates. The timing of several peaks in Protoperidinium abundance coincided with those of diatom blooms, suggesting a possible trophic dependance. During such peaks the biovolume or biomass of the THD community exceeded that of both pigmented dinoflagellates and ciliates. Occurrence patterns of individual THD species were closely related to water temperature; this may indicate the involvement of benthic resting cysts in population succession.

Small-scale vertical distributional patterns of THDs were also studied in an embayment with an average depth of 5 m. While two autotrophic dinoflagellate species displayed distinct daily vertical migration patterns, THD species did not; most species maintained a constant 2-5 m depth of maximum abundance, while two others had surface maxima.

Feeding behavior, as observed in 19 THD species (Oblea rotunda, Zygabikodinium lenticulatum and 17 species of Protoperidinium) fits the following pattern: a THD cell attaches a slender filament to a prey item (usually a diatom) while it is engaged in a characteristic, spiralling "dance". Subsequently, a pseudopod or "pallium" (a term defined here) emerges from the flagellar pore and envelops the prey within a minute. Ten to sixty minutes later the pallium is retracted and the prey (now a nearly-empty frustule) is discarded. Most species feed only on diatoms, but O. rotunda, Z. lenticulatum (both diplopsaloid species) and P. pyriforme also preyed upon dinoflagellates.

Ingestion and growth rates were determined in the laboratory where cultures of Protoperidinium hirobis were fed the diatom Leptocylindrus danicus. Feeding cycles were repeated as often as every 1.5 to 2 hours. Maximal ingestion rates of 23 diatoms$\cdot$day^{-1} supported unexpectedly high specific growth rates of up to 1.1$\cdot$day^{-1} (1.7 divisions$\cdot$day^{-1}). Half-maximal growth and grazing rates occurred at approximately 1000 diatoms cells$\cdot$ml^{-1}. Peak division frequencies

occurred at night, although feeding rate was nearly constant on a diel basis.

The ultrastructure of the feeding apparatus was studied in Protoperidinium spinulosum. The pallium, when deployed, is composed of a complex system of membranous channels, vesicles, and a few microtubular ribbons radiating from the flagellar pore. Inside this pore, the pallium is continuous with the contents of an elongate microtubular basket that extends towards the nucleus. The apical end of this basket opens adjacent to the nucleus; at this point its contents become continuous with the central cytoplasmic region. This region is distinguished from the relatively dense, peripheral cytoplasm by the presence of either large electron-lucent vesicles (containing, perhaps, digestive enzymes) or numerous small lipid droplets. Examination of a pre-feeding cell has revealed the likely source of the pallium membranes: dense membranous whorls lie within the microtubular basket. A narrow pseudopodal appendage in two non-feeding cells may constitute the tow filament used in prey capture. A complex myonemal system, including osmiophilic ring, striated collars and connecting bands is described. The microtubular basket and osmiophilic ring structures were also found in Protoperidinium hirobis, Protoperidinium punctulatum and Oblea rotunda.

This thesis has done much to further the understanding of a prevalent component of the protozooplankton, the thecate heterotrophic dinoflagellates. This progress, which was due in a large part to the culture success reported herein, includes new insights into the abundance, feeding behavior, food preferences, feeding rates, and ultrastructural basis of feeding in this preeminent group of the thecate heterotrophic dinoflagellates, the genus Protoperidinium.

Thesis Supervisor: Dr. Donald M. Anderson
Associate Scientist, Dept. Biology, W.H.O.I.

Acknowledgements

At this long-awaited personal milestone, it is good to have a chance to remember and thank those whose companionship and assistance in the lab has meant so much: John Lively, Dr. Brian Binder, Bruce Keafer, and especially Dave Kulis, the water bearer. To my supportive and enthusiastic thesis committee, including Diane Stoecker, John Waterbury, Penny Chisholm, O. Roger Anderson (of Lamont-Doherty), I am much indebted; they have made a big difference in my (as yet unfinished) development as a careful, critical student of nature. I am particularly indebted to Roger, who helped me find my way around the protistological literature and enhanced my ultrastructural investigations with his sharp eye. I owe more than I originally thought possible to my advisor and mentor, Don Anderson: the initial suggestion of working on heterotrophic dinoflagellates (together with a clever suggestion that I look up Kofoid and Swezy 1921, with its delightful watercolor illustrations), timely encouragement and challengingly high expectations, laboratory support, and valuable guidance in the fashioning of unambiguous, concise prose (nice try, Don!). I also thank Max Taylor for providing the opportunity to meet, at Friday Harbor, some of my dino collegues for the first time and to see my first feeding Protoperidinium; the company of Greg Gaines was appreciated as well.

My research was supported in part by a NSF graduate fellowship, a graduate research grant through the WHOI Coastal Research Center, and two NSF grants, OCE-8400292 and DCB-8520605. The WHOI Education office has come through with support at crucial times, especially the visit to Friday Harbor, for which I am grateful.

I thank my parents for the privileged opportunities they have provided me to pursue my love of nature and art.

To my wife, Paula, I am very grateful for over five years of continual emotional support and growth, and help in the struggle to keep my life in perspective. I promise you that I've outgrown vans in WHOI parking lots.

Finally, I dedicate this work, an examination of minute wonders, to the Artist who, with prolific creativity, has given us a world of surprising intricacies to appreciate, to investigate, and to cherish.

INTRODUCTION

This thesis focuses on a group of free-swimming marine planktonic organisms called peridinioid thecate heterotrophic dinoflagellates. Like most dinoflagellates, these single-celled organisms are propelled by two flagella. The root of "dinoflagellate" is the Greek word "dinos", referring to their whirling swimming motion; "peridineo" has the same meaning. Dinoflagellates are most popularly known by the "red tide" phenomena caused by certain photosynthetic, brown-pigmented species. The abundance and ubiquity of the non-photosynthetic (= heterotrophic), colorless dinoflagellates in most marine environments is only now becoming widely appreciated. The heterotrophic species, which constitute roughly half of the 2000 or so living dinoflagellate species, can be divided into two important classes: those with naked, soft-walls and those that are thecate or armored. The latter group is characterized by the presence of a rigid cellulose wall or theca composed of a series of polygonal plates (like a coat of armor), the arrangement of which is used extensively in dinoflagellate taxonomy. The presence of the theca in heterotrophic forms is of primary importance to this study; in the words of Calkins (1901), "...there is frequently an unbroken shell about the animal which makes it impossible for solid food to enter." Naked forms have no such barrier to ingestion, and have long been known to phagocytose diverse food particles. When my thesis began, the feeding habits of thecate species were a complete mystery.

The species investigated in this thesis represent the largest group of all living thecate heterotrophic dinoflagellates, which are found in

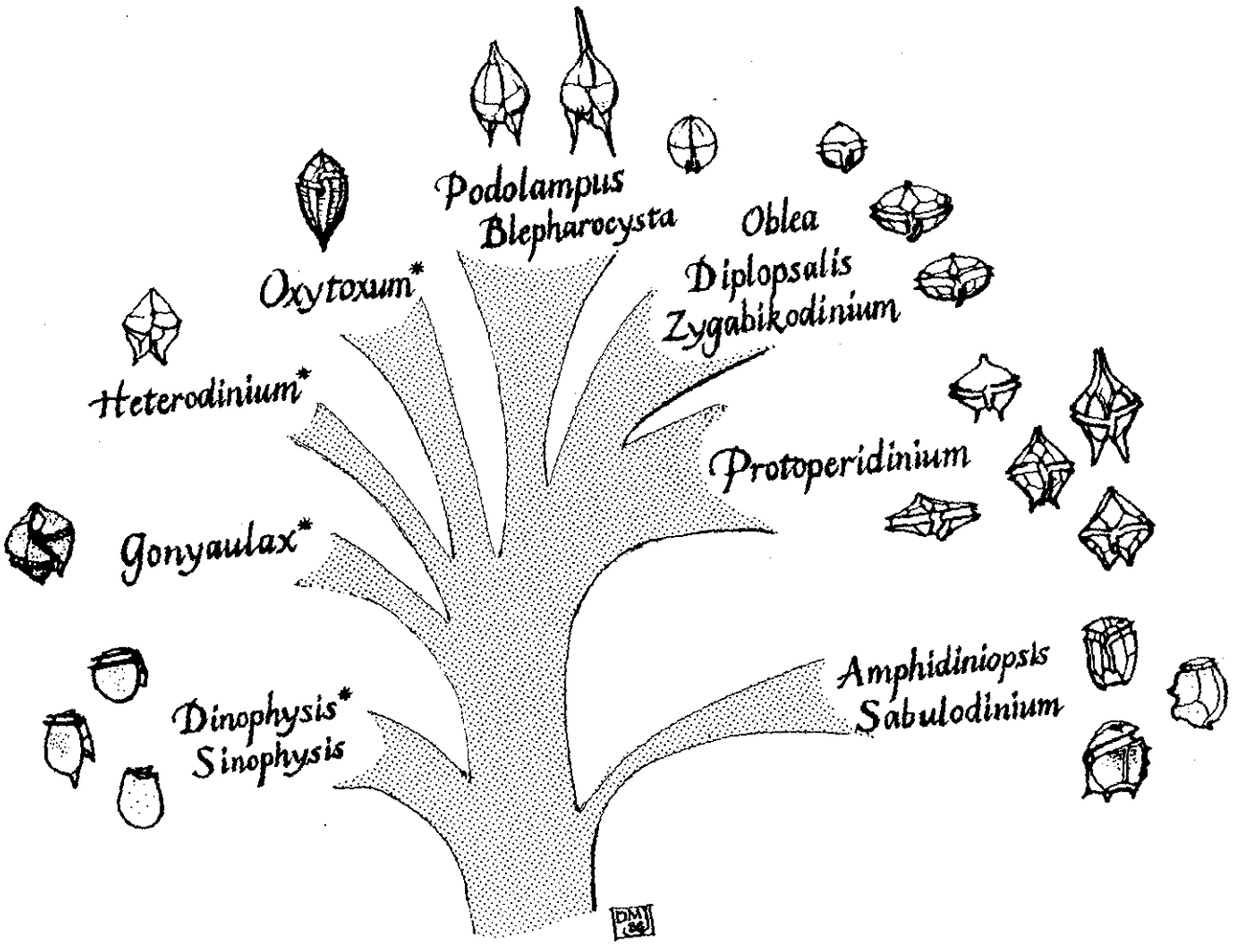

Fig. 1: Thecate Heterotrophic Dinoflagellates

*genera which possess photosynthetic species

at least a dozen genera (Fig. 1). The dinophysoid branch is composed of several elaborately shaped genera, most of which have algal endo- or exosymbionts, but the strictly heterotrophic (i.e., lacking any pigmented symbionts) species are found only in Dinophysis (formerly Phalacroma) and Sinophysis (see below). A single heterotrophic species has been discovered in both Gonyaulax (unpubl. obs.) and Heterodinium (Lessard and Swift 1986). Both Oxytoxum and Podolampus are composed of a mixture of heterotrophic and photosynthetic members, while Blepharocysta is composed of a single heterotrophic species. Several heterotrophs exist in an odd assortment of dorso-ventrally flattened genera known as "sand dinoflagellates" because they inhabit the interstitial waters of beach sand, including Amphidiniopsis (which can be found in the water column), Helicodinium (see Appendix), Sinophysis (related to Dinophysis), Planodinium and Sabulodinium (Saunders and Dodge 1984). Finally there are the heterotrophic peridinioid genera, including Protoperidinium, Diplopsalis, Dissodinium, Zygabikodinium and Oblea. It is on this group that my observations of feeding have been made. All of the hundreds of species in these genera are heterotrophic, although there is a single report of a photosynthetic Protoperidinium species (Lessard and Swift 1986) which needs further verification.

The term "peridinioid" may be a source of some confusion. Since Peridinium was among the first dinoflagellate genera to be named (by Ehrenberg), terms resembling this word (such as the french "peridinien") have been used to refer either to all dinoflagellates or to all thecate dinoflagellates (including, for example, Gonyaulax). My use of the term "peridinioid" refers to the genera listed above, plus the related

photosynthetic forms such as Peridinium (from which Protoperidinium was divided by Balech, 1974) and Scrippsiella. Interestingly, Podolampus and Blepharocysta, both of which have previously been seen to have behavior similar to that described here for Protoperidinium, are also considered to be related to the peridinioid dinoflagellates (Abé, 1966; Taylor, 1980)

Many taxa related to Protoperidinium form nearly indestructible benthic resting cysts which are found, often in good condition, in the marine fossil record. These microfossils have been extensively studied by marine micropaleontologists and palynologists, some of whom attempt to infer the nature of the ancient oceans (the study of paleo-oceanography) by analyzing the distributions of various dinoflagellate cysts and other microfossils. Clearly, key to this line of research is an understanding of the environmental requirements of the motile stage of those dinoflagellates that form cysts (Harland, 1983; Bujak, 1984). The insights that are presented in this thesis concerning the ecology of Protoperidinium will no doubt be of interest to palynologists studying the related cyst-based genera of Brigantedinium, Lejeunacysta, Selenopemphix, Xandarodinium and others.

The discovery of feeding in Protoperidinium, Zygabikodinium and Oblea (Chapter 2) has come after a long period of sustained dinoflagellate study. Dinoflagellates were first observed over two centuries ago by O.F. Muller, who described Ceratium in 1773. 65 years later, C.G. Ehrenberg described several genera of dinoflagellates, including Peridinium, as part of his study of "infusioria" which included ciliates, flagellates, and even rotifers. Somewhat amusingly

from our perspective, a single row of cilia was thought to exist in the girdle; the flickering appearance of the motile transverse flagellum was no doubt responsible for this misinterpretation. Accordingly, the dinoflagellates, together with some unrelated protists, were known as "cilioflagellates" until nearly the end of the 19th century. Despite the inclusion of a cingular row of cilia, Ehrenberg's illustrations were marvelously detailed, as can be seen in his Die Infusionsthierchen als Vollkommene Organsimen (1838). His polygastica theory, which is summarized by his title ("Infusioria as complete organisms") deserves a brief digression. Ehrenberg interpreted the uptake of carmine dye particles into food vacuoles in ciliates as the ingestion of food into permanent stomachs; contractile vacuoles were believed to be minute testes, stigmata were thought to be complete eyes, and an unseen system of nervous fibers was postulated. One cannot help but imagine his reaction if a specimen of the heterotrophic dinoflagellate Erythropsidinium, with its astonishingly complete eye-like ocellus, had been observed. On a certain level, the sort of intricacies thought by Ehrenberg to exist in protists have in fact been discovered (Chapter 5).

The study of the "infusoria" (so named because some of the earliest discoveries concerning protists were made from hay infusions) was dominated by zoologists well into the 20th century; consequently the ingestion of food by microorganisms, even green ones, was expected. Indeed, Stein (1883) demonstrated in Euglena the presence of a well-developed oral aperture that could ingest food. Kent (1880) figured Gymnodinium ingesting a small flagellate, and postulated the presence of an unseen oral aperture within the sulcus of Peridinium

(which, along with all other dinoflagellates, was figured in an inverted, antapex-up orientation; this condition was corrected for the most part by Stein (1883) although the illustrations in his marvelous plates of Oxytoxum and Ceratocorys were still inverted). The first descriptions of pseudopodal behavior in dinoflagellates was reported by Stein (1883) in the phototrophic species Ceratium cornutum. It is difficult to interpret these observations since such cytoplasmic extrusions can result from hypertonic stress. More elaborate pseudopodia were depicted by Schutt (1895) for Podolampus and Blepharocysta, but food capture was not described. These observations, made nearly a century ago, are especially remarkable in that they have not been repeated in Podolampus despite close scrutiny by Elbrächter (pers. comm.) and myself. Feeding in Blepharocysta has, however, been recently documented (Steidinger et al., 1968).

The study of heterotrophy in dinoflagellates was vigorously pursued in the first part of the 20th century by Biecheler (1936) who described some remarkable feats of dinoflagellate phagotrophy and by Kofoid (1921), who believed that the large, conspicuous pusules (permanent vacuoles often filled with a characteristic pink fluid) of Protoperidinium species were involved in the uptake of dissolved organic compounds. Hofeneder (1930) described a filopodial reticulum surrounding Ceratium hirundinella, an observation that has not since been confirmed. Droop (1959) characterized the chemical requirements for the hardy phagotroph Oxyrrhis, as did Provasoli and Gold (1957) for Crypthecodinium cohnii. In the '60s and early '70s, while the Cachons examined the structure and behavior of several exotic phagotrophic

dinoflagellates (Cachon and Cachon 1967, 1974), reports of heterotrophy declined (Bursa, 1961; Norris, 1969). The study of dinoflagellates, also called the Pyrrophyta (flame-plants, referring to bioluminescence) fell mostly at this time in the domain of botanists, and studies of phototrophic species were predominant. All dinoflagellates were regarded (and, in undergraduate biology classes, taught) as members of the phytoplankton; the existence of heterotrophic species (besides the well-known dinoflagellate Noctiluca) was unknown to me until this fact was brought to my attention by Don Anderson just a few year ago.

The pendulum of dinoflagellate study has, in recent years, swung back toward the zoologists, or more properly protozoologists. The current proliferation of reports of heterotrophic dinoflagellate phenomena developed in the late '70s, coinciding with the development of renewed interest in the microzooplankton that coexists with the larger, well-studied zooplankton (i.e., Beers et al., 1970; Heinbokel, 1978; Fenchel, 1982). Recent studies include the description of the peduncle, a small cytoplasmic appendage of naked dinoflagellates, by Lee (1977) and Spero (1979) and population dynamics studies by Smetacek (1981) and Kimor (1981). Fresh water phagotrophic behavior was also reported (Irish, 1979; Frey and Stoermer, 1980; Wedemayer and Wilcox, 1984). Currently, continuing the approach of Stein (1883), photosynthetic dinoflagellates are being examined for heterotrophic or "myxotrophic" behavior (Porter 1985). The work on thecate heterotrophic dinoflagellates reported below coincided with that of Lessard (1984) and Gaines and Taylor (1985).

The thesis which follows begins with a field study designed to

characterize the seasonal abundance of thecate heterotrophic dinoflagellates (as well as their non-thecate cousins); the vertical distributions of several of these organisms within the water column are presented in Appendix III. During the course of these studies the "diatomivorous", pseudopodal nature of feeding in these organisms was at last observed (by myself in company with Greg Gaines and F.J.R. "Max" Taylor in August 1983 at Friday Harbor, with its wonderfully diverse fauna and flora of dinoflagellates). This knowledge helped me to obtain several species of Protoperidinium in long-term laboratory culture (with the crucial employment of Diane Stoecker's rotating apparatus), which in turn enabled me to collect growth and grazing data, and to collect and prepare feeding cells for transmission electron microscopy, using methods kindly related to me by Larry Fritz from Rich Triemer.

The excitement that has been afforded me by certain species of Protoperidinium in the course of my research has, in retrospect, made this period at Woods Hole, (enlivened as it was both by the occasional disappointments of failed cultures and flawed T.E.M technique and the thrills of witnessing feeding behavior or of finally achieving a clean batch of formvar), one of great satisfaction.

REFERENCES

Abé, T. 1966. The amoured Dinoflagellata: I. Podolampidae. Publ. Seto Mar. Biol. Lab. 14:129-54.

Beers, J.R, F.M.H. Reid and G.L. Stewart 1969. Microzooplankton and its abundance relative to the larger zooplankton and other seston components. Mar. Biol. 4:182-189.

Bursa, A.S. 1961. The annual oceanographic cycle at Igloolik in the Canadian Artic. II. The phytoplankton. J. Fish. Res. Bd. Can. 18:563-615.

Cachon, J. and M. Cachon 1967. Cymbodinium elegans nov. gen. nov. sp., Peridinien Noctilucidae Saville-Kent. Protistologica 3:313-318.

Cachon, J. and M. Cachon 1974. Le systeme stomopharyngien de Kofoidinium Pavillard. Comparisons avec celui de divers Peridiniens libres et parasites.

Calkins, G.N. 1901. The Protozoa. MacMillian Co., New York. 347pp.

Droop, M.R. 1959. Water-soluble factors in the nutrition of Oxyrrhis marina. J. mar. biol. ass. U.K. 38:605-620.

Fenchel, T. 1982. Ecology of heterotrophic microflagellates. I. Some important forms and their functional morphology. Mar. Ecol. Prog. Ser. 8:211-2 .

Frey, L.C. and Stoermer 1980. Dinoflagellate phagotrophy in the upper Great Lakes. Trans. Am. microsc. Soc. 99:439-444.

Gaines, G. and Taylor, F.J.R. 1984. Extracellular digestion in marine dinoflagellates. J. Plank. Res. 6:1057-1061.

Heinbokel, J.F . 1978. Studies on the functional role of tintinnids in the southern California bight. II. Grazing rates of field populations. Mar. Biol. 47:191-197.

Irish, A.E. 1979. Gymnodinium helveticum Penard F. achroum Skuja. A case of phagotrophy. Br. phycol. J. 14:11-15.

Kent, W.S. 1880. A Manual of the Infusoria David Brogue, London. 472pp.

Kimor, B. 1981. Seasonal and bathymetric distribution of thecate and nonthecate dinoflagellates off La Jolla, California. CalCOFI Rep. 22:126-134.

Lee, R.E. 1977. Saprophytic and phagocytic isolates of the colorless heterotrophic dinoflagellate Gyrodinum lebouriae Herdman: J. mar. biol. ass. U.K. 57:303-315.

Lessard, E.J. 1984. Oceanic heterotrophic dinoflagellates: distribution, abundance, and role as microzooplankton. PhD thesis, University of Rhode Island. 146pp.

Lessard, E.J. and E. Swift 1986. Dinoflagellates from the North Atlantic, classified as phototrophic or heterotrophic with epifluorescence microscopy. J. Plank. Res. 8:1209-1215.

Norris, R.E. 1966. Unarmoured marine dinoflagellates. Endeavour (Oxf.) 35:124-128.

Provasoli, L. and K. Gold 1957. Some nutritional characteristics of Gyrodinium cohnii, a colorless marine dinoflagellate. J. Protozool. 4 (suppl.), 7.

Porter, K.G., E.B. Sherr, B.F. Sherr, M. Pace and R.W. Sanders. 1985. Protozoa in planktonic food webs. J. Protozool. 32:409-415.

SchÜtt, F. 1895. Die Peridineen der Plankton-Expedition. Lipsius and Tischer, Kiel, 170 pp.

Smetacek, V. 1981. The annual cycle of the protozooplankton in the Kiel Bight. Mar. Biol. 63:1-11.

Spero, H.J. 1982. Phagotrophy in Gymnodinium fungiforme (Pyrrhophyta): the peduncle as an organelle of ingestion. J. Phycol. 18:356-360.

Stein, F.R. von 1883. Der Organismus der Infusionthiere. Verlag von Wilhelm Engelmann, Leipzig. 30 pp., 24 pl.

Wedemayer, G.J. and L.W. Wilcox 1984. The ultrastructure of the freshwater, colorless dinoflagellate Peridiniopsis berolinense (Lemm) Bourrelly (Mastigophora, Dinoflagellida). J. Protozool. 31:444-453.

CHAPTER 1

Population Dynamics of Heterotrophic Dinoflagellates in a Temperate Estuary

Abstract

The annual cycle of heterotrophic dinoflagellate abundance in a shallow estuarine embayment was investigated in the context of the co-occurring phototrophic dinoflagellate and ciliate dynamics. Two groups of heterotrophic dinoflagellates, thecate forms (principally Protoperidinium spp., upon which attention was focused) and naked, phagotrophic forms (chiefly Polykrikos schwartzii) both occurred in brief, non-concurrent blooms with cell densities exceeding 50 ml^{-1}. The timing of several Protoperidinium blooms appears to have coincided with periods of diatom abundance; the largest peaks, which featured the simultaneous maxima of four species, occurred during a Skeletonema costatum bloom. These observations are consistent with recent laboratory evidence for diatom grazing by thecate heterotrophic dinoflagellates. Thecate heterotrophic dinoflagellates dominated the dinoflagellate community only in a few brief periods; phototrophic dinoflagellates, especially thecate forms, were typically dominant. The occurrence of most dinoflagellate species appears to be rather closely related to temperature.

The thecate heterotophic dinoflagellate community is thus seen to be composed of at least a dozen species, dominated by Protoperidinium, that occurred in a succession of brief, often overlapping pulses. Occasionally these populateions were sufficiently numerous to dominate the protozooplanktonic community, but on average their abundance was below that of their (likely) protozoan competitors, the ciliates. Co-occurance of half a dozen Protoperidinium species with diatom blooms suggest a trophic dependance.

INTRODUCTION

The protozooplankton, sensu Sieburth et al. (1978), has rapidly become a subject of extensive study, but methodological difficulties still prevent a clear understanding of how this diverse group of heterotrophic protists functions in marine food webs. The ecological role of thecate heterotrophic dinoflagellates, a ubiquitous component of marine protozooplanktonic communities, is particularly poorly understood. Mere description of this community, prior to the widespread availability of epifluorescence microscopy, had been problematic due to the difficulty in distinguishing many heterotrophic species from their photosynthetic congeners. Consquently, heterotrophic dinoflagellates have often been grouped with photosynthetic forms as members of the phytoplankton (i.e. Marschall, 1985). (To further confuse the issue, some photosynthetic dinoflagellates may actually be phagotrophs, or, more properly, mixotrophs: Porter et al., 1985). For this reason and for reasons of inadequate preservation in fixed samples, etc., little is known about the population dynamics of heterotrophic dinoflagellates in relation to other components of the microplankton. Incidental reports suggest that thecate heterotrophic dinoflagellates are prevalent and sometimes abundant in many habitats. Reid et al. (1970) found Protoperidinium depressum to be present year-round in the Southern California Bight, and P. depressum was also found to dominate a net tow taken in the Gulf of Maine (Bigelow, 1926). Some species of Protoperidinium may even form "red-tide" like discolorations in coastal

waters (Le Fevre, 1979). Lessard (1985) documented the seasonal abundance of heterotrophic dinoflagellates in transects across the Gulf Stream in the Mid Atlantic Bight. Highest concentrations (7 cells•l^{-1} were found in spring in the slope water/Gulf stream front. In all stations along the transect except the Sargasso Sea, heterotrophic species on occasion numerically dominated the dinoflagellate community. Species of Protoperidinium were noted in Norwegian fjords by Hasle and Smayda (1960). A small species, P. bipes, once exceeded 10^4 cells•l^{-1}, but most species >30μm in diameter rarely exceeded 10^3 cells•l^{-1}.

Few reports deal comprehensively with the protozooplanktonic community. A study by Smetacek (1981) shows that the aggregate biomass of heterotrophic protists can occasionally exceed that of the metazoan grazers, and, among the protists, that heterotrophic dinoflagellates can reach biomass densities comparable to those of ciliates. However, this time series analysis lacked the species resolution required to draw any specific inferences concerning predator/prey relationships. Lessard (1985) documented the numerical predominance of heterotrophic dinoflagellates over sarcodine protists in the open ocean.

The study which follows was designed to analyze the seasonal cycle of a protozooplanktonic community, focusing on the dinoflagellates, with sufficient detail so that events such as close temporal couplings between abundance peaks of predator and prey organisms (which might suggest food preferences of thecate heterotrophic dinoflagellates) could be documented. This approach was taken chiefly because all previous attempts to culture or observe feeding behavior in thecate heterotrophic dinoflagellates had met with failure at that time. The specific goals of

this report are: (1) to characterize the annual cycle of the dinoflagellate community; (2) to do so in the context of the co-occurring ciliate, diatom and "metazooplanktonic" cycles; and (3) to indicate the likely food resources used by thecate heterotrophic dinoflagellates in an estuarine embayment.

METHODS AND MATERIALS

The study site, Perch Pond, Falmouth, Massachusetts, is a shallow (mean low tide depth 1.5 m), estuarine (average salinity 25‰) backwater of a larger embayment, Great Pond, which is separated from the well-mixed waters of Vineyard Sound (salinity 31‰). The isolation of Perch Pond (Fig. 1) is enhanced by the presence of a shallow, narrow channel leading to Great Pond; this feature, together with the presence of a diverse dinoflagellate assemblage, makes the location attractive for studies of plankton populations. Tidal mixing can replace 40% of the pond's volume over 24 hours (Garcon et al., 1986).

Each week, a single composite sample was taken from Perch Pond between 11 AM and 1 PM by mixing, in a carboy, samples taken from five stations located along the pond's central axis. All samples were taken with a 2.2 m closable PVC tube; this resulted in a depth-integrated sample that minimized the risk of variability due to patchiness; a pair of duplicate samples yielded comparable species composition/abundance data. Near-surface (0.5 m) water temperatures were recorded. The sample was subsampled (after gently mixing the carboy) in two ways: a 500 ml aliquot was concentrated with a 20 μm Nitex screen to a reduced volume

of 50 ml, and a second, unconcentrated 50 ml aliquot was taken. Both subsamples were fixed in biological grade glutaraldehyde (final concentration 2%) and left in Zeiss settling chambers overnight. A concentrated, live sample was examined to note the presence of delicate, naked species that become distorted and difficult to identify once preserved. All counts were made on a Zeiss epifluorescence inverted microscope (filter set #487706), allowing unambiguous determinations of the presence or absence of chloroplasts (and chloroplast-containing food vacuoles). The smallest dinoflagellates and ciliates were enumerated at 400x from the 50 ml aliquot by counting adjacent fields along a central transect of the circular settling slide. Larger organisms were counted from the concentrated aliquot, examined at 160x or 250x. Depending on cell densities, one to several transects were examined until approximately 200 cells of the abundant species had been counted. All species encountered were measured in three dimensions to provide volume estimates. The entire slide was scanned at 100x for rare species and metazoans. The presence of Amoebophrya ceratii-parasitized dinoflagellates (which exhibit a conspicuous green autofluorescence) was noted. In vivo chlorophyll fluorescence was measured on a Turner fluorometer for the whole and <20 μ fraction of the sample; these measurements served to crudely monitor the aggregate abundance of the phytoplankton community.

On one occasion, feeding of Oblea rotunda was observed. Feeding frequency measurements were made using subsamples of the <64 μm fraction of a recently collected Perch Pond sample by the following method: 10 ml samples were drawn into a 2x10 mm bore rectangular glass

tube and examined live under a dissecting microscope. Care was taken not to count cells reduntantly. Approximately 20% of O. rotunda cells were feeding, that is carrying food particles within a pseudopodal sac. These cells were tallied according to the identity of their prey and compared with the number of total feeding cells.

Taxonomic Notes

Dinoflagellate identifications, aided by analysis of thecal structure using Nomarski optics and calcafluor fluorescence (Fritz & Triemer 1985) were based on Schiller (1933), Lebour (1925) and Hulbert (1957). Differential autofluorescence of heterotrophic dinoflagellates also aided species identification. (As an example, two species of similar size and appearance, Protoperidinium pellucidum and P. pyriforme were found to have, respectively, an extremely intense green autofluorescence and no detectable fluorescence). Several forms were encountered that could not be identified (Appendix B). Protoperidinium sp. A is related to P. leonis in tabulation and ornamentation, but is markedly compressed in an oblique dorso-ventral plane (see Appendix II). Protoperidinium sp. B. had the appearance of a colorless Scrippsiella; it lacks noticeable pusules and contains a large oblong waxy storage body located mid-cell. Protoperidinium sp. C is a small, 25 µm dorso-ventrally flattened cell with a pair of conspicuous pusules (Appendix II). Another enigmatic thecate heterotroph is Gonyaulax sp. A., a somewhat large (45 µm) species resembling a colorless G. scrippsae (Appendix II). Although this species was never abundant, the mere existence of a non-photosynthetic Gonyaulax species comes as a surprise, as the genus has been considered to be composed exclusively of phototrophs. All four species lack any

pigmentation with the exception of greenish accumulation bodies on the part of Gonyaulax sp. A, and have no conspicuous autofluorescence.

Scrippsiella trochoidea has recently been shown to have several related species of very similar appearance forming a S. trochoidea complex, casting doubt on routine field identifications (Steidinger and Balech 1977). Consequently, the species resembling S. trochoidea will be identified as Scrippsiella spp.. A separate, clearly recognizable Scrippsiella species with angular epithecal and small antapical spines is called Scrippsiella sp A.

RESULTS

The temperature cycle of Perch Pond over the 14 month duration of the study has a high amplitude with extremes of 2 and 26°C (Fig. 2). Over 80 species of dinoflagellates were encountered; the abundances of the 50 most common species, including the phagotrophic flagellate Ebria tripartata, are presented in Appendix I. Twenty-four of the 50 dinoflagellates were heterotrophic species; the thecate heterotrophs account for 18 of these 24 species. Among the photosynthetic dinoflagellates, 19 of 26 are thecate. The biomass (i.e., biovolume) concentration comparisons (which are presented as a quantity ecologically preferable to cell number) reveal a complex, temporally shifting picture. Fig. 3 reveals two major peaks in total dinoflagellate biomass density, the first in September/October dominated by Scrippsiella spp. and the naked Gonyaulax rugosum, the second December/January dominated by Heterocapsa triquetra and Katodinium rotunda. On a yearly basis,

phototrophic H. triquetra was the most abundant, pervasive species in Perch Pond. With the exception of a bloom in December, thecate phototrophic species usually dominated the phototrophic dinoflagellate community (Fig. 4b,5). Scrippsiella sp. A and Dinophysis acuminata are two other occasionally dominant phototrophic species. In vivo fluorescence (Fig. 6) fluctuated in a similar pattern to the biomass estimate, showing two distinct peaks through time. Microflagellates were not identified with the exception of Apedinella sp. which formed a massive bloom, detected in January. The pattern of diatom abundance was strongly episodic and seemed to be coincident with the abundance of Protoperidinium species. (Fig. 7).

Heterotrophic dinoflagellates occasionally dominated the dinoflagellate community; this is most clearly evident in Fig. 5. The greatest heterotrophic peak (Fig. 4a) was composed chiefly of Polykrikos kofoidii together with lower abundances of another large naked phagotroph, Gyrodinium spirale. Ingested H.triquetra and Scrippsiella sp. A cells were found within Polykrikos cells. A third exceptionally large phagotroph Gymnodinium abbreviatum (with a length of 110 μm) never became abundant, and was not seen to have recognizable particles within food vacuoles. Another phagotroph, Ebria tripartata, a prevalent but rarely abundant species, was observed with ingested chains of Fragillaria sp. and Skeletonema costatum, as previously reported by Smayda (1973).

The smaller of the two major heterotroph peaks occurred in late August and was composed almost exclusively of thecate heterotrophic dinoflagellates of the genus Protoperidinium (species include

Protoperidinium sp. A, P. minimum, P. oblongum, and P. spinulosum with cell densities of 26, 18, 10 and 5 cells•ml^{-1}, respectively)(Fig. 8). Polykrikos appeared in low numbers at the end of this peak.

While all species of Protoperidinium found in Perch Pond were strongly seasonal, two diplosaloid species, Oblea rotunda and Zygabikodinium lenticulatum were present year-round. The latter never attained significant densities, but O. rotunda did exhibit several marked peaks (Fig. 9), with cell numbers exceeding 50•ml^{-1}. Feeding on the part of O. rotunda was witnessed in Perch Pond on 11 May 1984, allowing the documentation of feeding frequencies (Table 2). The dominant dinoflagellate, H. triquetra, was the favored food taken by O. rotunda. However, two other dinoflagellates were taken as well (Dinophysis acuminata and O. rotunda itself) in direct proportion to their abundance. Pennate diatoms and nanoflagellates were also preyed upon with a combined frequency of 19% of the feeding O. rotunda cells, but their abundance was not determined.

The presence of dinoflagellates parasitized by Amoebophrya ceratii, a dinoflagellate that proliferates within the host nucleus, was noted in 17 of 50 samples during the months of February-May, August-September, and November. Heterocapsa triquetra was the most prevalent host, with as much as 10% of the population being infected at one time; in one sample (17 May 1984) parasitized dinoflagellates reached a density of 87 cells•ml^{-1}. In late August and September when H. triquetra was nearly absent, A. ceratii was found parasitizing Protoperidinium minutum, again reaching an infection frequency of 10%. Several other species were parasitized at lower frequencies; they include Scrippsiella spp., Oblea

rotunda, Zygabikodinium lenticulatum, Protoperidinium pellucidum, Kryptoperidinium foleaceum, Gonyaulax tamarensis, Prorocentrum gracile and Gyrodinium areolum.

The aggregate biovolume of the heterotrophic dinoflagellates on occasion exceeded that of the ciliates, as shown in Fig. 10; however, the ciliate community usually contributed the largest biovolume fraction of the protozooplankton. Non-loricate forms were typically more abundant than tintinnids. One abundant tintinnid, Favella sp. is known to select small dinoflagellates for prey (Stoecker et al., 1981) and was on one occasion found to have ingested Protoperidinium minutum. Metazoan zooplankters that could potentially act as predators of heterotrophic dinoflagellates can also become abundant in Perch Pond (Figure 12).

DISCUSSION

This report provides the most detailed account of the seasonal abundance of thecate heterotrophic dinoflagellates to date. Previous work featured quarterly sampling (Lessard, 1985), failed to distinguish heterotrophs from phototrophs, or did not report population dynamics of these dinoflagellates on a species basis. The original motivation of this study was to determine which factors control the abundance of these dinoflagellates, which had not been cultured at that time. Now that the diatom grazing behavior of the genus Protoperidinium and Zygabikodinium (and to a lesser degree, Oblea) has become known through culture experiments (Chapters 2 and 3), some evidence of a Protoperidinium/ diatom correlation should be present in these data. In this context,

Zygabikodinium lenticulatum never rose above a low background concentration in Perch Pond, although this species is often dominant among dinoflagellates in the perennially diatom-rich waters of Vineyard Sound (unpubl. obs.). For most of the year in Perch Pond, Protoperidinium densities were rather low but abundance peaks of various magnitudes covary with several of the seven or so diatom blooms (Figs. 7,8). The most striking episode occurred in late August 1983, when four species of Protoperidinium (P. minutum, P. oblongum, P. spinulosum and Protoperidinium sp. A) reached their highest densities of the year on the same day (as sampled) simultaneously with a major diatom bloom (Fig. 8). It would obviously be better if a more detailed data set with daily samples were available, but this clear correlation stands as the first field demonstration of a thecate heterotrophic dinoflagellate/diatom linkage. The diatom community during this period was overwhelmingly dominated by Skeletonema costatum, a species known to support maximal growth of P. spinulosum in culture (unpubl. obs.).

While no other "significant" biomass peaks (from the perspective of Fig. 2) can be attributed to the genus Protoperidinium, three minor peaks coincided with diatom blooms, involving P. pellucidum, P. conicum and P. oblongum. Of the two remaining diatom blooms lacking associated Protoperidinium spp., one (in January) was poorly sampled due to ice; therefore a Protoperidinium/diatom correlation can be demonstrated for four out of five adequately sampled episodes of diatom maxima. It should be noted that some of these diatom blooms seem to occur during spring tides associated with full moons, which may transport diatoms from Vineyard sound or simply resuspend local populations.

The strong but not perfect covariation between diatom availability and Protoperidinium blooms does not rule out the possible suitability of other, non-diatom phytoplankters as food for Protoperidinium species. The absence of Protoperidinium blooms during the two remaining diatom blooms may be related to predation mortality as well as food limitations. Furthermore, temperature obviously plays an important role in controlling the occurrence of dinoflagellates (Smayda 1980). Indeed, many dinoflagellate species, both heterotrophs and phototrophs, occur in brief, seasonally characteristic intervals while other species have eurythermal, year-round characteristics (Fig. 12). Table 1 categorizes the seasonal species, and lists the temperature ranges through which they occurred, as well as the temperature range of maximal cell densities. Some species occur only in the cold winter-spring period, while others are restricted to the temperature maximum of summer. One species, Protoperidinium conicum, like Gonyaulax tamarensis, appears both in the spring and again in the fall, although at somewhat dissimilar temperature ranges. As many Perch Pond dinoflagellates (22 out of 50) are known to have benthic resting stages or cysts, it is likely that temperature-controlled germination of the cysts leads to the formation of seasonal planktonic populations of motile cells (D. M. Anderson, unpubl. data). This has already been shown to be the case for Gonyaulax tamarensis (Anderson and Morel 1979). It should be noted that a number of seasonal heterotrophic species such as Protoperidinium sp. C, P. pellucidum and P. spinulosum do not as yet have known cyst stages. Either an elusive cyst stage does exist or the species in question are introduced each year as vegetative cells from adjacent regions.

When the data set is scrutinized further, another potential predator/prey relationship emerges, that of Oblea rotunda and Heterocapsa triquetra (Fig. 9). In April of both 1983 and 1984 an O. rotunda bloom occurred at the end of a massive bloom of H. triquetra. Further, the larger of the two O. rotunda blooms (with peak cell density of $57 \cdot ml^{-1}$) was associated with the largest H. triquetra bloom, of 7000 $cells \cdot ml^{-1}$. In culture, maximal growth of O. rotunda (one $doubling \cdot day^{-1}$) are sustained by H. triquetra densities of 5000 $cells \cdot ml^{-1}$ or greater; half maximal growth occurs at 1300 $cells \cdot ml^{-1}$ (unpubl. data). The first O. rotunda bloom occurred in the presence of H. triquetra cell densities less than $1000 \cdot ml^{-1}$. It is possible that small scale H. triquetra cell densities could be higher than the water-column average as measured by the sampling protocol, since this species is known to form discrete, vertically migrating bands (See Chapter 2). The O. rotunda/H. triquetra interaction is further confirmed by the feeding frequency observations which show that O. rotunda readily feeds on H. triquetra in a Perch Pond assemblage, although the grazers do not appear to discriminate among the available dinoflagellate species, O. rotunda included. Further, O. rotunda did not appear in significant numbers during blooms of Dinophysis acuminata (the other dinoflagellate seen to be taken as food) or any other dinoflagellate. A special relationship seems to exist between O. rotunda and H. triquetra, even though other food sources may be acceptable.

The ingestion of diatoms by species of Protoperidinium suggests that these dinoflagellates compete with much larger heterotrophs such as copepods for food. While it is too early to accurately assess the

feeding capacity of the entire Protoperidinium community, grazing rate measurements have been made for one small species, Protoperidinium hirobis (Chapter 3); maximum individual daily ingestion rates exceeded 20 Leptocylindrus danicus cells$\cdot d^{-1}$. This ingestion rate datum can be compared with that of the dominant copepod in Perch Pond, Acartia hudsonica. Deason (1980) reported an individual daily ingestion rate of $6.5 \cdot 10^4$ Skeletonema costatum cells for A. hudsonica. Since S. costatum cells are smaller than those of L. danicus by roughly a factor of five, P. hirobis is assumed for sake of comparison to have a S. costatum ingestion rate of 100 cells$\cdot day^{-1}$. It follows that approximately 650 P. hirobis cells can collectively ingest as many diatom cells as a single copepod. Since the Protoperidinium cells in Perch Pond often outnumber copepods by a factor of 1000 or more, it is concluded that the Protoperidinium community may in some cases rival copepods as important diatom grazers. In light of the maximal Protoperdinium cell concentrations of $6 \cdot 10^4 \cdot l^{-1}$, as many as $6 \cdot 10^6$ diatom cells may be cropped each day, although Protoperidinium grazing pressure is undoubtly much lower during non-bloom periods.

The presence of the parasitic dinoflagellate Amoebophrya ceratii in both phototrophic and heterotrophic species has been previously noted (Taylor, 1968). Infection of thecate heterotrophic dinoflagellates obviously would reduce their population growth rate, but observed infection frequencies of 10% or lower would not likely have a profound effect on community population dynamics.

In conclusion, this study has fulfilled the aims of documenting the various components of the dinoflagellate community with particular

emphasis on the thecate heterotrophs. It also suggests the likely food preferences of thecate heterotrophic dinoflagellates in Perch Pond since these microheterotrophs can become very abundant for brief intervals during blooms of diatoms; at other times their numbers remain at a low background. Thecate heterotrophic blooms do not coincide with those of naked heterotrophs as a consequence, no doubt, of non-overlapping food requirements. Thecate heterotrophic dinoflagellates, like other dinoflagellates, display several seasonal occurence patterns that are probably temperature-dependant. The intermittent survival of dinoflagellates as benthic resting cysts may be involved in the maintenance of these repetitive patterns. Heterotrophic dinoflagellates as a class can occasionally out-number, on a biomass basis, the other major protozooplanktonic class, the ciliates. While some thecate heterotrophs have diets similar to those of some ciliates (i.e., predation upon dinoflagellates) the larger diatoms which are readily preyed upon by species of Protoperidinium are not available to ciliates. This report, then, adds an additional level of complexity to the microbial food web in marine waters. Further work on food specificity of heterotrophic dinoflagellates can be expected to increase this level of complexity yet further.

References

Anderson, D.M. and F.M.M. Morel 1979. The seeding of two red tide blooms by the germination of benthic Gonyaulax tamarensis hypnocysts. Est. and Coast. Mar. Sci. 8:279-293.

Bigelow, H.B. 1926. Plankton of the offshore waters of the Gulf of Maine. Bull. Bur. Fisheries, Doc. No. 968, 40 (1924) Part II, pp. 1-509.

Deason, E.E. 1980. Grazing of Acartia hudsonica (A. clausi) on Skeletonema costatum in Narrangensett Bay (USA): influence of food concentration and temperature. Mar. Biol. 60:101-113.

Fritz, L. and R.E. Triemer 1985. A rapid, simple technique utilizing calcofluor white M2R for the visualization of dinoflagellate thecal plates. J. Phycol. 21:662-664.

Garcon, V.C., K.D. Stolzenbach and D.M. Anderson 1986. Tidal flushing of an estuarine embayment subject to recurrent dinoflagellate blooms. Estuaries 9:179-187.

Hasle, G.R. and T.J. Smayda 1960. The annual phytoplankton cycle at Drobak, Oslofjord. Nytt. Mag. Botanikk 8:53-75.

Hulbert, E.M. 1957. The taxonomy of unarmoured Dinophyceae of shallow embayments of Cape Cod, Massachusetts. Bio. Bull. 112:196-219.

Lebour, M.V. 1925. The Dinoflagellates of Northern Seas. Marine Biological Association, Plymouth. 250pp.

Le Fevre, J. 1979. On the hypothesis of a relationship between dinoflagellate blooms and the "Amoco-Cadiz" oil spill. J. Mar. Biol. Assoc. U.K. 59:525-528.

Lessard, E.J. 1984. Oceanic heterotrophic dinoflagellates: distribution, abundance, and role as microzooplankton. PhD dissertation, University of Rhode Island. 146pp.

Marschall, H.G. 1985. Comparison of phytoplankton concentrations and cell volume measurements from the continental shelf off Cape Cod, Massachusetts, U.S.A.. Hydrobiologia 120:171-179.

Reid, F.M.H., E. Fuglister and J.B. Jordan 1970. V. Phytoplankton taxonomy and standing crop. In The ecology of the phytoplankton off La Jolla, California, in the period April through September, 1967. Strickland, J.D.H. (ed.) Bull. S.I.O. 17:51-66.

Schiller, J. 1933. Dinoflagellatae (Peridineae). In Rabenhorst, L. (ed.) Kryptogamen-Flora. 10:1-590.

Sieburth, J.M., V. Smetacek and J. Lenz 1978. Pelagic ecosystem structure: heterotrophic compartments of the plankton and their relationship to plankton size fractions. Limnol. Oceanog. 23:1256-1263.

Smayda, T.J. 1973. The growth of Skeletonema costatum during a winter-spring bloom in Narragansett Bay, Rhode Island. Norw. J. Bot. 10:219-247.

_____ 1980. Phytoplankton species succession. In Morris, I. (ed.) The Physiological Ecology of Phytoplankton. pp. 493-570.

Smetacek, V. 1981. The annual cycle of protozooplankton in the Kiel Bight. Mar. Biol. 63:1-11.

Steidinger, K.A. and E. Balech 1977. Scrippsiella subsalsa (Ostenfeld) comb. nov. (Dinophycea) with a discussion on Scrippsiella. Phycologia 16:69-73.

Stoecker, D., R.R.L. Guillard and R.M. Kavee 1981. Selective predation by Favella ehrenbergii (Tintinnia) on and among dinoflagellates. Biol. Bull. 160:136-145.

Taylor, F.J.R. 1968. Parasitism of the toxin-producing dinoflagellate Gonyaulax tamarensis by the endoparasitic dinoflagellate Amoebophyra ceratii. J. Fish. Res. Bd. Canada 25:2241-2245.

Table 1. Categories of thecate heterotrophic dinoflagellate patterns of occurrence in Perch Pond.

	Months of occurrence	Temp. range (occurrence)[a]	Temp range (abundance)[b]
Spring species			
Protoperidinium sp.B	Dec-May	2-12°C	6-8
P. punctulatum	Feb-March	2-8	-
P. bipes	Feb-March	2-9	9
P. conicoides	Feb-March	2-9	-
Protoperidinium sp.C	Feb-April	2-20	7-10
P. pellucidum	Feb-April	3-12	6-10
Spring/Fall species			
P. conicum	May-June, Nov	9-22	18
Summer species			
P. oblongum	June-Oct	9-26	13-25
P. spinulosum	July-Oct	15-23	21-25
Protoperidinium sp.A	May-Sept.	8-25	20-25

[a] Temperature range during periods of detectable abundance.
[b] Temperature range during periods of half-maximal cell abundance or greater.

Table 2. Feeding by Oblea rotunda captured together with a field assemblage from Perch Pond on 11 May 1984.

prey species	availability[a]	feeding frequency[b]	feeding frequency[c]
Heterocapsa triquetra	86.6	82.7	67
Oblea rotunda	9.4	13.8	11
Dinophysis acuminata	4.0	3.5	3
pennate diatoms	---	---	5[d]
nanoflagellates	--	---	14[e]
		n=29	n=36

[a] Percentage of total free swimming dinoflagellates available as food to O. rotunda.

[b] Percentage of O. rotunda cells observed feeding on a given prey species out of the subpopulation of O. rotunda cells which were feeding on any of the 3 dinoflagellate species.

[c] Percentage of O. rotunda cells observed feeding on given prey species out of total feeding population of O. rotunda; this later population constituted approximately 20% of the total O. rotunda population.

[d] Pennate diatoms were not counted in bulk sample.

[e] Nanoflagellates out-numbered H. triquetra by a factor of at least 35.

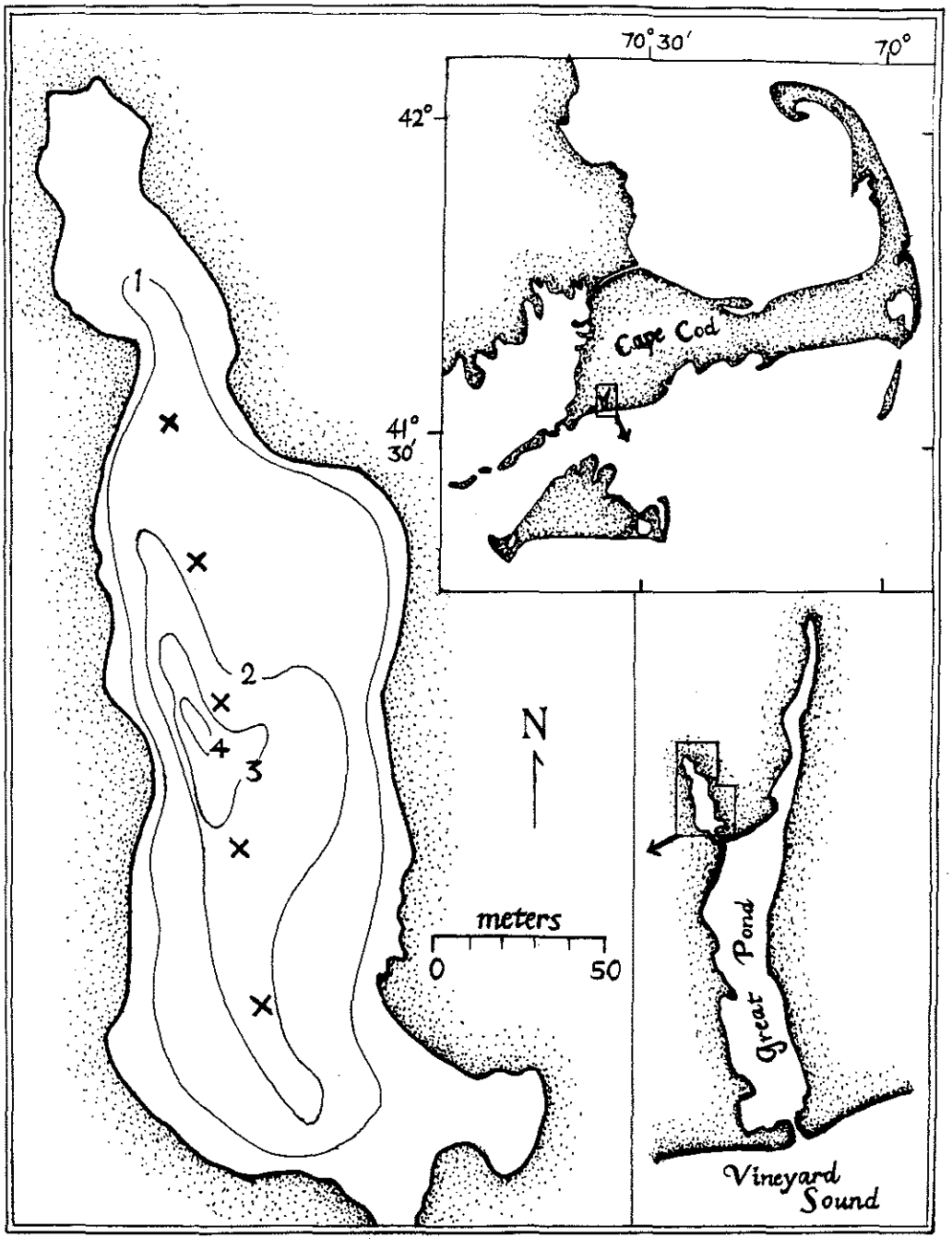

Figure 1. Map of Perch Pond, Massachusetts. Sample transect denoted by x's, depth in meters.

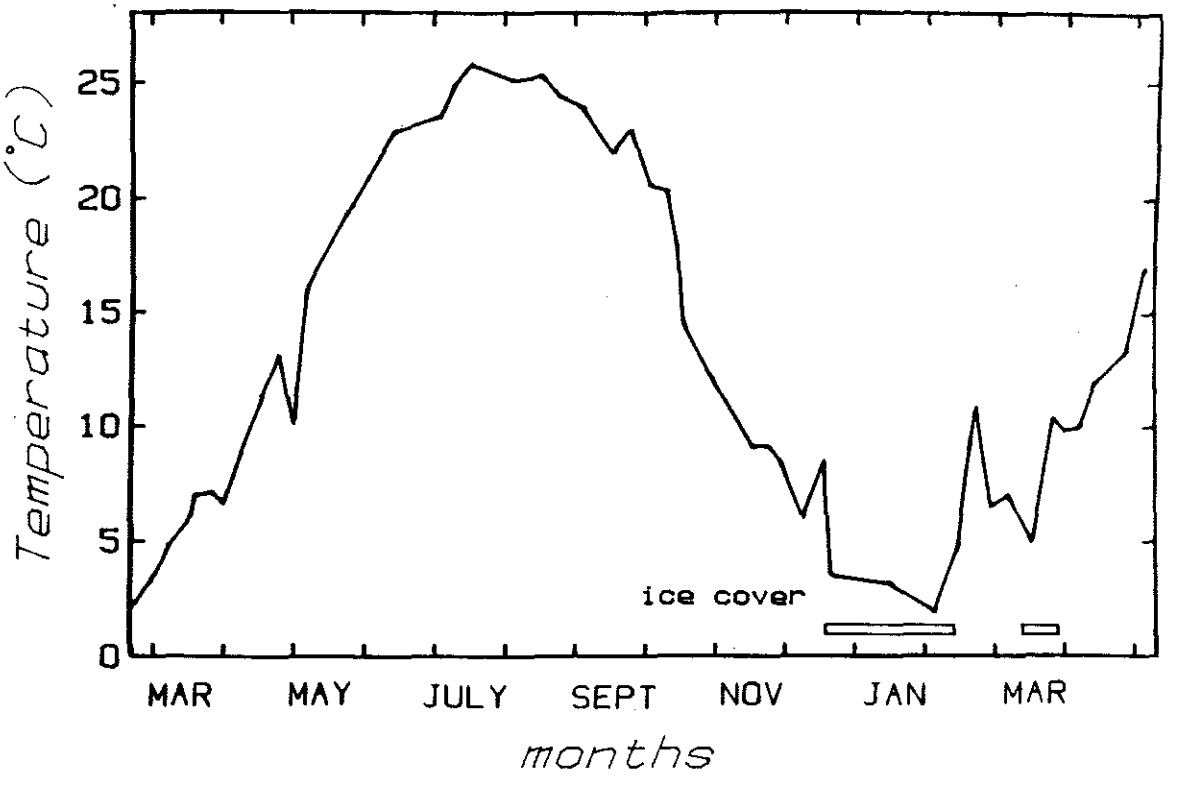

Figure 2. Record of surface water temperature in Perch Pond, 1983-1984. Intervals of ice cover indicated by horizontal bars.

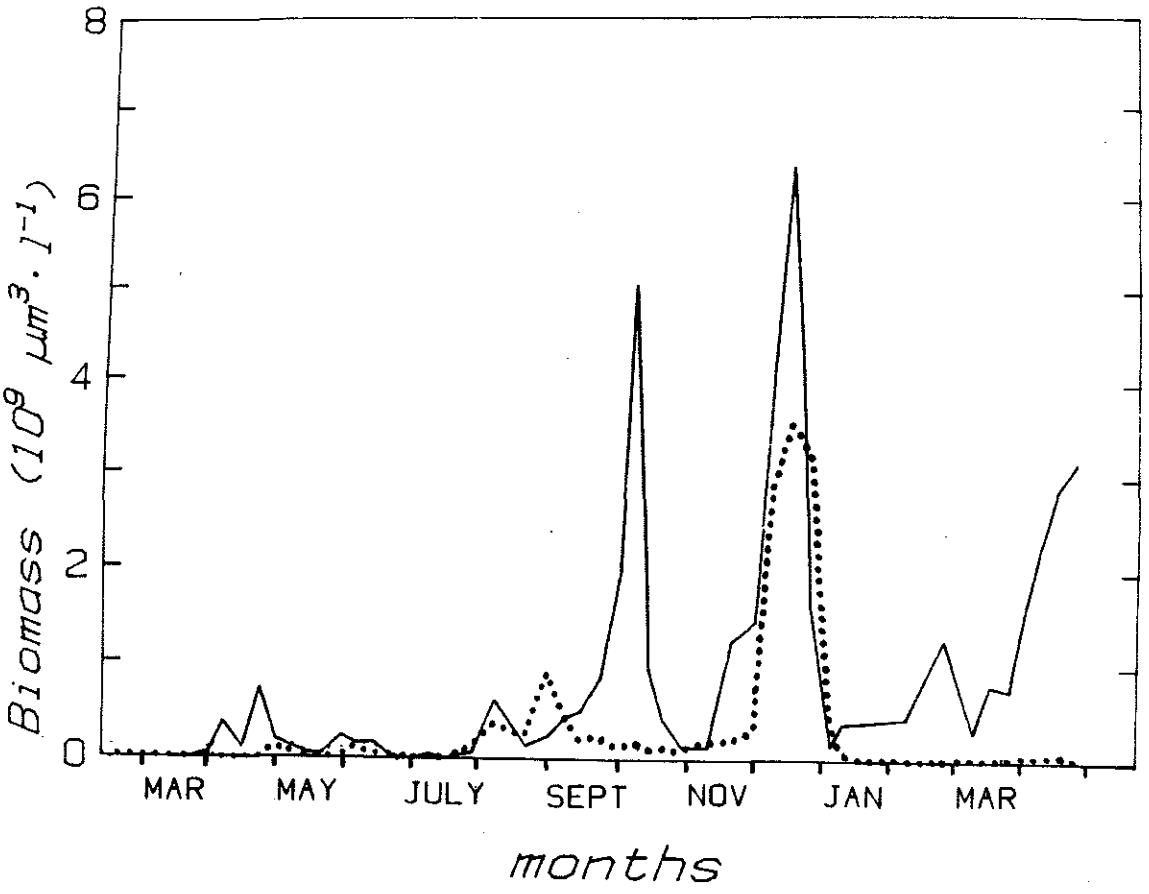

Figure 3. Volume-weighted abundance ("biomass") of dinoflagellates in Perch Pond. Solid line = total phototrophs; dotted line = total heterotrophs.

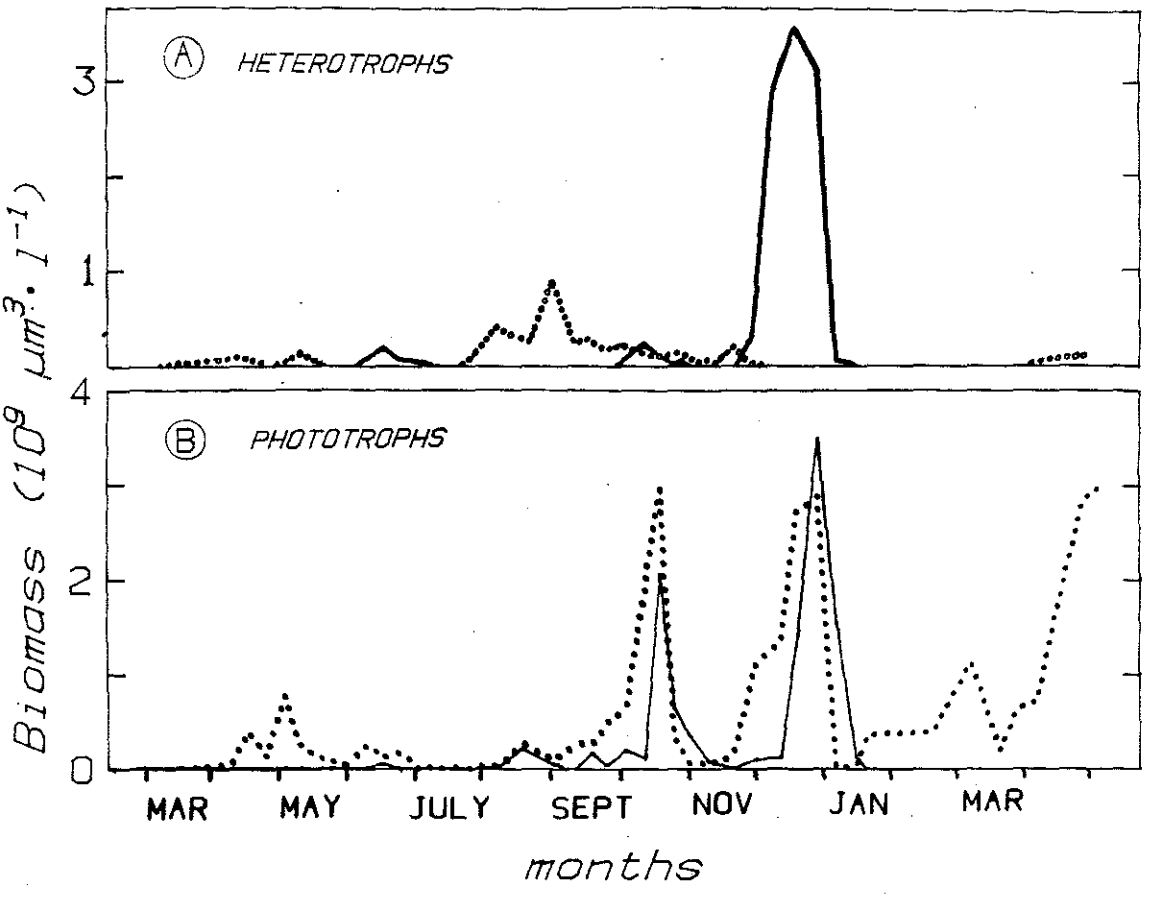

Figure 4. Volume-weighted abundance of dinoflagellates in Perch Pond.

Solid line = naked species.
Dotted line = thecate species.

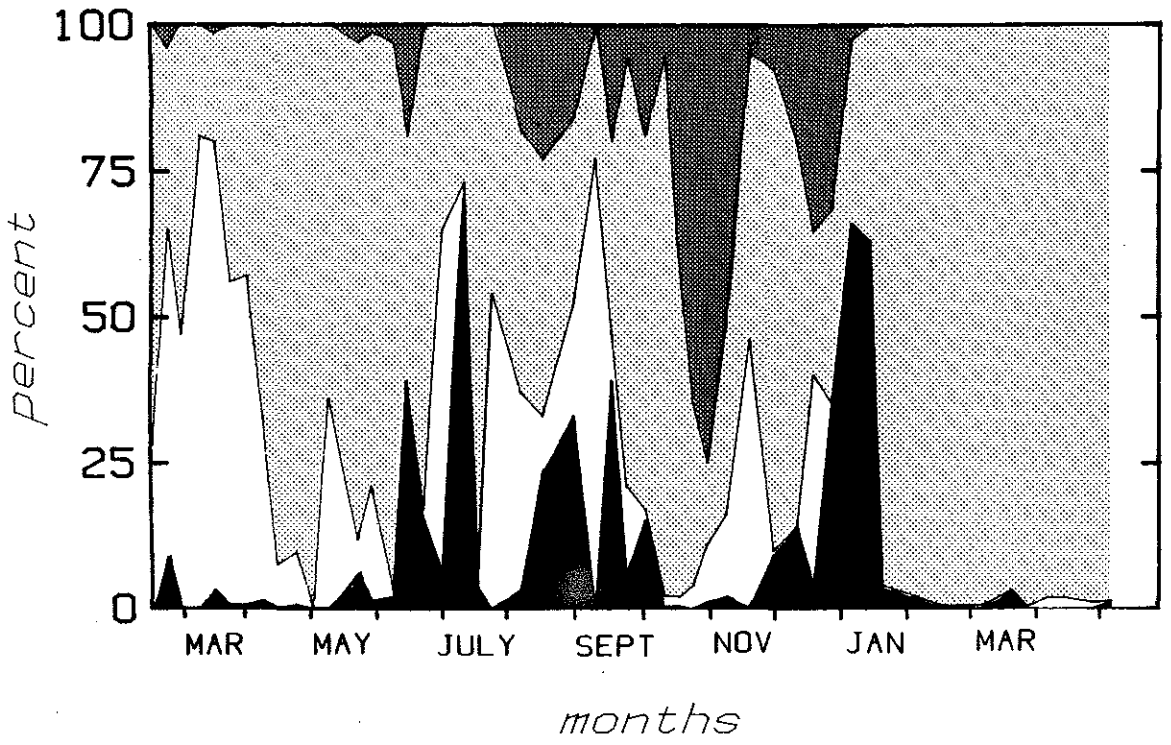

Figure 5. Relative composition of the dinoflagellate community in Perch Pond.

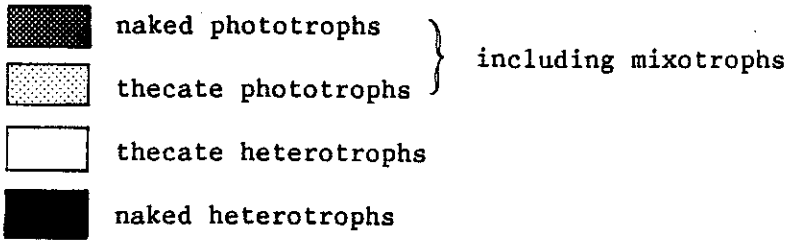

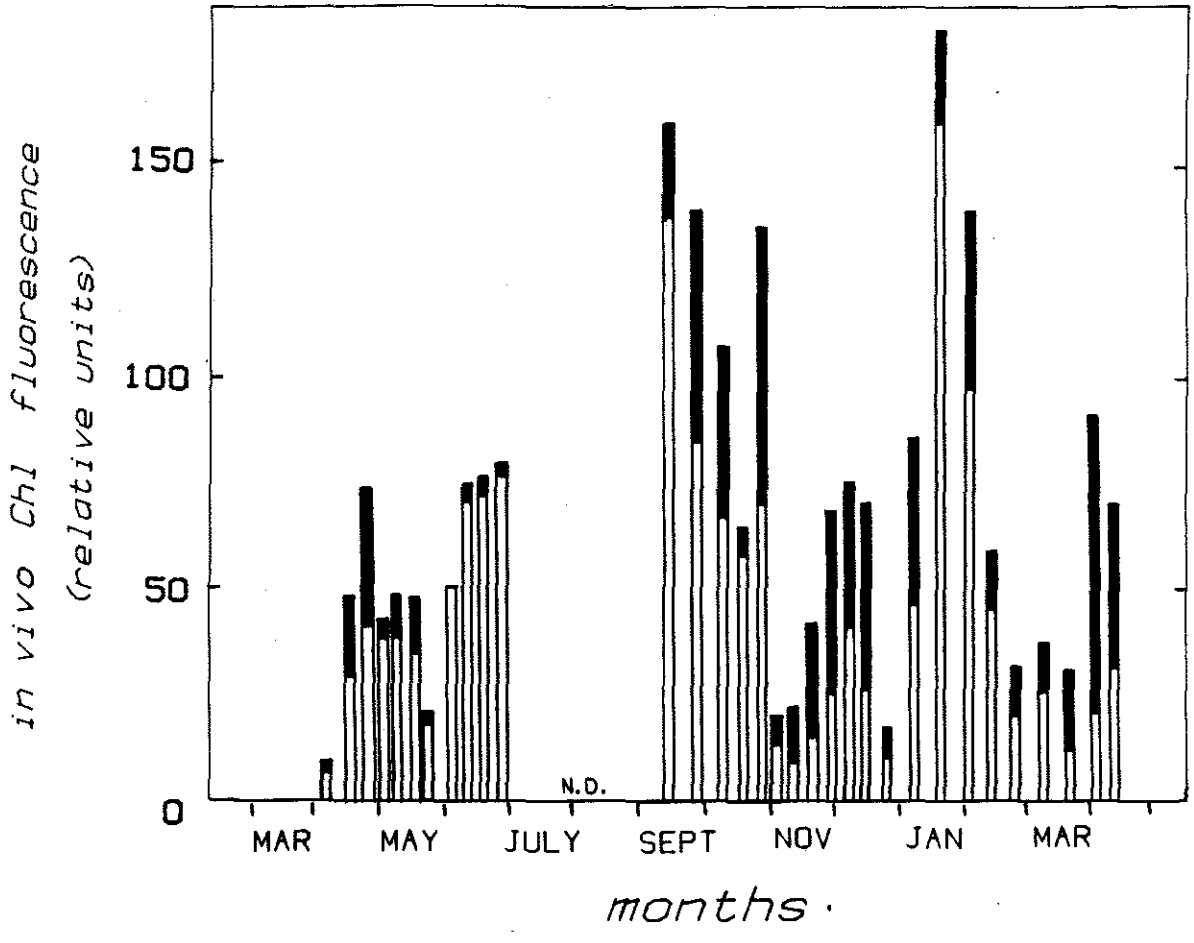

Figure 6. In vivo fluorescence in Perch Pond. Light segments = <20μm size fraction. Darkened segment (>20μm fluorescence) obtained by subtracting <20μm fraction from whole, unfiltered sample.

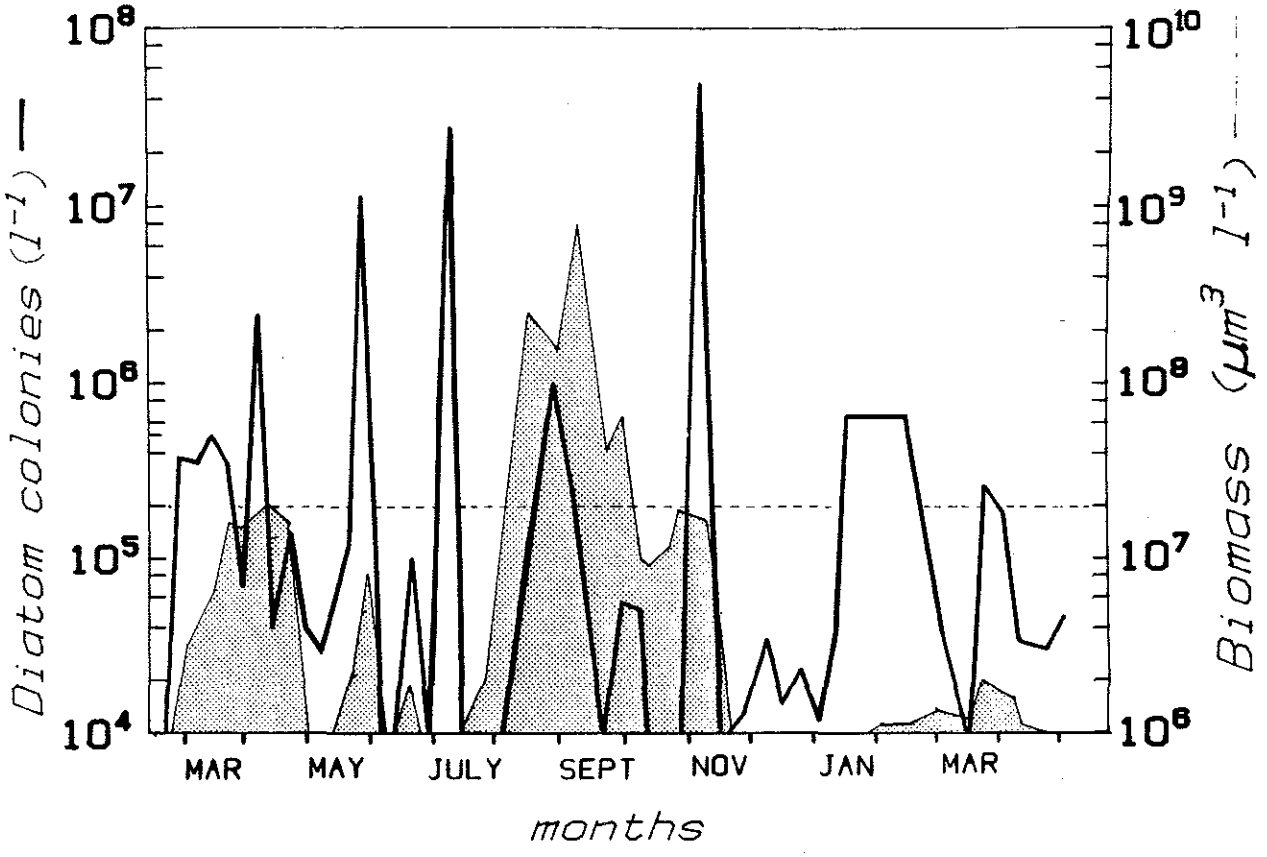

Figure 7. Diatom and Protoperidinium + Zygabikodinium species abundance in Perch Pond. Colonies, typically on the order of 10 cells in length, were enumerated as ecologically pertinent food units. Dashed line = $2 \cdot 10^6 \cdot l^{-1}$, an arbitrary threshold concentration (see Figure 8).

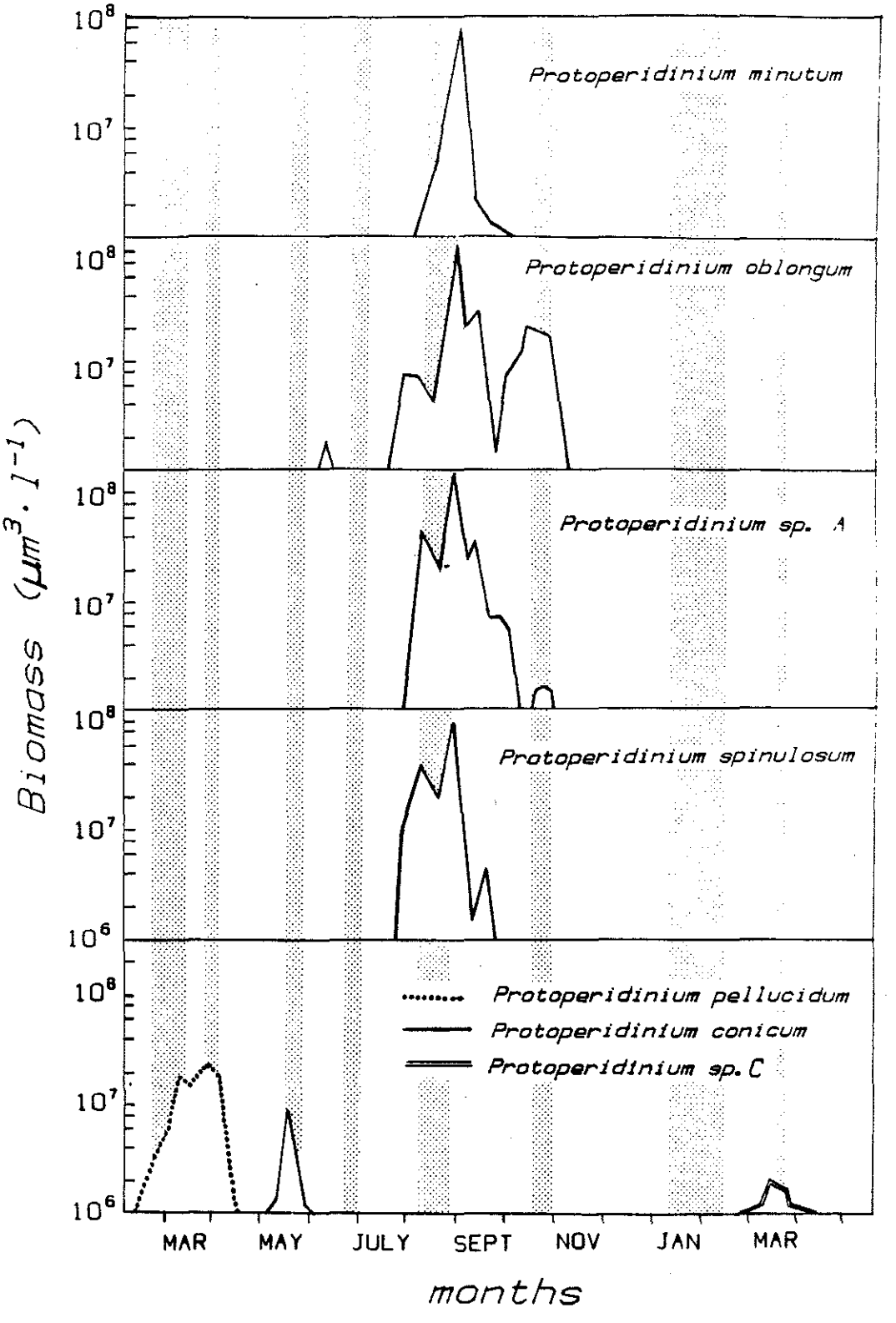

Figure 8. Volume-weighted abundances of individual species of Protoperidinium through time. Peaks of diatom blooms indicated by shaded bands where they exceed $2 \cdot 10^5$ colonies$\cdot l^{-1}$ (see dashed line in Fig. 7).

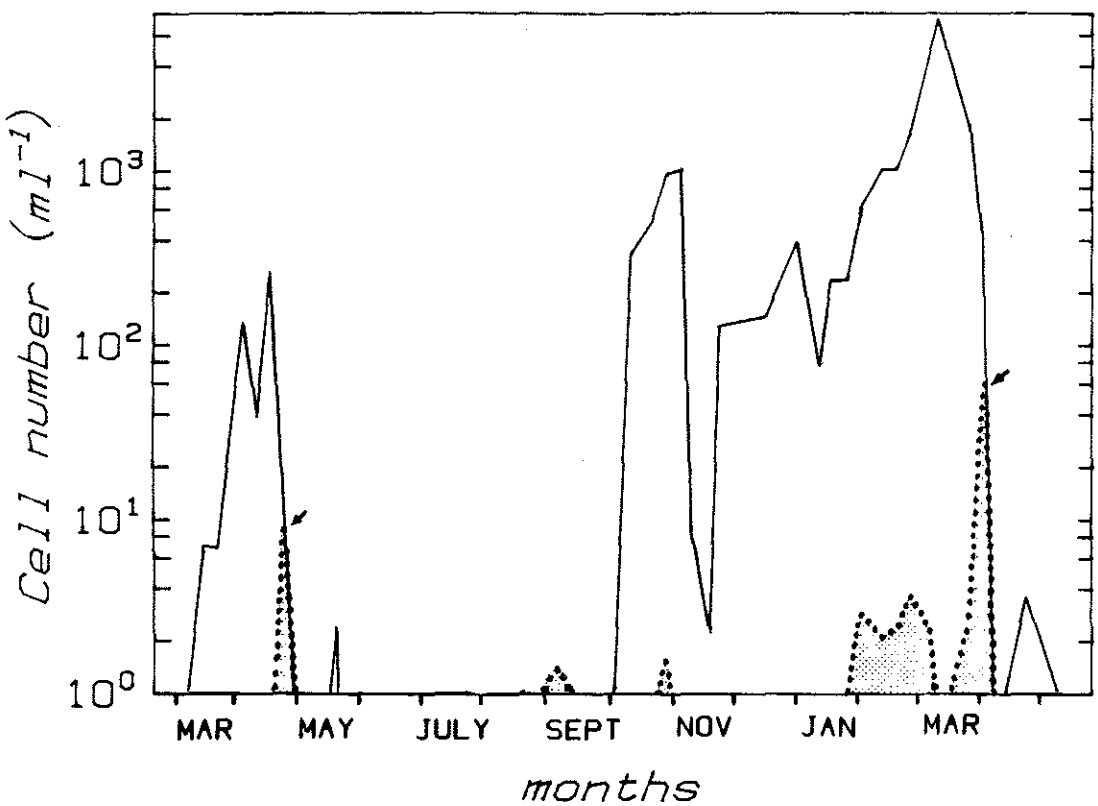

Figure 9. Numerical abundance of Oblea rotunda (dotted line with stipple) and Heterocapsa triquetra (solid line). Arrows denote two annually recurrent O. rotunda blooms.

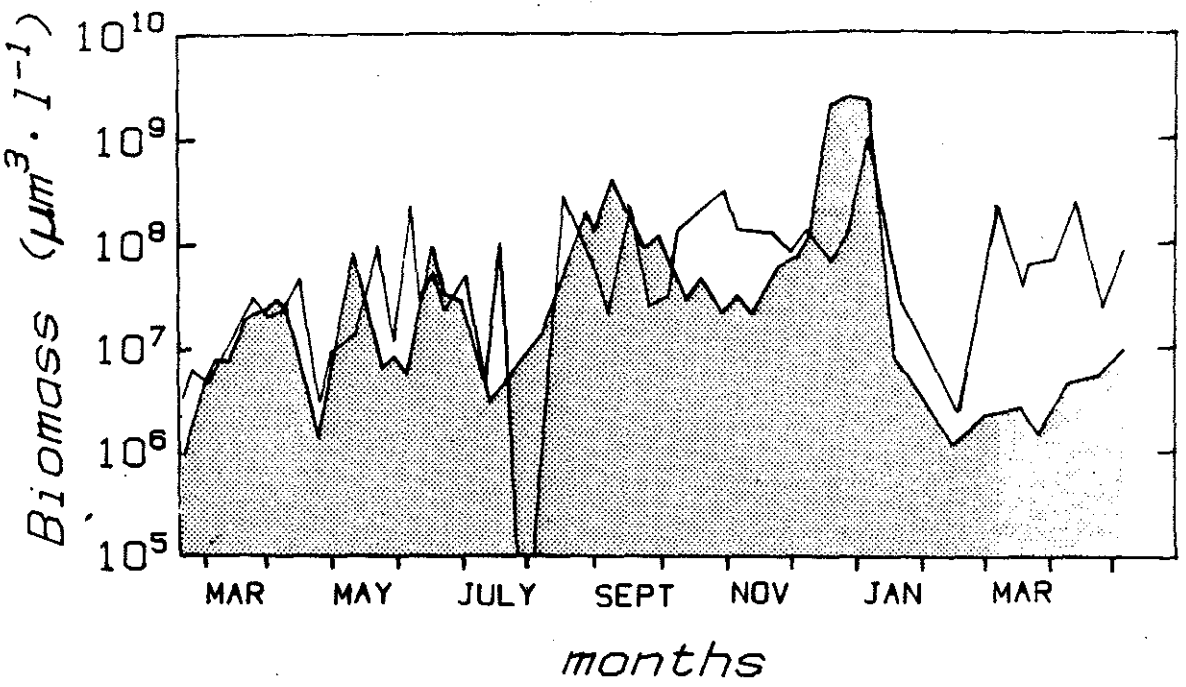

Figure 10. Volume-weighted abundance of total heterotrophic dinoflagellates (shaded area) and ciliates in Perch Pond.

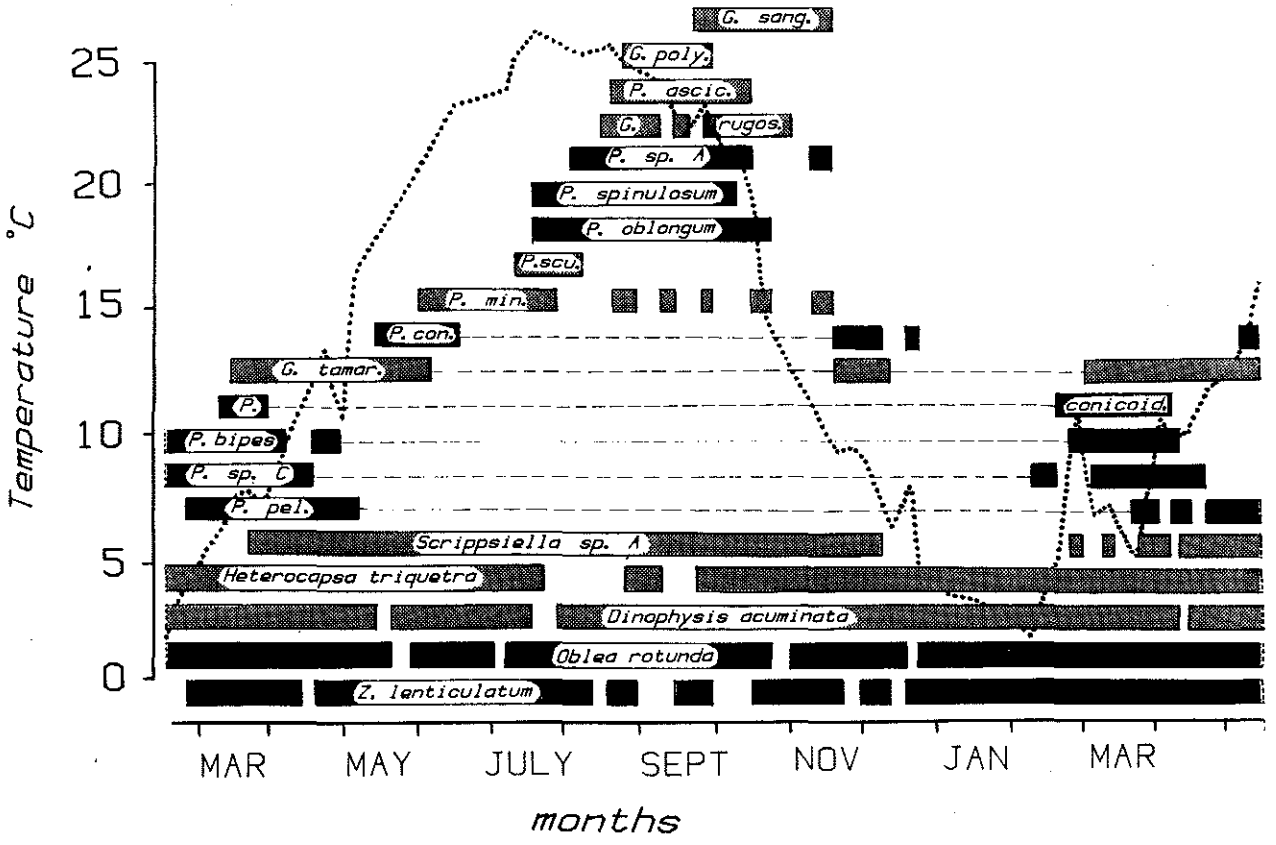

Figure 11. Seasonal occurence patterns of selected dinoflagellates in Perch Pond, plotted together with surface water temperature (dotted line). Black bars = heterotrophs
Grey bars = phototrophs

Abbreviations:

G. sang. = Gymnodinium sanguinium
G. poly. = Gonyaulax polyedra
P. ascic. = Peridinium asciculiferum
G. rugos. = Gonyaulax rugosa
P. sp A. = Protoperidinium sp. A
P. spinulosum = Protoperidinium spinulosum
P. oblongum = Protoperidinium oblongum
P. scu. = Prorocentrum scutellum
P. min. = Prorocentrum minutum
P. con. = Protoperidinium conicum
G. tamar. = Gonyaulax tamarensis
P. conicoid. = Protoperidinium conicoides
P. bipes = Protoperidinium bipes
P. sp. C = Protoperidinium sp. C
P. pel. = Protoperidinium pellucidum
Z. lenticulatum = Zygabikodinium lenticulatum

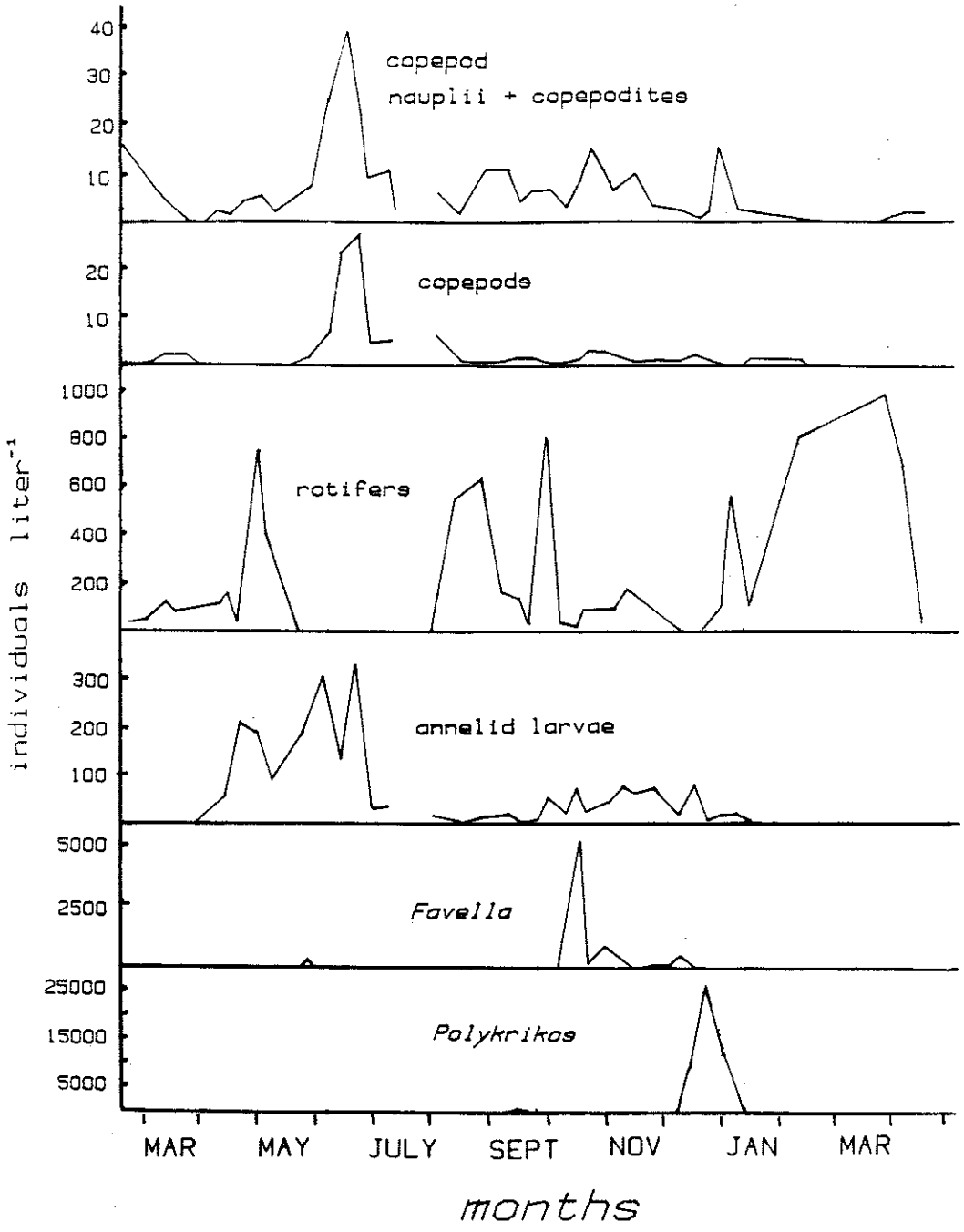

Fig. 12. Numerical abundance of potential predators of thecate heterotrophic dinoflagellates, including both metazoans and protozoans.

CHAPTER 2

Thecate Heterotrophic Dinoflagellates: Feeding Behavior and Mechanisms

by

Dean M. Jacobson

and

Donald M. Anderson

ABSTRACT

The feeding of 19 species of thecate heterotrophic dinoflagellates from three genera (Protoperidinium, Oblea, Zygabikodinium) can be described within one general framework. These species engulf diatoms and other prey with a pseudopod (herein termed a "pallium") which originates at the flagellar pore in the sulcus. The pallium is a highly plastic, membranous organ which easily stretches to accommodate spines and other protrusions, and has been observed to enclose as many as 58 diatom cells in a chain. Feeding episodes, during which the contents of the phytoplankton prey are liquified and transported through the pallium, typically last from 7 to 30 minutes, but may continue for as long as 2 h. In cases of diatom predation, empty, intact frustules are discarded at the meal's conclusion. Thus far, with few exceptions, Protoperidinium species have been observed feeding only on diatoms, whereas two diplopsaloid species feed on dinoflagellates and prasinophytes as well. In four species from the three genera studied, a capture filament has been observed that connects the food to the dinoflagellate prior to extension of the pallium, sometimes allowing the cell to pull the food while swimming. A distinctive precapture swimming behavior is also described for six species, suggesting that the dinoflagellates are selective grazers.

INTRODUCTION

Thecate heterotrophic dinoflagellates equipped with a rigid cell wall or theca have long been an enigma in the planktonic community. They are widely abundant and have attracted much study, but their feeding mechanisms, preferences, and rates remain a mystery. Holozoic dinoflagellates which lack a cellulose theca are regularly observed to contain phagocytosed food particles, but the thecate species show no evidence of food ingestion. One exception is an account by Bursa (1961) of a Protoperidinium ingesting a flagellate, which is reinterpreted below. The most likely food uptake orifice through the theca - the flagellar pore - is too small for the passage of any particle larger than a bacterium (Abé 1981). Other feeding strategies that have been considered are uptake of dissolved materials (osmotrophy) or uptake of decaying organic matter (saprotrophy). Osmotrophy seems unlikely since surface-to-volume ratios suggest that it would be difficult for an organism as large as a dinoflagellate to compete with bacteria for dissolved organic carbon in the sea (Morey-Gaines and Elbrachter, 1987). The recent report of the feeding behavior of two Protoperidinium species by Gaines and Taylor (1984) did much to resolve the mystery as they described a large "feeding veil" that the dinoflagellates deployed to completely envelope relatively large diatoms whose cell contents were then dissolved. The veil was deployed over a large area, only a portion of which was occupied by the diatom food. The work reported here, based on observations of 18 species from three genera, demonstrates that feeding is far more selective than the "feeding veil" description would suggest.

MATERIALS AND METHODS

Organisms were captured with net tows from Perch Pond or Vineyard Sound, Massachusetts (average salinities 26 and 32‰ , respectively). The <80 µm plankton fraction was incubated at 15°C for 2 to 16 hours, with added diatoms, in 15 ml polypropylene centrifuge tubes mounted on a slowly rotating apparatus. When the ratio of thecate heterotrophic dinoflagellates to detritus was too low, desired cells were transferred via micropipette to filtered seawater, with cultured diatoms or natural phytoplankton assemblages added. Such short term "cultures" typically yielded 0-5% feeding dinoflagellates at a given time. Feeding cells were either monitored with a Nikon dissecting microscope or transferred to wet mounts for observation with the phase and Nomarski optics of a standard Zeiss compound microscope. For ease of relocation, 6 mm coverslips, supported by small lumps of modeling clay, were used. Nomarski optics simplified analysis of thecal plate arrangements needed for taxonomic assignment, but two species (Protoperidinium species A and B) could not be identified and may constitute new species. Cells with deployed pseudopodia had to be manipulated gently as they readily aborted feeding by retracting or detaching their pseudopod when disturbed. Use of 2 mL settling slides with a Zeiss inverted compound microscope allowed direct observations to be made on samples at high magnifications without the need for further isolation. Feeding durations were determined either by continuous surveillance of an undisturbed cell held in a 15 mL petri dish or by transferring cells seen to have recently captured food (i.e. those with long attachment filaments) to microwell plates so that several

individuals could be monitored simultaneously. Swimming velocities and trajectories were determined from videotaped recordings by tracing from the video monitor. Bouins fixative was used to preserve the pseudopod apparatus intact. For documentation, a Nikon photomicrography system, a JVC S-100CH color video camera with a Panasonic 1/2 inch VCR and an MTI black and white video camera with a Panasonic 3/4 inch VCR were employed. For preliminary transmission election microscopy (see Chapter 4), single isolated cells were added to a mixture of 2% cacodylate-buffered glutaraldehyde and 1% osmium tetroxide at 0°C for 30 min, washed in seawater, embedded in 1% agar and passed through dehydration and Epon-Araldite infiltration series. Cells were ultimately flat-embedded and then excised and reoriented on a resin stub for microtomy. Thin sections were stained with uranyl acetate and lead citrate.

RESULTS

To date, 19 species of thecate heterotrophic dinoflagellates have been observed to employ a pseudopodal mechanism to feed on living particulate food. With the exception of Protoperidinium pyriforme and possibly Protoperidinium species B (an organism resembling a colorless Scrippsiella), the food consumed by Protoperidinium species consists exclusively of diatoms, whereas two diplopsaloid species fed on diatoms, dinoflagellates and prasinophytes (Table 1). While hundreds of dinoflagellates have been seen feeding on intact phytoplankters, several cells of Oblea rotunda and Zygabikodinium lenticulatum have also been seen to capture and envelop small transparent detrital particles. Several bacteria were seen on one such particle stained with DAPI. The

list of acceptable food species varies according to the number of observations made on the various dinoflagellates. In many instances, the dinoflagellates consumed prey much larger than themselves. This typically involved consumption of diatom chains but on occasion, large cells (e.g. Coscinodiscus) were enveloped and digested individually. Spines on bristly food species such as Chaetoceros presented no obstacle to the enveloping pseudopod. No diel variation in feeding has yet been detected; most observations were made during the organisms' light phase.

Feeding behavior in the species observed follows a consistent pattern marked by distinctive precapture, capture, pseudopod deployment, digestion, and pseudopod retraction phases.

Precapture

Precapture behavior has been observed in six species (Oblea rotunda, Zygabikodinium lenticulatum, Protoperidinium spinulosum, Protoperidinium punctulatum, Protoperidinium conicum and Protoperidinium claudicans). Other species may also have this same behavior but the likelihood of witnessing the initial moments of feeding events (which seem to occur infrequently) is terribly small. Most cells swim in a relatively straight course that is punctuated by occasional abrupt direction changes and usually pass by diatoms that are close to the swimming path without outwardly indicating recognition or attraction. However, a cell is sometimes seen that, when it encounters a diatom, swims in tight circles about the prey for usually one minute or less, occasionally up to 2 min. The path of P. spinulosum around a chain of Chaetoceros traced from a video recording illustrates this behavior (Fig. 1). With the exception of P. punctulatum, the species listed above display a characteristic,

punctuated swimming pattern as they circle the prey. This pattern, symbolized in Figure 1 by the dashed line, consists of a series of small pulses as the cell pitches its apex in a sawtooth pattern at a rate of three or four cycles per second. Their swimming speed in this mode is typically reduced from 350 $\mu m \cdot s^{-1}$ to 100 or 150 $\mu m \cdot s^{-1}$. The conspicuous "sawtooth" behavior was not observed in P. punctulatum, whose swim path around a chain of Leptocylindrus danicus was a smooth, uninterrupted spiral. Oblea rotunda is distinctive because of its high velocity swimming behavior around its typically small prey. The swim path is punctuated by brief jerks or twitches, comparable to the slower sawtooth pattern of larger species but more difficult to resolve.

Capture

Precapture behavior flows directly into capture, except when the cell abandons its potential prey item and departs, returning to straight swimming. While diatoms are obviously passive, other prey may be able to escape capture. An individual O. rotunda cell was observed as it attacked quiescent Heterocapsa triquetra cells, but in each of five successive encounters, the potential food organisms distanced themselves from the predator with brief pulses of swimming, thereby evading capture.

Successful captures occur as follows. Without pausing from spiraling and sawtooth-swimming, a cell may resume straight swimming with the prey suddenly trailing behind. Clearly, a linkage was established in a fraction of a second in the form of a filament too thin to detect with a dissecting microscope. The moment of filament attachment is often signaled by particularly rapid, high frequency twitches of the predator. Unfortunately, the erratic and rapid swimming of dinoflagellates makes

observation with higher magnifications of the brief, infrequent capture event impractical. However, observations of the capture behavior of O. rotunda with dark field illumination allowed both the longitudinal flagellum and the "tow filament" to be simultaneously visible. These two thread-like appendages appear to have the same diameter of approximately 1 μm. The tow filament has also been observed during food capture in P. spinulosum, P. conicum, and Z. lenticulatum. As illustrated in Fig. 2, the emerging pseudopod appears to extend along the filament; at the same time the filament is either contracted or retracted, pulling the prey closer. Similar, previously unreported filament-assisted capture behavior has been frequently observed both in Oxyrrhis marina and Gyrodinium cf. dominans. These naked heterotrophic dinoflagellates promptly phagocytosed their filament-anchored food cells (unpublished observations).

On three occasions a filament was not observed during capture by P. spinulosum. One such instance is depicted in Fig. 1. After a minute of looping around a Chaetoceros chain, the cell halted, then rolled and pitched so that its antapex was directed toward the diatom, then extended its tongue-like pseudopod toward the diatom. It is possible that a filament was present. However, the dinoflagellate did not pull the diatom until the pseudopod had become attached, so that the existence of a primary filament attachment could not be established.

Pseudopod Deployment

In P. pellucidum, P. punctulatum, O. rotunda and Z. lenticulatum, the pseudopod appears to emerge from the sulcal pore as a narrow tongue, advancing at a rate of 2-6 μm • s^{-1}. In Z. lenticulatum, the

leading edge of the pseudopod was observed to flare as it approached its prey, broadening from a diameter of 6 μm to 12 μm (Fig. 2). This broadening can be more pronounced in P. conicum, in which a pseudopod reached 75 μm laterally as it approached a filament-tethered Corethron cell (Fig. 2c). A recently excysted cell of Protoperidinium sp. A (closely related to P. leonis) rapidly protruded a lobate pseudopod when compressed beneath a coverslip (Fig. 8). An ovoid body next to the large sac pusule was darkly stained by Lugol's iodine solution; the nature of this body is not known. Most frequently, however, the pseudopod maintains a narrow (5-10 μm) cylindrical form resembling an umbilical cord (Figs. 2 and 12) until it contacts the diatom, over which it spreads, forming a close-fitting envelope. This hyaline envelope is usually inconspicuous and can easily escape detection by an observer. The pseudopod conforms to projections such as spines, coating them in a thin sheath (Figs. 6,7,12). The long slender projections that follow and enclose spines can expand to form a continuous sheet around peripheral particles (Fig. 22). Filopodia may project from a pseudopodal envelope enclosing a spineless diatom; on spinose diatoms it is difficult to distinguish filopodia from enveloped spines. Filopodial cross bridges occasionally connect adjacent spines. As many as 58 cells from three mutually entangled chains of Chaetoceros have been simultaneously enveloped and consumed by a single cell of P. spinulosum. Several cells of P. spinulosum can attach to a single diatom, and two cells of O. rotunda have been seen attached to a single Heterocapsa cell. When the dinoflagellate is attached to the concave surface of an arched diatom chain, the pseudopod spreads out to form a rather two-dimensional sheet

in the plane of the diatom, in the fashion of a webbed foot (Fig. 22c). A radial fibrillar structure is evident in such a web, converging on the dinoflagellate's sulcal pore.

Digestion

Little conspicuous activity occurs after the pseudopod has reached its maximal extension. The dinoflagellate is often motionless, unable to swim with large diatom chains, although the transverse flagellum continues to undulate. Such cells often sink to the bottom of the observation chamber, greatly simplifying the acquisition of detailed observations with the inverted microscope. Sometimes the dinoflagellate may be able to pull a small food particle. Oblea rotunda, which often preys on flagellates smaller than itself (Fig. 3) swims rapidly throughout the digestion phase. Granular cytoplasmic streaming at a velocity of $5\mu m \cdot s^{-1}$ through the pseudopod is visible at high magnifications. Parenthetically, the observation of this streaming, traveling both proximally and distally, is enhanced by viewing video-taped sequences at increased tape speeds.

One subtle change that occurs during digestion is that of the dinoflagellate's placement relative to the prey. Whereas the diatom may have been tethered to the end of a pseudopodal 'stalk' resembling an umbilical cord 50 μm in length early in the deployment phase (Fig 12), this distance is reduced to around 20 μm at the end of deployment (Figs. 6,14). The dinoflagellate-diatom attachment point location can change during the course of feeding, as if the pseudopod stalk is drifting laterally across the envelope (Fig. 22).

Changes in the prey cytoplasm occur gradually, but are conspicuous when the end points of feeding are compared, i.e. Figs. 18-20. In one case (not illustrated) of Z. lenticulatum feeding on Stephanopyxis, no morphological change occurred in the diatom's cytoplasm for the first 50 min of feeding. Then, the evenly distributed chloroplast began to cluster, forming unpigmented regions in the diatom, and proceeded until only a few condensed globules remained in the most proximal frustules at the end of the 110 min feeding episode. The diatom cells more distant from the dinoflagellate showed less complete degradation. In contrast, very rapid initial changes were seen to occur in the cytoplasm of a cell of Ditylum brightwellii (100 μm in length) captured by P. spinulosum. Within seconds of pseudopod attachment, the diatom plasmalemma pulled away from the frustule near the point of contact with the pseudopod. After 15 s the entire diatom cytoplasm had become condensed, forming two spheres with diameters of 10 and 20 μm. No further gross changes occurred until after 7 min when the smaller sphere disintegrated into a cluster of pigmented particles, most of which vanished by the end of the 19 min feeding episode. Usually the silica frustule of diatoms maintain their original form throughout the course of feeding. However, the frustules of thin-walled diatoms such as Ditylum and Leptocylindrus may be bent and distorted within the pseudopod (Fig. 4).

In the latter part of digestion, streaming of granules toward the dinoflagellate becomes most conspicuous. The volume of the sack pusule of Z. lenticulatum in one case was reduced by half during the digestion phase. Pusular volume changes have not yet been determined for other species. At the end of feeding, diatoms have entirely lost the

refractive appearance characteristic of living cells, and only a few small residual particles remain inside the frustule (Fig 19).

With the exception of Oblea rotunda, the duration of most feeding events falls between 6 and 30 min; the 110 min event described above is exceptionally long. Oblea rotunda commonly remains attached to prey items for an hour or longer.

Retraction

This phase consists of the mass movement of the pseudopod back toward the dinoflagellate. It is the most spectacular aspect of dinoflagellate feeding, since the pseudopod flows inward from all directions at a rate of 10 $\mu m \cdot s^{-1}$. The membranous material accumulates at the flagellar pore (a bottleneck, with its diameter of only 2 or 3 μm) and forms a pulsating mass at the antapex of the dinoflagellate (Fig. 9,17). A retraction sequence of P. spinulosum on Chaetoceros curvetus is illustrated in Figs. 14-17. Note the manner in which the pseudopod becomes taut as tension is applied, evidently from the sulcal origin of the pseudopod. In one case, the retracted pseudopodal mass of P. spinulosum occupied a volume of 5000 μm^3 or nearly 20% of the non-pusular volume of the cell. This mass took 5 min to completely reenter the theca.

DISCUSSION

Thecate heterotrophic dinoflagellates in three genera (Oblea, Zygabikodinium, and Protoperidinium) appear, from our observations, to be

unified by their feeding behavior, sharing similar precapture behavioral patterns, capture mechanisms (involving the use of a previously unreported filament) and pseudopod deployment and digestion techniques. The capture filament, only briefly manifested, may well be a genus-wide characteristic. The 4 species (out of 19 encountered) in which this filament has been detected are also the species whose feeding behavior has been most extensively observed. The manner in which the pseudopod tightly fits the prey organism, and the close proximity of the dinoflagellate to its food (so that the pseudopodal attachment is hidden) conspire to make feeding behavior inconspicuous, and helps explain why this phenomenon has for so long been unknown.

The pseudopod structures described above are clearly similar to those reported by Gaines and Taylor (1984). They observed P. depressum as it deployed a disc-shaped pseudopodal sheet that spread broadly to form a circular "feeding veil". One edge of the veil made contact with a diatom which was drawn close to the dinoflagellate when the veil was retracted, somewhat like the entrapment of fish within a purse seine. Our interpretation of their observations is that of a pseudopod spreading evenly across the glass slide upon which the dinoflagellate had settled. The appearance of a veil covering a large area lacking diatoms may be due to the proximity of the smooth, flat surface of the glass slide, and may not have formed had the cell been suspended in water. In only one case (involving P. conicum) out of the dozens of captures observed (none of which occurred against a glass surface) was the pseudopod laterally expanded prior to diatom engulfment. In other capture events involving P. conicum, as well as O. rotunda, Z. lenticulatum, P. spinulosum and P.

punctulatum, the emerging pseudopod held the form of a narrow cylinder, spreading laterally only after contact was made with the prey. The presence of a capture filament helps explain how the pseudopod is directed towards its target. We have not yet observed capture behavior in P. depressum (the species described with a feeding veil by Gaines and Taylor, 1984) but in cells observed in the process of feeding, the pseudopod appeared as a close-fitting envelope, as is the case for the other species we have observed.

The search and capture behavior described above shows that swimming thecate heterotrophic dinoflagellates, which persistently spiral tightly around potential prey items before effecting their capture, are not nonspecific predators using a broad net mechanism to obtain food randomly. Rather, they actively select a particular prey item, anchor themselves to this particle with a filament, and then deploy their pseudopod.

The sudden contraction of the cytoplasm of a captured diatom occurring after pseudopodal attachment as described earlier for Ditylum is very similar to a phenomenon described by Drebes and Schnepf (1982) occurring during the peduncular feeding of the naked dinoflagellate Paulsenella sp. upon the diatom Steptotheca. This phenomenon very likely reveals the rapid release of an enzyme from the pseudopod or peduncle or an associated sudden pH shift that can alter the permeability of the diatom membranes.

The pseudopodal feeding mechanism of thecate heterotrophic dinoflagellates has been described as "extra-cellular digestion" (Gaines and Taylor, 1984). Strictly speaking, if the pseudopod membrane is able

to surround a prey item completely, digestion is intra-cellular since it occurs within a feeding vacuole, albeit a vacuole outside the theca. If the pseudopod can engulf only a portion of an elongate prey, digestion occurs in an extra-cellular (that is, not entirely membrane-contained) manner. The distinctions between "extra-cellular", "intra-cellular", and phagotrophic feeding are in this case rather artificial.

Large, colonial diatoms are currently believed to be grazed only by organisms at least the size of copepods, while microzooplankters such as oligotrich ciliates are thought to be limited to small, often flagellated phytoplankters. This study helps to establish a new trophic link within the marine planktonic food web, that is, the grazing of thecate heterotrophic dinoflagellates upon large diatoms.

Pseudopodia are not new to flagellates. Amoeboflagellates are heterotrophs akin to "true" amoebae, except for a brief flagellated stage prior to encystment (Schuster, 1963). A number of photosynthetic chrysophytes (Rhizochrysis, Chrysamoeba, Rhizochromulina) and a xanthophyte (Rhizochloris) apparently have flagellate/amoeboid alternation life cycles, the persistent amoeboid form displaying radiating filopodia (Hibberd & Chretiennot-Dinet, 1979). In Chrysamoeba alone is the amoeboid stage flagellated, but the flagellum does not contribute to cell motility (Hibberd, 1971). Small, bactivorous monads are certainly phagotrophic, and diminutive pseudopodia have been described in Cercomonas (Mignot and Brugerolle, 1975). This brief survey suggests that the thecate heterotrophic dinoflagellate pseudopod is unlike that of any flagellate yet described. The pseudopod is manifest in flagellated, vegetative, motile cells, and is certainly more elaborate

that those observed in other flagellates.

Pseudopodal structures as elaborate as those described here are found in foraminiferans and radiolarians. Filopodia are conspicuous in these "rhizopoda", and are often elaborated into anastomosing reticulopodial networks (Leidy, 1879; Anderson, 1983). The pseudopodia of thecate heterotrophic dinoflagellates do form filopodia but they are few in number. Occasionally they can converge and fuse to form lamellipodia in a manner similar to that of reticulopodia. However, a comparison of the details of food engulfment as revealed by transmission electron microscopy accentuates the unique nature of this pseudopod. In radiolaria, Anderson (1983) has described how reticulopodia that contact food develop thickened, microfilament-rich "coelopods" that envelop and forcibly rupture the prey exoskeleton. This allows pseudopods to gain access to the internal tissue of such prey as copepods. In foraminiferans, Anderson and Bé (1976) reveal reticulopodia that surround food such as copepods and secrete an adhesive substance to anchor the prey item in place. Reticulopodia find their way within the exoskeleton and transport bits of tissue and oil droplets to the large cell aperture and on into the endoplasm. In contrast, thin sections through a feeding dinoflagellate cell (unpublished data) show that the transparent envelope surrounding the diatom food is composed merely of empty membrane vesicles within a continuous membrane sheath (Fig. 13). This delicate structure apparently cannot rupture a diatom frustule. Instead, degenerative enzymes presumably diffuse through the diatom pores to liquify the prey cytoplasm, which then diffuses out through the pores, leaving the silica frustule intact. This situation is reminiscent of arachnid feeding, in

which the contents of captured arthropods are liquified and ingested, leaving an empty exoskeleton.

The uniqueness of the thecate heterotrophic dinoflagellate pseudopod leads us to propose a new term, "pallium", Latin for the sheet-like garment worn in ancient Greece. This term emphasizes the manner in which the membranous pseudopod envelops food particles.

Further analysis of the pallium and comparisons with different protists requires completion of ultrastructural/cytochemical work. The organization of the pallium, especially in regard to microtubules, and the spatial relationships between the internal manifestations of the pallium, the sac and collecting pusules, and the two flagella, all of which are associated with the flagellar pore, will be of particular interest.

The observation of size changes of the sac pusule in Z. lenticulatum suggests that this organelle may play a role in feeding. The sac pusule, the larger of two, is most conspicuous in thecate heterotrophic dinoflagellates (Kofoid, 1909), much less so in naked heterotrophic and most photosynthetic dinoflagellates. In some heterotrophs the sac pusule can occupy as much as half of the cell volume, yet it appears to contain only seawater. The pusules, despite much attention and imagination, are still in want of a proven function. One of the most convincing hypotheses is one of excretion or osmoregulation (Dodge, 1972) but uptake of dissolved substances (Kofoid and Swezy, 1921) and buoyancy (Norris, 1966) have also been proposed. The streaming of cytoplasm out of and into the theca through the flagellar pore during feeding suggests a different function for the sac pusule, that of volume regulation. One

might expect its volume to increase upon deployment of the pallium or its volume to decrease during import of food materials and pallium retraction. Indeed, a decrease in sac pusular volume of approximately 50% has been observed during digestion in a cell of Z. lenticulatum, as noted above. Further work is needed to test this hypothesis; considerable care must be taken to avoid artifacts because of the sensitivity of the pusule to stresses associated with microscopic observation.

The description made by Bursa (1961) of a Protoperidinium sp. ingesting a flagellate, which is illustrated by a drawing, matches the appearance of a cell retracting its pallium. The drawing shows irregular protrusions that radiate from a mass at the sulcus, which we reinterpret to be its pallium. Drawings by Schütt (1895) which depict cells of Podolampus bipes and Blepharocysta splendor-maris with pseudopodal extensions protruding through the flagellar pore lead us to suggest that the pallium may be present in these tropical dinoflagellates as well. Indeed, such a phenomenon was again observed by Steidinger et al. (1967) in Blepharocysta splendor-maris.

The 19 predator species listed in Table 1 have widely differing numbers of prey species; as mentioned before, this is primarily an artifact of the number of observations. At this time little can be said of selection among diatom species; prey species tend to be amongst the most abundant diatoms at the time of capture. However, a clear pattern emerges with regard to diatoms vs. non-diatom species. Generally speaking, Protoperidinium species graze exclusively on diatoms, while the two diplopsaloid species (O. rotunda and Z. lenticulatum) also take

dinoflagellates, and in the case of Oblea, prasinophytes as food. While this hypothesis holds true, so far, for 14 species of Protoperidinium, two other species, P. pyriforme and Protoperidinium sp. B may feed on dinoflagellates. It is interesting that while P. pyriforme frequently fed on Protogonyaulax (=Gonyaulax) tamarensis, this toxic species was not preyed upon by O. rotunda even when offered as its sole food. O. rotunda will consume other dinoflagellates of similar size.

The fact that O. rotunda and Z. lenticulatum and perhaps other species can capture and feed upon detrital "marine snow" type particles show that bacterial consumption undoubtedly occurs. Consumption of diatoms alone would also result in assimilation of bacterial carbon, as well as other commensal organisms living on or near diatoms. The intensity of bactivory among thecate heterotrophic dinoflagellates is not clear, and may be most significant in diatom-poor regions. This may explain uptake of labeled bacterial carbon by thecate heterotrophic dinoflagellates observed by Lessard (1985).

Although thecate heterotrophic dinoflagellates are delicate, fastidious organisms that reveal their secrets only after prolonged coaxing, much has been learned of them. In summary, three genera have been found to share the pallium feeding system, including the use of a filament to initially secure their prey. Swimming behavior prior to capture indicates that the predators are potentially selective grazers. Indeed, while the genus Protoperidinium restricts its diet almost entirely to diatoms, two diplopsaloid species also prey upon dinoflagellates and prasinophytes, as well as bacteria-colonized detrital particles.

Much remains to be discovered of the ultrastructure, chemosensory abilities, diel feeding patterns and trophic rates of these remarkable microzooplankters.

ACKNOWLEDGEMENTS

We thank S. Watson for the use of high resolution video equipment and O. R. Anderson for helpful discussions. This research was supported in part by a National Science Foundation doctoral fellowship (to DMJ), by the Education Program and the Coastal Research Center at the Woods Hole Oceanographic Institution, and by National Science Foundation grant OCE-8400292 (to DMA). Contribution number 6044 from the Woods Hole Oceanographic Institution.

REFERENCES

Abé, T. H. 1981. Studies on the family Peridinidae. An unfinished monograph of the armored dinoflagellata. SETO Mar. Biol. Spec. Publ. 6:1-413.

Anderson, O. R. 1983. Radiolaria. Springer-Verlag, New York, 355 pp.

Anderson, O. R. & Bé, A. W. H. 1976. A cytochemical fine structure study of phagotrophy in a planktonic foraminifer, Hastigerina pelagica (d'Orbigny). Biol. Bull. 151:437-449.

Bursa, A. S. 1961. The annual oceanographic cycle at Igloolik in the Canadian Arctic. II. The phytoplankton. J. Fish. Res. Board. Can. 18:563-615.

Dodge, J. D. 1972. The ultrastructure of the dinoflagellate pusule: a unique osmoregulatory organelle. Protoplasma 75:285-302.

Drebes, G. & Schnepf, E. 1982. Phagotrophy and development of Paulsenella cf. chaetoceros (Dinophyta), an ectoparasite of the diatom Streptotheca thamesis. Helgolander Meeresunters. 35:501-515.

Gaines, G. & Taylor, F. J. R. 1984. Extracellular digestion in marine dinoflagellates. J. Plank. Res. 6:1057-1061.

Hibberd, D. J. 1971. Observations on the cytology and ultrastructure of Chrysamoeba radians Kleb (Chrysophyceae). Br. Phycol. J. 6:207-223.

Hibberd, D. J. & Chretiennot-Dinet, M. J. 1979. The ultrastructure and taxonomy of Rhizochromulina marina gen. et sp. nov., an amoeboid marine chrysophyte. J. Mar. Biol. Assoc. U. K. 59:179-193.

Kofoid, C. A. 1909. On Peridinium steinii Jorgensen, with a note on the nomenclature of the skeleton of the Peridinidae. Arch. Protistenk. 16:25-47.

Kofoid, C. A. & Swezy, O. 1921. The free living unarmored Dinoflagellata. Mem. Univ. Calif. 5:1-562.

Leidy, J. 1879. Freshwater rhizopoda of North America. Rep. U.S. Geol. Surv. 12:1-324.

Lessard, E. J. & Swift, E. 1985. Species-specific grazing rates of heterotrophic dinoflagellates in oceanic waters, measured with a dual-label radioisotope technique. Mar. Biol. (Berl.) 87:289-296.

Mignot, J. P. & Brugerolle, G. 1975. Etude ultrastructurale de Cercomonas Dujardin (=Cercobodo Krassilstchick), protiste flagelle. Protistologica 11:547-554.

Morey-Gaines, G. & Elbrachter, M. 1987. Heterotrophy in dinoflagellates. In Taylor, F. J. R. [Ed.] The Biology of Dinoflagellates. Blackwell Scientific, Oxford.

Norris, R. E. 1966. Unarmoured marine dinoflagellates. Endeavour (Oxf.) 35:124-128.

Schuster, F. 1963. An electron microscope study of the amoebo-flagellate Naegleria gruberi (Schardinge). I. The amoeboid and flagellate stages. J. Protozool. 10:297-313.

Schütt, F. 1895. Die Peridineen der Plankton-Expedition. Lipsius and Tischer, Kiel, 170 pp.

Steidinger, K. A., Davis, J. T. & Williams, J. 1967. A key to the marine dinoflagellate genera of the west coast of Florida. Fla. Bd. Conserv. Mar. Lab., Tech. Ser. 52:1-45.

TABLE 1. Predator/ prey relationships in thecate heterotrophic dinoflagellates.

Predator species	Size[a]	Food species	size[a]	type[b]
Oblea rotunda	30	Pyramimonas sp. (13-10)	10	pras
		Micromonas sp. (DW8)	8	pras
		Heterocapsa triquetra	30	dino
		Prorocentrum minimum	25	dino
		Dinophysis acuminata	40	dino
		Gonyaulax tricantha	35	dino
		Protoperidinium pellucidum	45	dino
		Oblea rotunda	30	dino
		Nitzchia closterium	30	s.d.
		Amphiprora sp.	20	s.d.
		Ditylum brightwellii	80	s.d.
		Leptocylindrus danicus		c.d.
		Eucampia zoodiacus		c.d.
		colorless detrital particle	50	
Zygabikodinium lenticulatum	50	Prorocentrum scutellum	30	dino
		Heterocapsa triquetra	30	dino
		Coscinodiscus sp.	60	s.d.
		Amphiprora sp.	120	s.d.
		Ditylum brightwellii	80	s.d.
		Nitzchia sp.	35	s.d.
		Licmophora sp.	40	s.d.
		Chaetoceros sp.		c.d.
		Thalassiosira sp.		c.d.
		Guinardia flaccida		c.d.
		colorless detrital particle	40	
Protoperidinium spinulosum	45	Chaetoceros affinis		c.d.
		C. curvetus		c.d.
		Leptocylindrus danicus		c.d.
		Skeletonema costatum		c.d.
		Eucampia zoodiacus		c.d.
P. pellucidum	45	Licmophora sp.	40	s.d.
		Thalassiosira sp.		c.d.
		Asterionella japonica		c.d.
		Leptocylindrus danicus		c.d.
		Chaetoceros sp.		c.d.
P. conicum	55	Corethron hystrix	35	s.d.
		Thalassiosira sp.		c.d.
		Chaetoceros sp.		c.d.
		Lithodesmium sp.		c.d.
P. cf. hirobis	25	Leptocylindrus danicus		c.d.
		Skeletonema costatum		c.d.

Predator species	Size[a]	Food species	size[a]	type[b]
P. punctulatum	55	Rhizosolenia sp.	200	s.d.
		Leptocylindrus danicus		c.d.
P. curtipes	60	Ditylum brightwellii	80	s.d.
P. achromaticum	35	Leptocylindrus danicus		c.d.
P. minutum	40	Licmophora sp.	40	s.d.
		Guinardia flaccida		c.d.
		Chaetoceros sp.		c.d.
P. pentagonum	50	Lauderia sp.		c.d.
P. excentricum	60	Ditylum brightwellii	80	s.d.
		Coscinodiscus sp.	50	s.d.
P. claudicans	60	Chaetoceros curvetus		c.d.
P. quarnerense	40	Thalassiosira sp.		c.d.
P. oblongum	60	Chaetoceros sp.		c.d.
P. pyriforme	40	Protogonyaulax tamarensis	40	dino
		Heterocapsa triquetra	35	dino
		Scrippsiella sp.	40	dino
		Nitzchia sp.	30	s.d.
P. depressum	120	Thalassiosira sp.		c.d.
Protoperidinium sp. A	50	Chaetoceros sp.		c.d.
Protoperidinium sp. B	30	Oblea like cell	17	

[a] Diameters in µm.

[b] pras.=prasinophyte; dino.=dinoflagellate; s.d.=solitary diatom; c.d.= colonial diatom, with lengths ranging from 100-400µm.

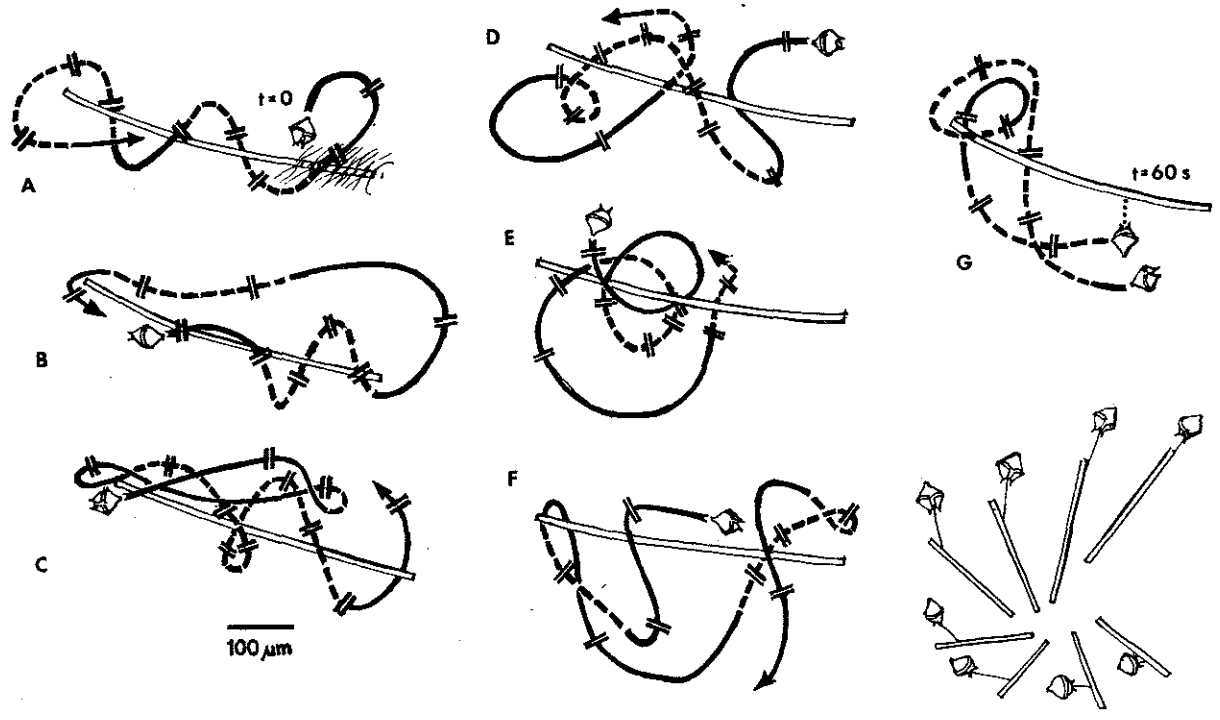

Fig. 1. Sequence of 60 s duration showing swim path of Protoperidinium spinulosum immediately prior to capture of Chaetoceros chain. Frame A depicts portion of diatom spines. Dashes signify one second intervals. Each frame commences at dinoflagellate symbol (drawn to scale) and concludes with arrow. Dashed lines indicate sawtooth swimming behavior (see text for details). Frame G indicates location of pseudopod attachment. Last frame shows dinoflagellate with slender pseudopodal attachment slowly pulling (foreshortened) diatom.

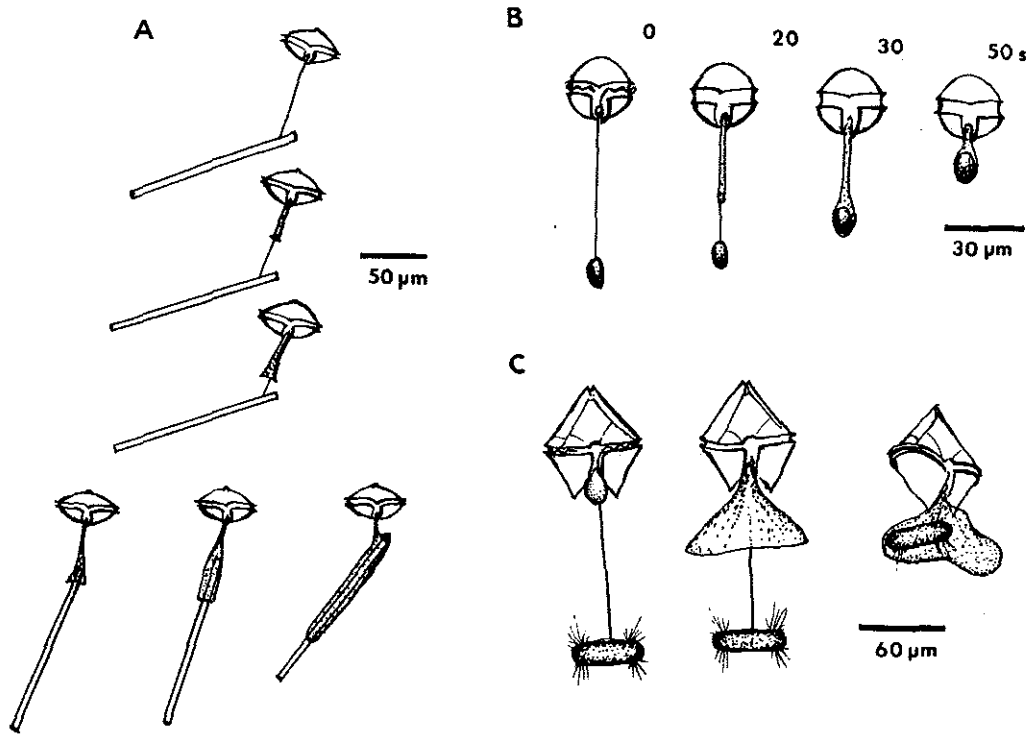

Fig. 2. Psuedopod deployment in thecate heterotrophic dinoflagellates.

A. Sequence of approx. 3 min duration showing pseudopod deployment of Zygabikodinium lenticulatum feeding upon Leptocylindrus danicus. Note primary attachment filament.

B. Similar sequence of Oblea rotunda feeding on Pyramimonas sp., with times given.

C. Protoperidinium conicum feeding on Corethron hystrix. Note broadness of emerging pallium.

Figs. 3-12. Light micrographs of pseudopodal feeding in thecate heterotrophic dinoflagellates. Scale bars = 25 μm.

Fig. 3. Zygabikodinium lenticulatum feeding on Ditylum brightwellii showing normal appearance of diatom cytoplasm.

Fig. 4. D. brightwellii enveloped by pallium of Z. lenticulatum; the diatom has sustained frustular distortion and cytoplasmic degradation.

Fig. 5. Z. lenticulatum attached to Chaetoceros sp. (chain of 4 cells). Edge of frustule, within pallium, shown by arrow.

Fig. 6. Protoperidinium pellucidum feeding on Chaetoceros sp.. Note stalk-like attachment of pallium (arrow).

Fig. 7. Same cell as before; P. pellucidum cell is above focal plane. Note cytoplasmic sheaths surrounding diatom spines (arrow).

Fig. 8. Protoperidinium sp. A, recently excysted cell, with pallium (see text).

Fig. 9. P. pellucidum, cell depicted in Figs. 6 and 7, after pallium retraction, with accumulation of pseudopod material at sulcus.

Fig. 10. P. pellucidum enveloping Licmophora sp. and slender pennate diatom.

Fig. 11. P. pyriforme feeding on Protogonyaulax tamarensis (pseudopod not conspicuous).

Fig. 12. Oblea rotunda with recently captured temporary cyst of Heterocapsa triquetra.

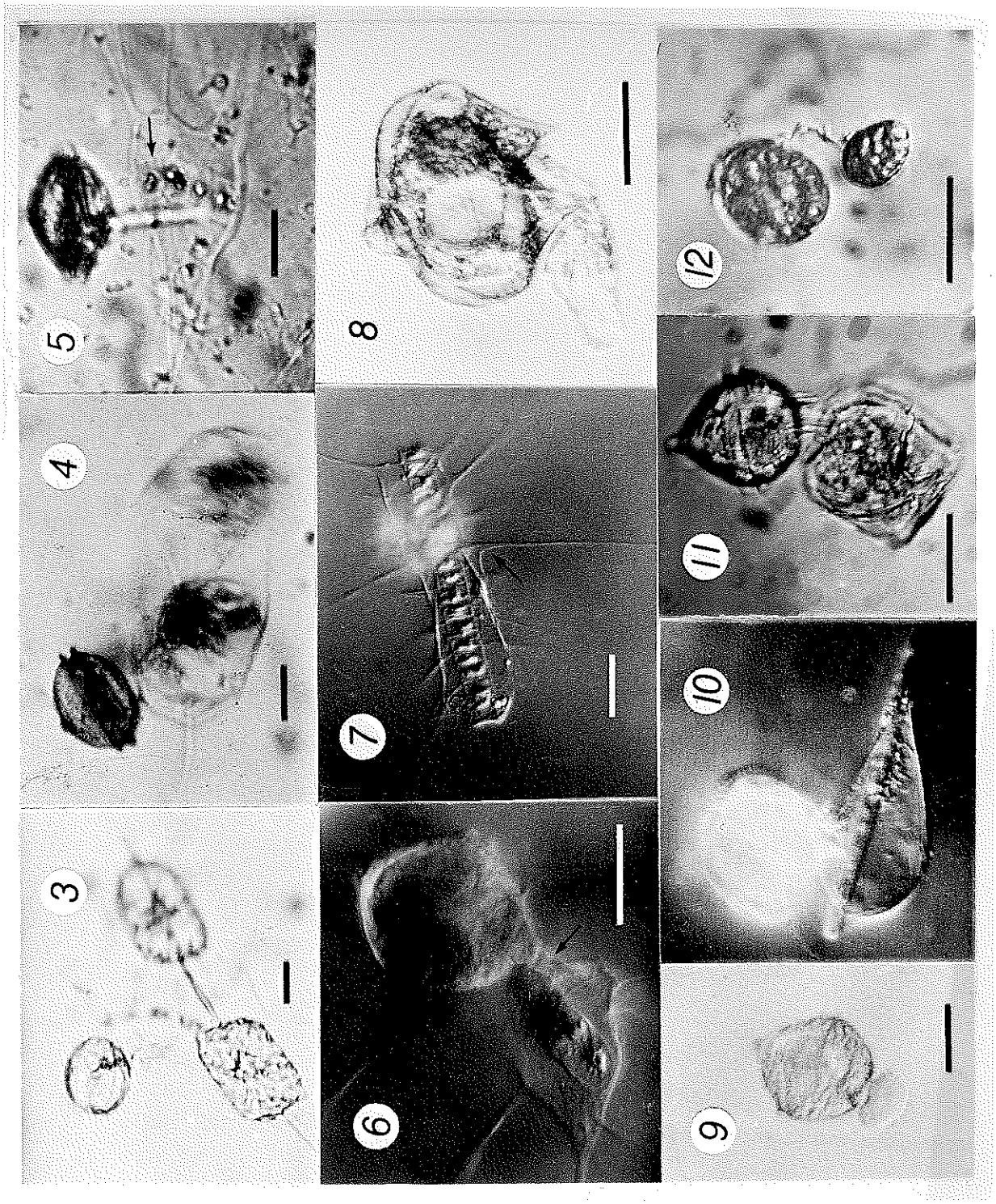
5
8
12
4
7
11
3
6
10
9

Figs. 13-21. Pseudopodal feeding in thecate heterotrophic dinoflagellates, cont'd. Scale bar of Fig. 13 = 5 μm; all others = 25 μm.

Fig. 13 Transmission electron micrograph of longitudinal section through Protoperidinium spinulosum feeding on Eucampia zoodiacus with pallium fitting through flagellar pore. Corners of two frustules visible (arrow).

Figs. 14-17. Video sequence of pseudopod retraction in P. spinulosum feeding on Chaetoceros curvetus. T=0, 8, 12, 20s respectively. While the pallium seems to be spreading, the concave edge (arrow) is actually being pulled taut. Note radial structure and accumulation of pseudopod material at antapex of cell. In Figure 17, moments before departure of cell, the edge of the pseudopod mass appears as a crescent-shaped highlight (arrow).

Fig. 18. Zygabikodinium lenticulatum engulfing Stephanopyxis turris with hyaline envelope (arrow). Dinoflagellate cytoplasm clouded by Bouins fixation.

Fig. 19. S. turris after digestion. Pallium membrane still attached (arrow) as Z. lenticulatum was accidentally detached from diatom during fixation. Note "folded" arrangement of four diatom frustules.

Fig. 20. Normal appearance of S. turris. Fig. 21. P. conicum feeding on Chaetoceros sp.. Compare appearance of of diatom cytoplasm within and beyond pallium (arrow). Chaetoceros spines to the right of the arrow lack cytoplasmic sheaths and are not, therefore, visible.

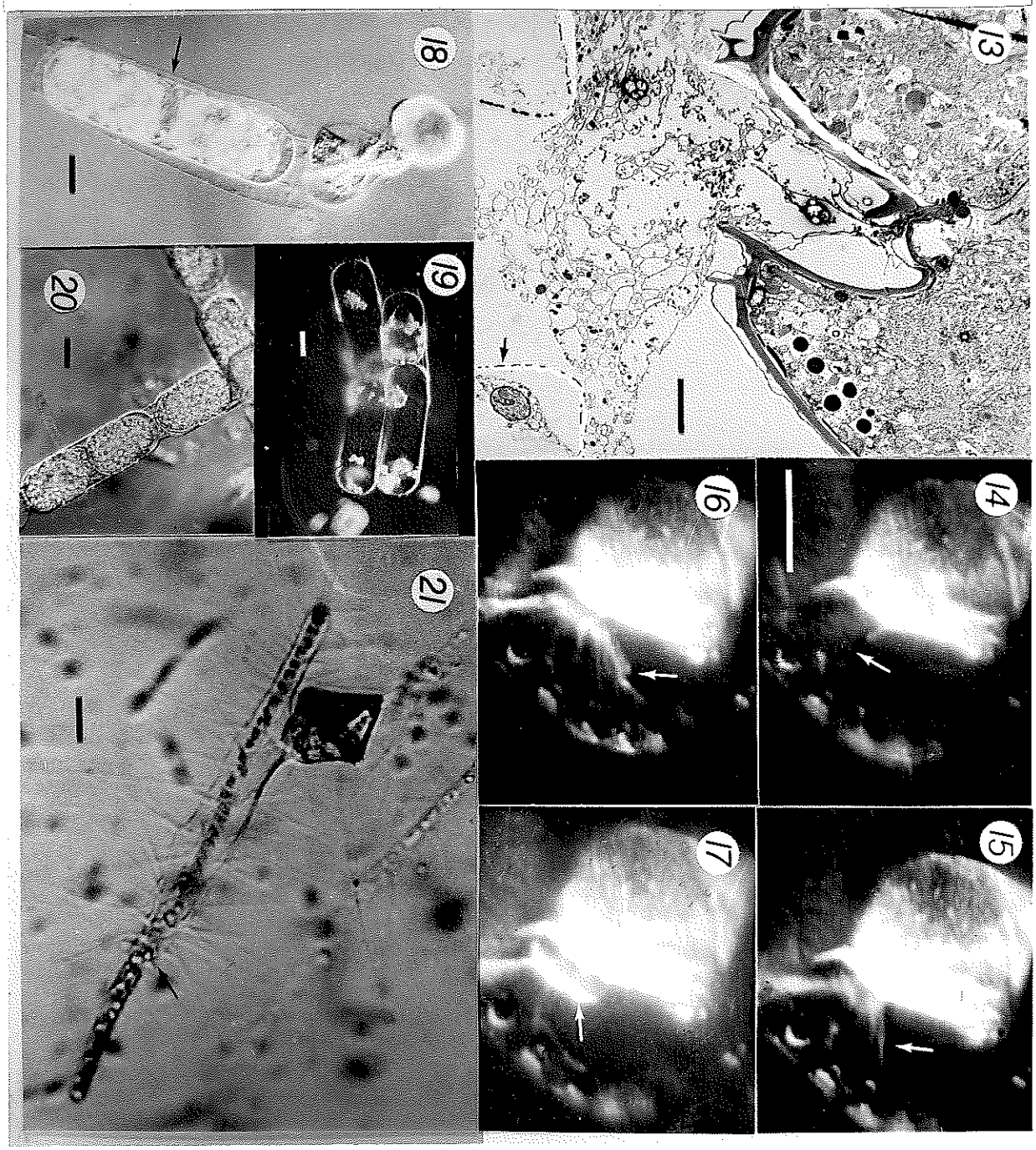
13
14
15
16
17
18
19
20
21

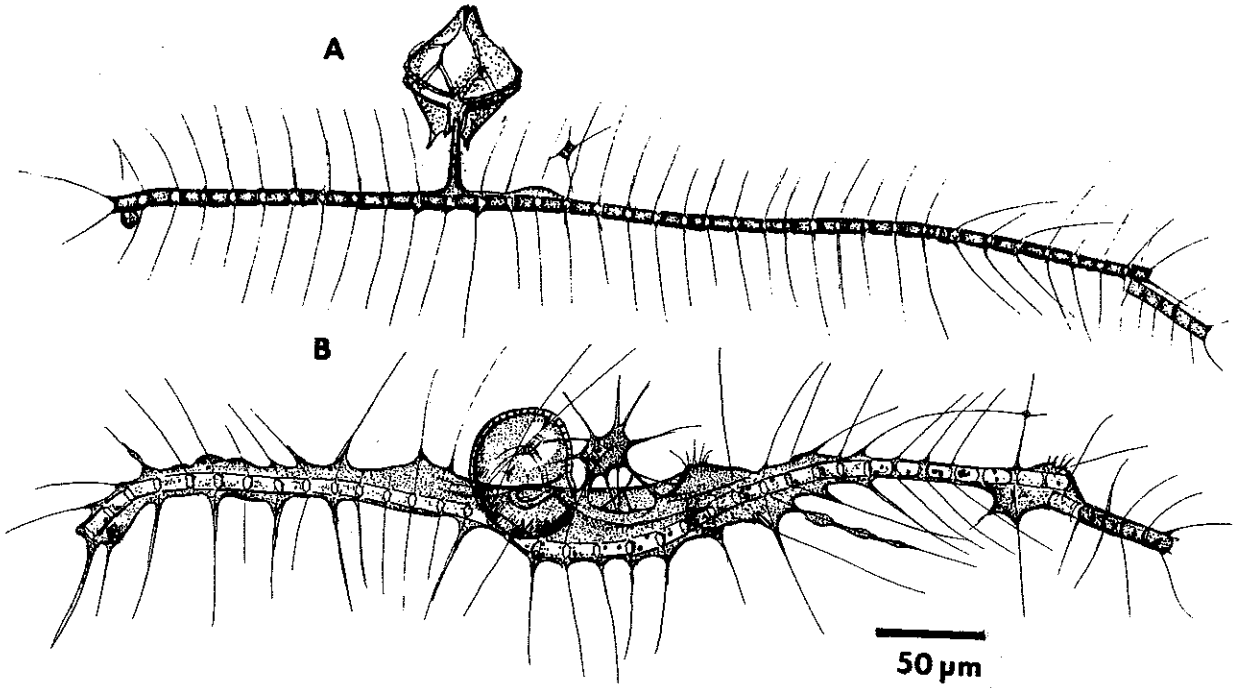

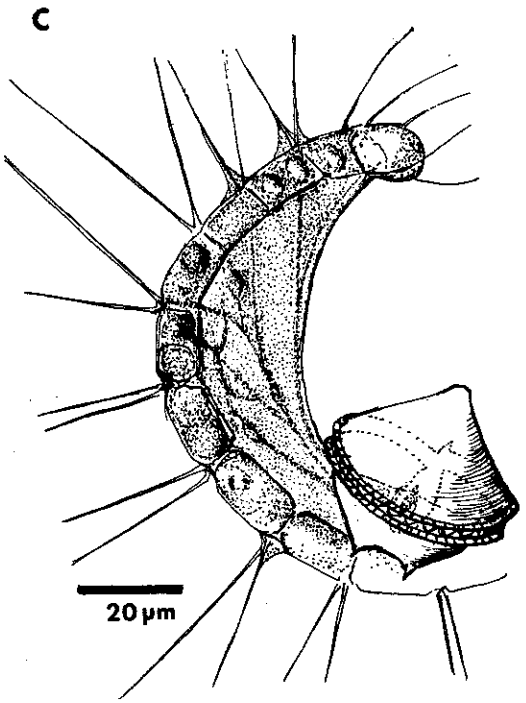

Fig. 22. Protoperidinium spinulosum feeding on Chaetoceros sp. as drawn from video recording. A. Soon after capture, early in deployment phase.
B. Approx. 15 min later; note formation of lamellipod surrounding 2-cell diatom to right of dinoflagellate.
C. Another P. spinulosum cell feeding on Chaetoceros curvetus, illustrating radial fibrillar structure within web-like pallium.

CHAPTER 3

Growth and Grazing Rates of *Protoperidinium hirobis* Abé, a Thecate Heterotrophic Dinoflagellate

Abstract

Growth and feeding rates of a small thecate heterotrophic dinoflagellate, Protoperidinium hirobis Abé, grown on the diatom Leptocylindrus danicus, were measured in batch cultures. Ingestion rates were determined directly by the enumeration of empty diatom frustules produced by dinoflagellate feeding. Both growth and feeding rates saturated at diatom concentrations of approximately 10^4 cells•ml^{-1}, and reached maximum values of 1.7 divisions•day^{-1} and 23 diatoms•$grazer^{-1}$•day^{-1}, respectively. This rate of cell division is notably high for dinoflagellates, which seldom grow faster than one division per day. Inferred feeding durations ranged from 43 min. to 1 h. Timing of cell division and grazing rate patterns were also examined; while mitosis occurred chiefly during the dark period, no diel variations in feeding rate were detected. These rates, the first direct growth and ingestion measurements to be made for a thecate heterotrophic dinoflagellate, serve to underscore the potential importance of a function these dinoflagellates perform within the microzooplanktonic food web: that of transforming the substance of large diatoms into particles more easily ingested by microzooplankters.

INTRODUCTION

Until recently, the nature of feeding in thecate heterotrophic dinoflagellates was unknown. Now it is clear that a pseudopodal mechanism is employed by Protoperidinium species and others to feed on phytoplankton, especially on the diatoms (Gaines and Taylor 1984, Jacobson and Anderson 1986). The only pertinent data on feeding rates in these organisms are that of Lessard and Swift (1985) who used a single-cell isolation radioisotope technique to measure feeding rates of field-captured thecate heterotrophic dinoflagellates. They reported rather high "clearance" rates with most species assimilating ^{14}C-labelled material (i.e., algae), while a few species incorporated ^{3}H-thymidine-labelled material (i.e., bacteria). Such data are useful, but there is a clear need for direct measurements of ingestion rates by techniques which are not subject to carbon recycling or other uncertainties associated with mixed assemblages. There is also a need to examine the growth rate of these microheterotrophs when supplied with different food concentrations. To these ends, this chapter reports the direct, simultaneous measurement of feeding and growth in one of the first thecate heterotrophic dinoflagellate species to be successfully maintained in culture.

METHODS and MATERIALS

Culture Conditions and Organism

Protoperidinium hirobis Abé was isolated by DMJ from Vineyard Sound, Massachusetts (31‰ salinity). This unialgal but non-clonal strain is identical to the original description of P. hirobis in all but one respect: the two antapical spines are consistently 40% shorter in length than reported by Abé (1936)(Fig. 1). Small cells with diameters ranging from 11 to 15 μm (compared to a normal mean diameter of 23 μm) (Fig. 1) appeared in cultures but never exceeded 10% of the population. P. hirobis was fed the diatom Leptocylindrus danicus (also isolated by DMJ from Vineyard Sound) and cultured in completely full, capped 16 ml polypropylene centrifuge tubes, which were rotated end-over-end on a "ferris wheel" apparatus. The dinoflagellates were maintained by diluting aliquots of dinoflagellates and diatoms into fresh f/2 media (Guillard and Ryther, 1976). Additional diatoms were added when cultures became food-depleted. All culturing and experiments were carried out in the same incubator (20°C, L:D 14:10 at approx. 100 $\mu E \cdot m^{-2} \cdot s^{-1}$).

Ingestion Rates

Ingestion data were derived from the enumeration of empty diatom frustules created by dinoflagellate pseudopodal feeding. With unconventional optics (i.e. an off-centered bright-field stage condenser) both the thin silica frustule walls and a small characteristic golden-brown residual particle constituting the remains of the diatom cytoplasm within the nearly empty frustule are visible at low

magnifications. (The cylindrical frustules are inconspicuous under bright field illumination, and although the frustule wall is well defined under phase optics, the color of the residual particle is less distinct.) The golden-brown residue was never seen in non-grazed diatom cultures, even when lysed, deteriorating cells were present; therefore the identification of grazed frustules was unambiguous. Ingestion rates (I) were calculated as follows:

$$I = \frac{f_t - f_o}{\bar{X} \cdot t}$$

where f_t and f_o are final and initial frustule concentrations, respectively, t is the time interval, and $\bar{X}$ is the average grazer concentration during this time interval. Average number of grazers (i.e. dinoflagellates) was estimated according to Heinbokel (1976) as follows:

$$\bar{X} = \frac{d_1 - d_0}{[\ln(d_1) - \ln(d_0)]}$$

where d_1 and d_0 are the final and initial dinoflagellate concentrations, respectively. Clearance rates were calculated by dividing ingestion rate by food concentration.

Experimental Protocol

Two consecutive experiments (hereafter termed grazing/growth experiments) were performed using dinoflagellate/diatom suspensions in order to simultaneously measure both the rate of grazing and growth as a function of food concentration. A series of equivalent dinoflagellate innocula was exposed to seven food densities (with targeted levels of 100, 500, 1000, 2000, 3000, 6000 and 10000 diatom cells$\cdot ml^{-1}$) in 32ml

polycarbonate centrifuge tubes; each treatment was performed in triplicate. For unknown but convenient reasons, the strain of L. danicus used grew as single or double cells, ranging in length from 30 to 60 µm, instead of in their usual colonial configuration, which can stretch hundreds of micrometers in length. These standardized food dimensions simplified the interpretation of the grazing data. The stock culture of dinoflagellates and their food was allowed to stand in a graduated cylinder for several hours in order to minimize the inclusion of diatoms and empty diatom frustules when the culture was used as an innoculum. In the first of two experiments, an initial dinoflagellate concentration of 100 cells•ml^{-1} was used, but this resulted in rapid depletion of the diatom standing crop, making data interpretation difficult; therefore complete frustule counts were not made, and the experiment was repeated using an initial dinoflagellate concentration of 25 cells•l^{-1}. Replicate samples of dinoflagellate innocula were preserved for enumeration of initial empty frustules, and replicate diatom control suspensions (i.e., without dinoflagellates) of 3000 cells•ml^{-1} were similarly sampled. After 24 hours the three lowest diatom treatments had become diatom-depleted, and additional diatoms were introduced to restore the target concentration. The food concentrations in the high diatom treatments (>3000 cells•ml^{-1}), however, had increased; neutral density screens were attached to these tubes in order to limit diatom growth. It seems reasonable to assume that grazing rates would be influenced to a greater extent by food concentration than by light intensity, an assumption which is supported by a diel experiment (see below). Tubes were sampled once every 24 hours for three days. The

sampling procedure involved gently pouring the media back and forth between two small beakers, followed by the transfer of a 2 ml aliquot to a vial holding 100µl Lugol's iodine solution. The colorless dinoflagellates were rendered more conspicuous by the iodine stain, but the color characteristics of grazed diatoms were not affected. Samples were subsequently transferred to settling slides and enumerated on a Zeiss inverted microscope. The entire sample was examined for dinoflagellates and empty frustules, except when frustule density was excessively high, whereupon random fields were examined at 400x until over 200 frustules had been encountered. Diatom growth during the experiment is indicated by horizontal error bars around growth and grazing rate data points. Grazing rate calculations were based on the first 48 hours of the experiment, while growth rates were based on the full 72 hour period.

Diel Time Course experiment

A second experimental protocol was designed to examine growth and feeding on a diel cycle under conditions of optimal food abundance. This time course experiment consisted of taking 2 ml samples from a single 300 ml centrifuge tube (with approximate densities of 300 dinoflagellates$\cdot ml^{-1}$ and 10^4diatoms$\cdot ml^{-1}$.) every 3 hours over a 30 hour period. Aliquots were fixed with formalin (3%) and stained with 4,6-Diamidino-2-phenylindole (DAPI: Sigma Chemical Co.) at a final concentration of 10µg$\cdot ml^{-1}$ for 30 minutes without washing and observed with Zeiss filter #487702 in order to enumerate dividing nuclei. Since doublet cells (i.e., daughter cells having completed cytokinesis but still attached) were most easily detected when viewed

with another fluorescence filter set (#487706) in which the unstained cytoplasm of P. hirobis auto-fluoresced intensely green, the samples were counted twice, first for dividing nuclei and again for doublet cells and total cell number. A drawing of a cell undergoing karyokinesis is shown in Fig. 1c: note the oblong, obliquely oriented nucleus. The time course of total cell number was used to compute the instantaneous specific cell division rate as a function of time. The following equation was used with 2 h time steps to obtain a finite-difference approximation of μ (h^{-1}), according to Nelson and Brand (1979):

$$\mu_t = \frac{N_{t+2h} - N_{t-2h}}{4\ N_t}$$

where N_t is the dinoflagellate abundance at sampling time t and N_{t-2h} and N_{t+2h} are the dinoflagellate abundances of the immediately preceding and immediately following sampling times, respectively. Ingestion rates were determined as for the previous experiment. The frequency of feeding cells as a function of time was also measured. Because all fixatives tested failed to quantitatively preserve the dinoflagellate-diatom connection of feeding cells intact, a live count technique was employed, as follows: 100 to 200µl samples were transferred in a series of drops onto the surface of a small sheet of plexiglass and examined under a dissecting microscope. This volume was chosen because the number of dinoflagellates per drop had to be limited to 5-10 (depending on dinoflagellate density) due to the rapid swimming speed of the cells. All counts were made within the experimental incubator; a red filter was utilized during the dark phase. Between 50 and 100 cells were examined for each calculation of feeding frequency.

Cell size was determined using an occular micrometer. Duration of feeding was determined by transferring cells that had just initiated feeding to 2 ml depression wells, where they were monitored once every 5 min. until they released their diatom prey. The volume of P. hirobis was estimated using a geometric model consisting of a cone atop a solid hemisphere.

RESULTS

Grazing/Growth Experiments

The first grazing/growth experiment yielded an average dinoflagellate specific growth rate of 1.15•day^{-1} for the highest diatom treatments; in treatments with <2000 cells•ml^{-1} growth was submaximal (Fig. 2) and grazing rates were not calculated due to the significant food depletion that had occurred. Both growth and grazing rates as a function of food concentration were measured in the second grazing/growth experiment. Growth curves were again exponential for food-replete cultures (Fig. 3) Both the growth and the grazing curves have the form of a hyperbolic Michealis-Menton saturation equation: the growth rate curve plateaus at μ=1.23•day^{-1} (corresponding to 1.7 divisions•day^{-1} and a generation time of 15 h) (Fig. 4) and the ingestion rate reaches a maximum of 23 diatoms•grazer^{-1}•day^{-1} (Fig. 5). Clearance rates ranged from 0.5 µl•grazer^{-1}•h^{-1} in low food conditions to .1 µl grazer^{-1} h^{-1} in conditions of high food abundance (Fig. 6). Half-staturation food concentration (K_m) values are similar for the two curves; a half maximal grazing rate

occurred at a food concentration of 1400±700 diatoms•ml^{-1}, while the corresponding growth rate occurred at 800±400 diatoms•ml^{-1}. Mean dinoflagellate size decreased with decreasing food abundance (Fig.7). Food-replete dinoflagellates had a mean diameter of 22µm, while food depleted cells had a mean diameter of 18µm, a volume decrease of approximately 45%.

Diel Time Course experiment

The dinoflagellate growth curve obtained during the diel time course experiment exhibited a form which deviated slightly from a smooth exponentially increasing function. There was an initial lag phase lasting several hours followed by growth at a specific rate of 1.08•day^{-1} (Fig. 8). The frequency of dividing nuclei and doublet cells is shown in Fig. 9, together with an instantaneous growth rate function derived from Fig. 8; mitotic cells were found throughout the dark phase with a major peak at 0400hr, 1.5 hours prior to the end of the dark phase. Two distinct peaks are apparent in the growth rate function, which has maximal values at 2300 and 0600 hr. The low frequency of doublet cells reflects the relatively short duration of this stage. A distinct population of small cells, with diameters of 11 to 15µm, was also noted (Fig. 1), but the abundance of these cells never exceeded 10% of the total population.

During this experiment, an ingestion rate of 20.2 diatoms•grazer^{-1}•day^{-1} was measured. The time course of empty frustule accumulation, which records the progress of feeding, is shown in Fig. 10. Since the actual dinoflagellate concentration through time is known (Fig. 8) a hypothetical frustule accumulation curve can be

calculated assuming a constant ingestion rate of 20.2 diatoms•grazer^{-1}•day^{-1}. This curve, also plotted in Fig. 10, fits well with the empirical data; however, early in the time course the slope of the frustule production curve was somewhat greater than the slope of the calculated curve. This relationship was reversed around 2300 hours, when the empirical slope flattened. At 1100 hours the empirical slope once again exceeded the slope of the hypothetical curve. This pattern is not unexpected since the cytological reorganization occurring during mitosis would presumably render the pseudopod apparatus inoperative for a period of time.

Finally, feeding frequency (the proportion of cells attached to diatoms at any given time) through time remained fairly constant at 25-30% (Fig. 11). The duration of feeding measured in seven cells ranged from 40 to 78 minutes, with a mean of 63 minutes.

DISCUSSION

The present study provides the first direct measurements of growth and grazing in a thecate heterotrophic dinoflagellate. The unique pseudopodal grazing mechanism of these microzooplankters provides an opportunity to measure grazing rates directly and precisely. Conventional grazing procedures consist of measuring the difference food abundance in separate grazed and control food treatments. Such studies necessarily require the assumption of identical growth characteristics of phytoplankton with and without grazers, even though nutrient regeneration and related factors are not identical in the two treatments. Grazing

rates calculated in this study avoid this uncertainty.

Ingestion rates reached a maximum of 23 diatoms •grazer•day^{-1}; this datum, together with the corresponding doubling time of 17 hours (during which 13.4 diatoms are ingested) can be used to estimate the gross growth efficiency of P. hirobis. Although cell carbon measurements have not yet been made for the species involved, cell volumes of the dinoflagellate and diatom are easily calculated. The plasma volume of the diatom is harder to estimate, however. If one assumes a plasma volume: cell volume ratio of 0.25, it follows that one grazer ingests approximately 2.5 times its own plasma volume prior to cell division. This corresponds to a gross growth efficiency of 40%, a typical protozoan value; however, this important parameter needs to be determined in a more rigorous fashion.

Clearance rates of P. hirobis ranged from 0.1 to 0.5 µl•grazer^{-1}•h^{-1}, depending on food abundance. These rates are somewhat lower that those obtained by Lessard and Swift (1985), who reported clearance rates ranging from 1 to 28µl•grazer^{-1}•h^{-1} for species of Protoperidinium . However, it is difficult to compare these clearance rates with the ingestion rates obtained in this study. The concept of clearance rate is of limited value when applied to raptoral feeders such as Protoperidinium. Food abundance has a strong influence on clearance rate measurements, and the food densities used by Lessard and Swift (who obtained their food assemblage from an open ocean net tow, which was then diluted) may have been lower than that used in the present study. This would probably result in higher clearance rates, even though this measurement was based on the assumption that only

organisms in the <20μm size fraction constituted the available food for the dinoflagellates. (In fact, it is possible that larger food particles may have been selected).

The growth rates of Protoperidinium hirobis grazing on the diatom Leptocylindrus danicus are surprisingly high. Most dinoflagellates have inherently slow growth rates with few reports of division rates in excess of one division•day^{-1} or $\mu = 0.69 \cdot day^{-1}$ (Loeblich 1967). Growth rates measured in these three experiments range from 1.1 to 1.2•day^{-1}. The maximum value corresponds to 1.7 divisions•day^{-1} or a generation time of 15 hours. This rate of growth is among the highest ever recorded for a dinoflagellate. The double-peaked form of the μ vs. t function (Fig. 9) may be a direct consequence of this "ultradian" or greater-than-daily-division mode of growth.

This study is the first to document the diel pattern of cell division in a thecate heterotrophic dinoflagellate. Phototrophic dinoflagellates typically divide in the hours near dawn with a "division gate" duration of 5 to 7 hours (Chisholm 1981). Division within the P. hirobis population persists through a rather lengthy period of at least 16 hours, beginning at the start of the dark phase and extending well into the light phase. Although this heterotroph presumably has no direct interaction with light as do phototrophs, P. hirobis maintains a periodic cell division rhythm.

The rates, frequencies and durations measured in the Diel Time Course experiment can be interrelated to test for internal consistency. Since diatom particles range from one to two cells in length, one may assume an average meal size of 1.5 diatom cells. Thus an ingestion rate of 20.2

diatoms•day^{-1} corresponds to 13.5 meals•day^{-1}. Given a feeding frequency of 25% (Fig. 10), a feeding duration of .44h or 27 min. can be calculated using the following relationship:

$$\text{Feeding duration (h)} = \frac{f \bullet 24}{n \bullet 100}$$

where f = % feeding frequency and n = number of meals•day^{-1}. This result is shorter than the directly measured mean feeding duration of 60 min, which may be overestimated due to suboptimal conditions imposed upon the isolated cells. The feeding frequency, on the other hand, may be underestimated since these dinoflagellates very readily release their tethered tethered diatom when disturbed. Although there are some discrepancies among the data, it can be concluded that feeding durations fall between 0.5 and 1 hour.

The above mentioned meal frequency, that is the number of meals taken each day, indicates that the interval between meal cycles is somewhat less that two hours. Given a meal duration of up to one hour, roughly an hour would still be available for the completion of cytoplasmic processes that would allow the repeated deployment of the pallium (the pseudopodal apparatus described by Jacobson and Anderson (1986)).

Protoperidinium hirobis can grow very rapidly and can graze diatoms at a rate of approximately one cell•h^{-1}. P. hirobis is a small thecate heterotrophic dinoflagellate whose growth rate may be greater than larger species, but larger species may well have a larger feeding capacity than P. hirobis. Because of this uncertainty, it is difficult to extrapolate to the entire Protoperidinium community. However, if one assumes a maximum Protoperidinium abundance in neritic waters of

$10^4 \cdot 1^{-1}$ and an ingestion rate of 20 diatom cells$\cdot$day^{-1}, a community ingestion rate of $2 \cdot 10^5$ diatoms cells$\cdot 1^{-1} \cdot$day^{-1} is suggested. This daily ingestion can represent a significant fraction (20%) of the standing crop of a diatom bloom having a density of 10^6 cells$\cdot 1^{-1}$. It should be noted that Protoperidinium abundances of 10^4 cells$\cdot 1^{-1}$ have been observed only for short lived blooms (see Chapter 1 and Hasle and Smayda 1960); their abundance typically ranges from 10^1 to 10^3 cells$\cdot 1^{-1}$. The role of these heterotrophs should also be examined in the context of the microzooplanktonic food web. The flow of energy from large diatoms (which are available principally to larger zooplankters) into smaller particles in the form of thecate heterotrophic dinoflagellates may be important for the nutrition of microzooplankters such as ciliates, many of which can ingest only small (<40μm) particles.

This study has examined only one species of Protoperidinium feeding on one diatom species. The existence and nature of food selection, the influence of food quality on growth rate, and many other topics can now be studied under controlled conditions and with relative ease using cultured thecate heterotrophic dinoflagellates.

REFERENCES

Abé, T.H. 1936. Report of the Biological Survey of Mutsu Bay. 3. Notes on the protozoan fauna of Mutsu Bay. I. Peridiniales. Sci. Report Tohoku Ser. 4 (Bio) 10:639-86.

Chisholm, S.W. 1981. Temporal patterns of cell division in unicellular algae In T. Platt (ed.) Physiological Basis of Phytoplankton Ecology. Bull 218 Can. J. Fish. Aquatic Sci. Ottawa.

Gaines, G. and F.J.R. Taylor. 1984. Extracellular digestion in marine dinoflagellates. J. Plank. Res. 6:1057-61.

Guillard, R.R.L. and J.H. Ryther 1962. Studies of marine planktonic diatoms. I. Cyclotella nana Hustedt and Detonula confervacea (Cleve). Can. J. Microbiol. 8:229-39.

Heinbokel, J.F. 1978. Studies of the functional role of tintinnids in the Southern California bight. I. Gazing and growth rates in laboratory cultures. Mar. Biol. 47:177-89.

Jacobson, D.M. and D.M. Anderson 1986. Thecate heterotrophic dinoflagellates: Feeding behavior and mechanisms. J. Phycol. 22:249-58.

Lessard, E.J. and E. Swift. 1985. Species-specific grazing rates of heterotrophic dinoflagellates in oceanic waters, measured with a dual-label radioisotope technique. Mar. Biol.(Berl.) 87:289-96.

Nelson, D.M. and L.E. Brand 1979. Cell division periodicity in 13 species of marine phytoplankton on a light: dark cycle. J. Phycol. 15:67-75.

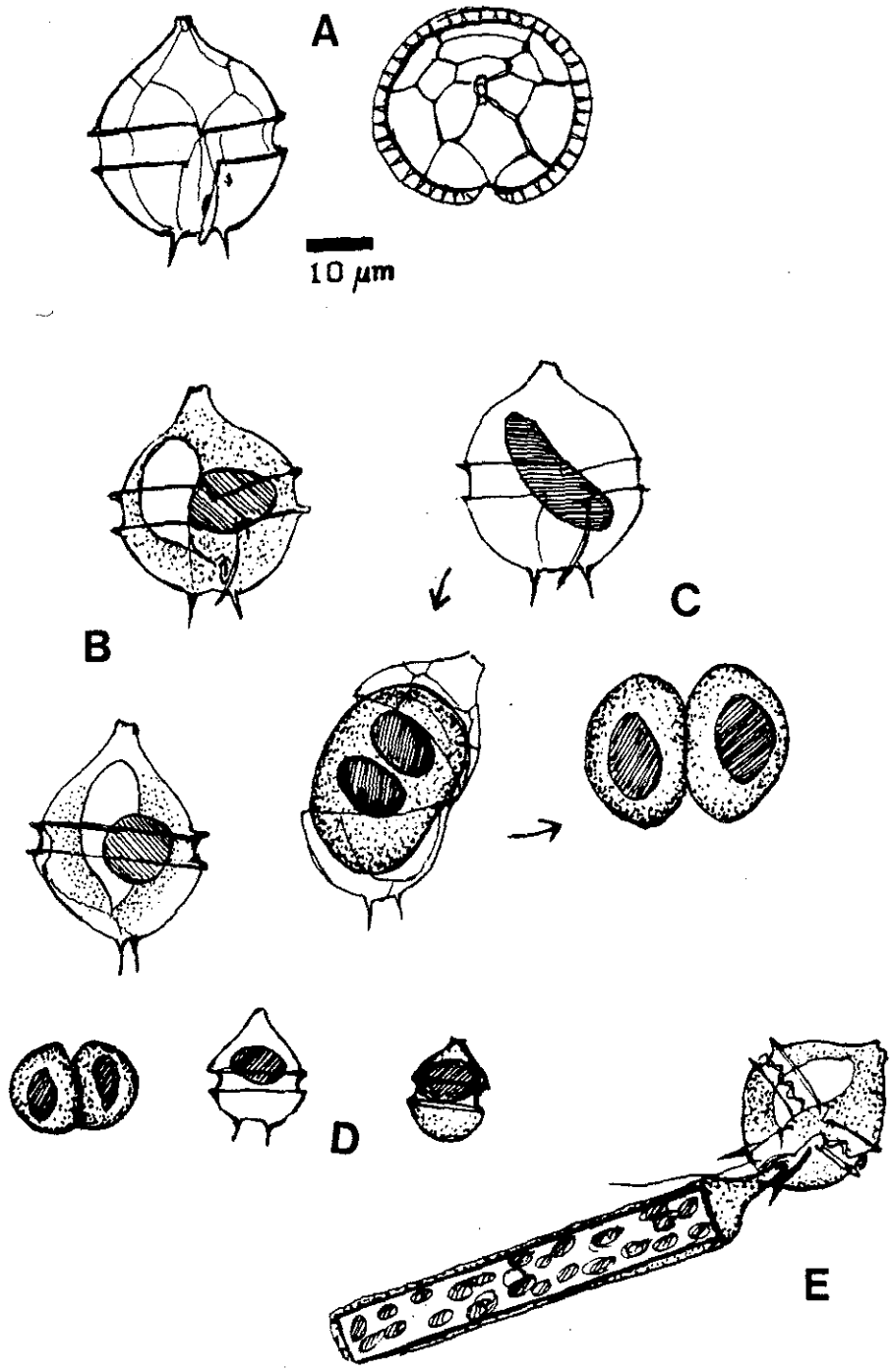

Fig. 1. Morphology of Protoperidinium hirobis.
A. Tabulation.
B. Interphase positions of nucleus and sac pusule.
C. Shape of nucleus in various mitotic stages. In regards to Fig. 8, the first two stages were counted as having dividing nuclei and the third stage was counted as a doublet cell.
D. "Small" cells.
E. Feeding cell, with pallium surrounding Leptocylindrus danicus.

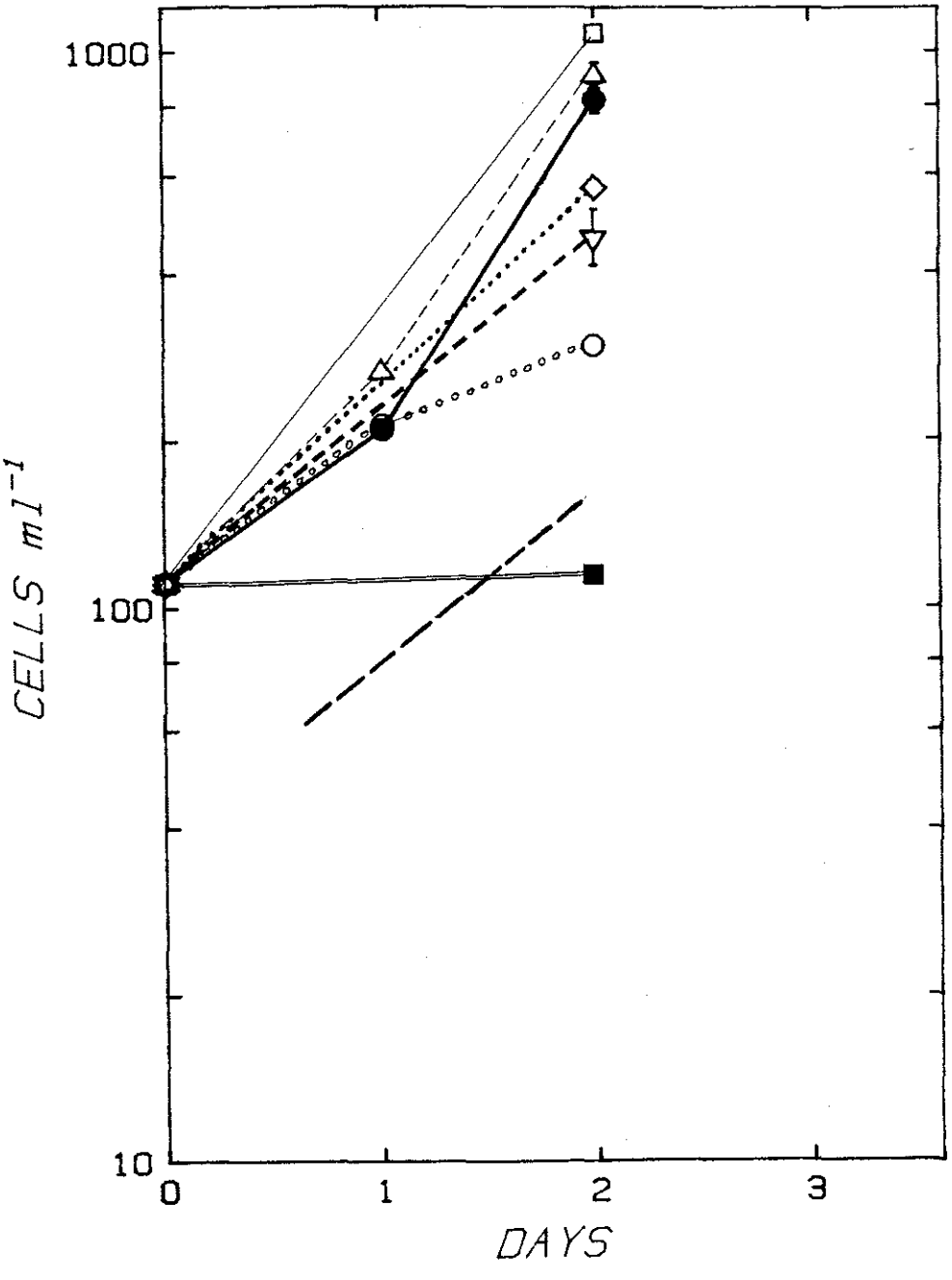

Fig. 2. Growth curves of Protoperidinium hirobis fed Leptocylindrus danicus, first grazing/growth experiment. Dashed line represents one division•day^{-1}, error bars represent one s.e.. Each curve shows a separate food treatment, as follows:

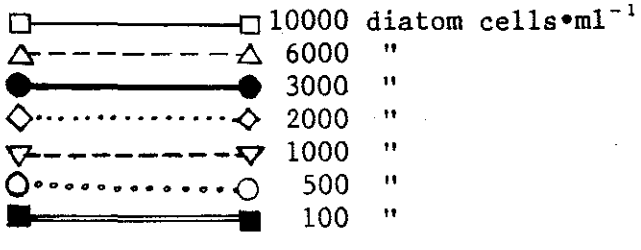

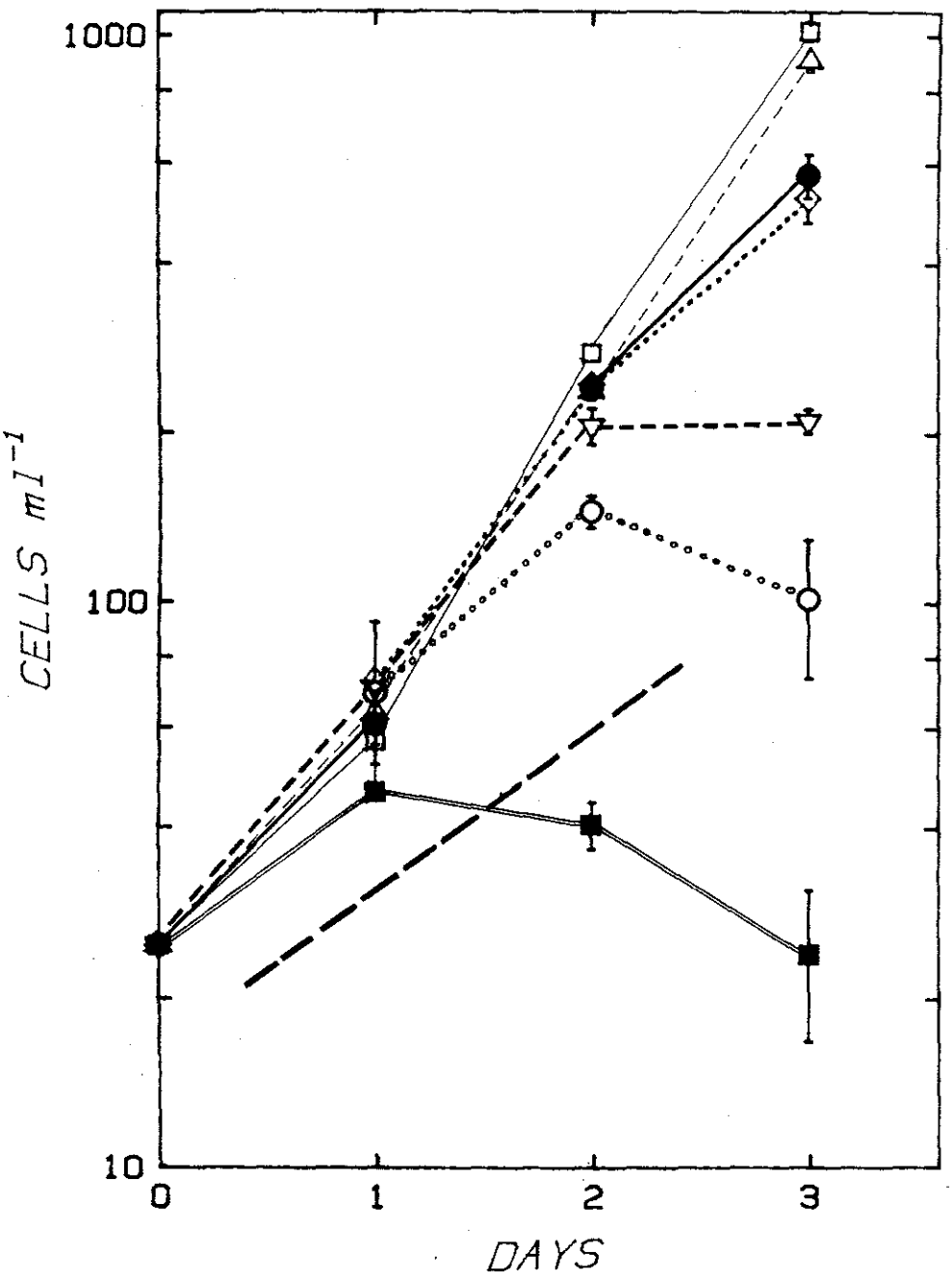

Fig. 3. Growth curves of Protoperidinium hirobis, second grazing/growth experiment; symbols as in Fig. 2.

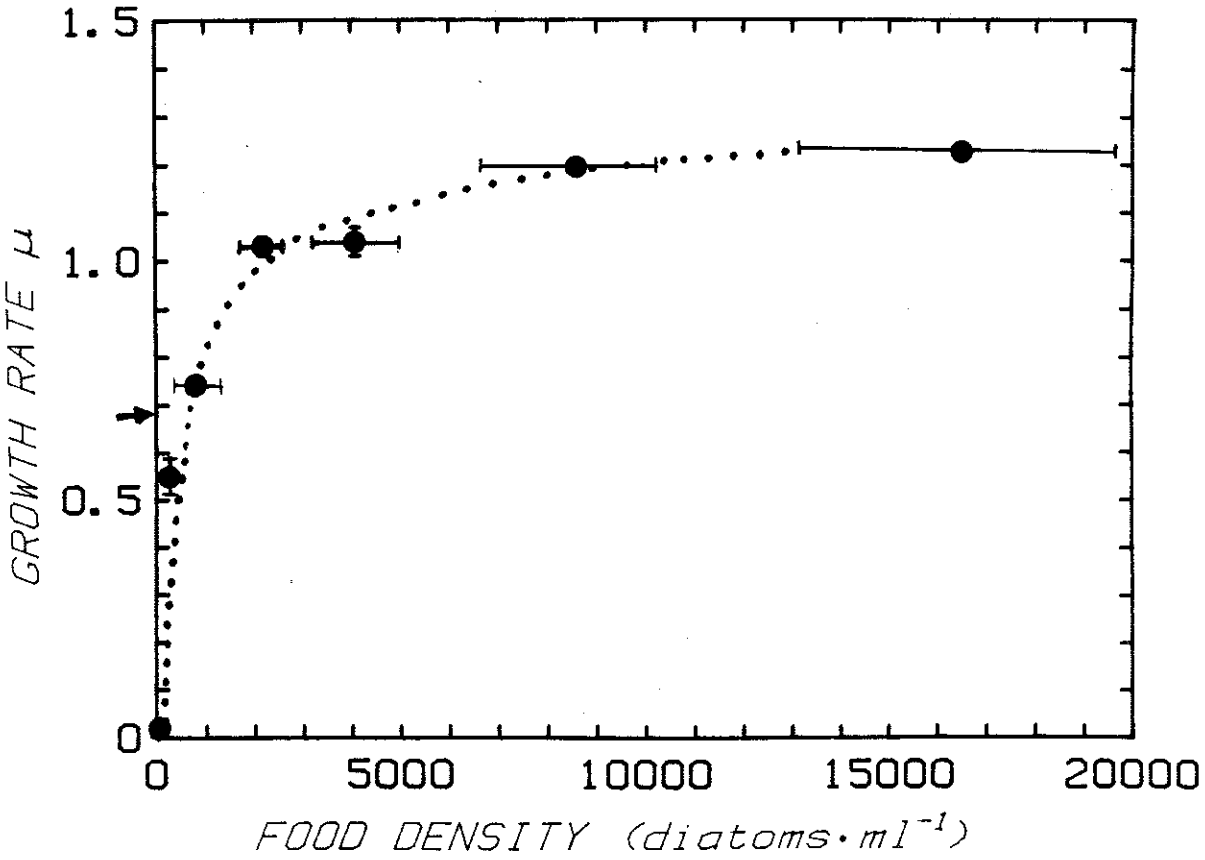

Fig. 4. Daily growth rate of Protoperidinium hirobis plotted as a function of food abundance using the second grazing/growth experiment data. Arrow indicates μ=.69 or one doubling per day. Horizontal error bars = empirical range of diatom concentration. Vertical error bars = 1 s.e..

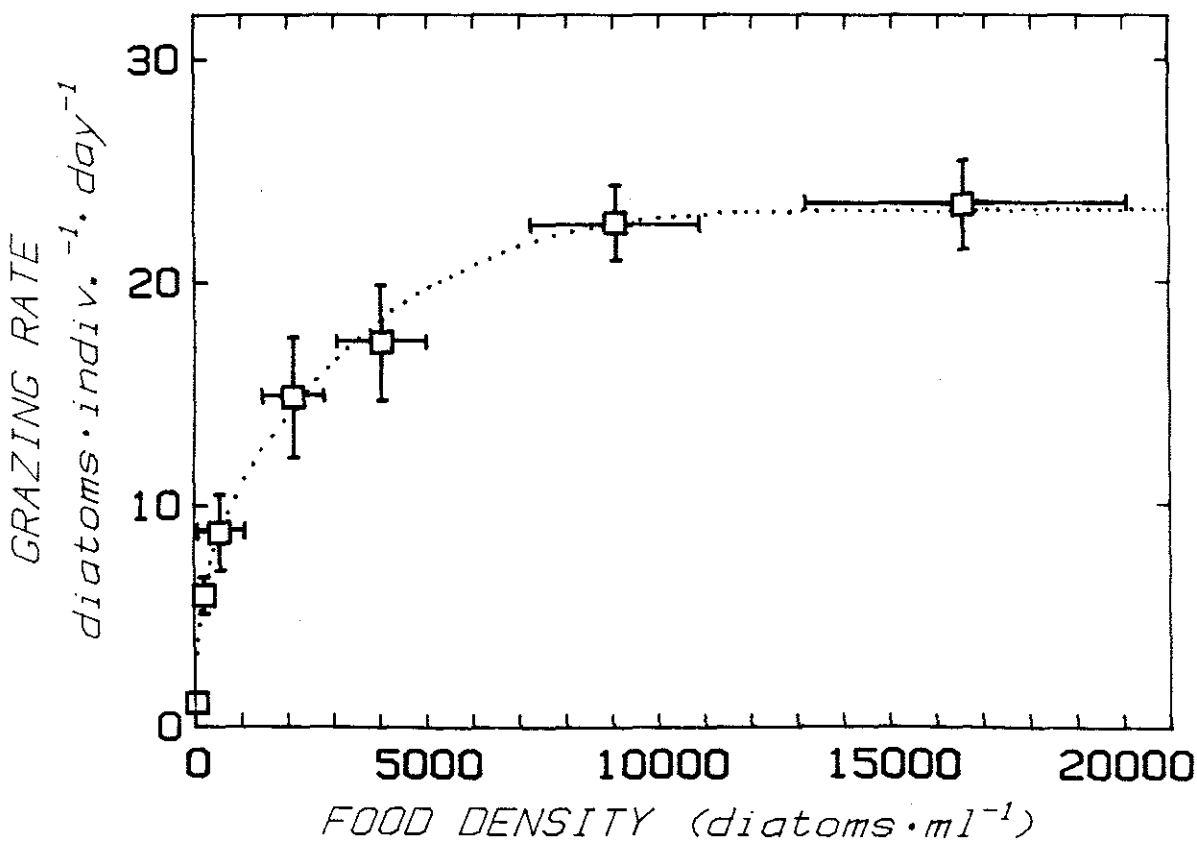

Fig. 5. Ingestion rate of Protoperidinium hirobis plotted as a function of food abundance, as in Fig. 4.

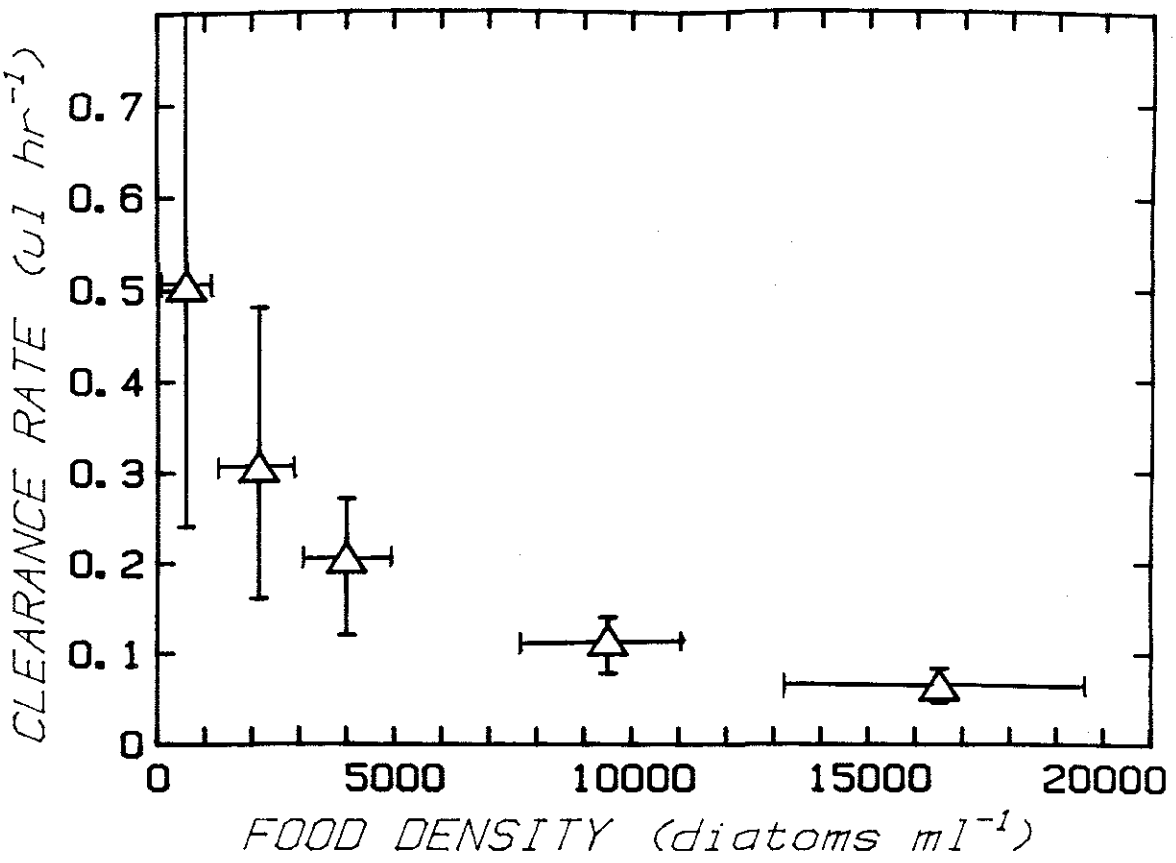

Fig. 6 Clearance rates of Protoperidinium hirobis calculated from the data shown in Fig. 5.

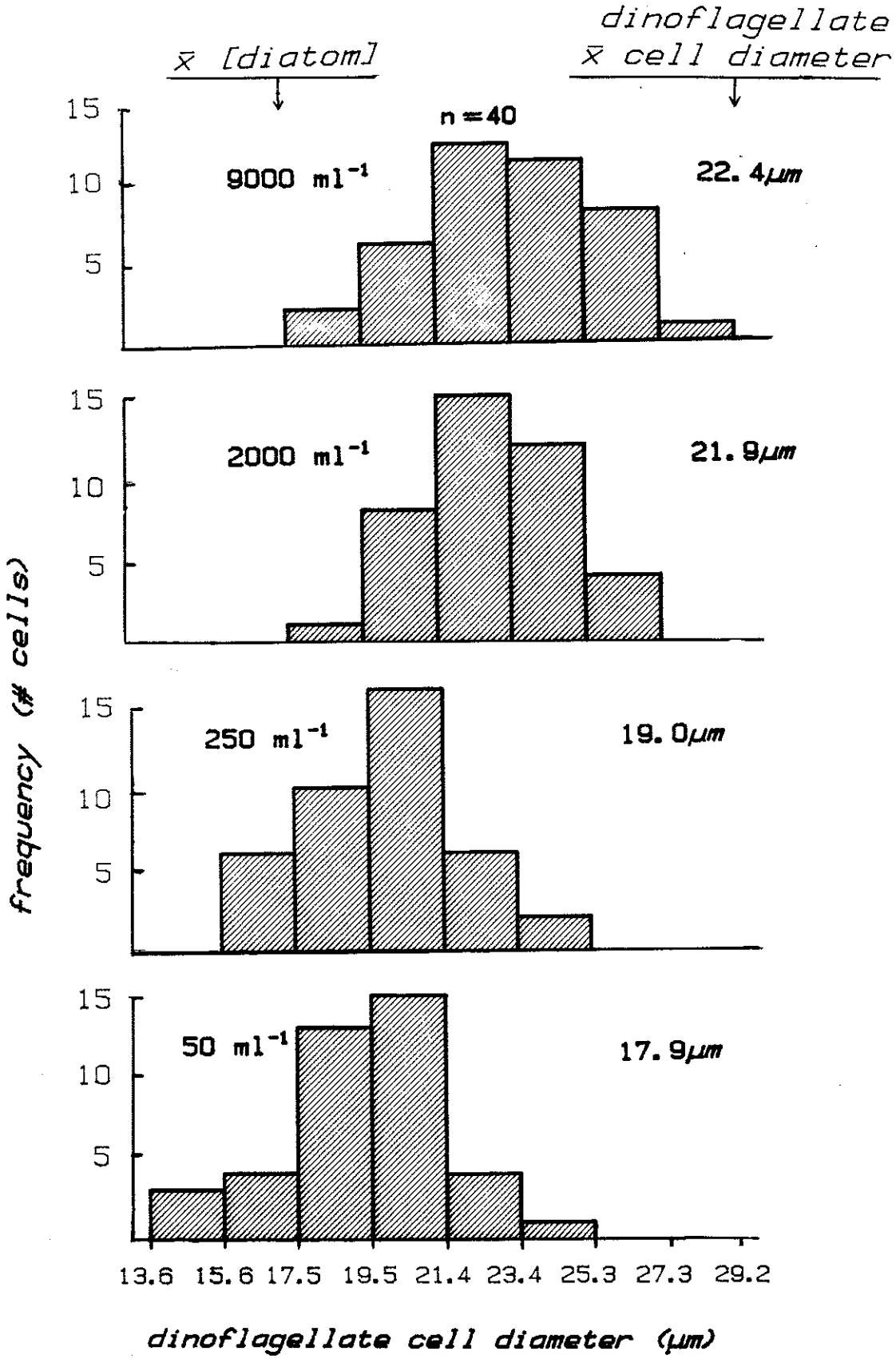

Fig. 6. Protoperidinium hirobis cell diameter-frequency histogram from four of the seven food treatments of the second grazing/growth experiment.

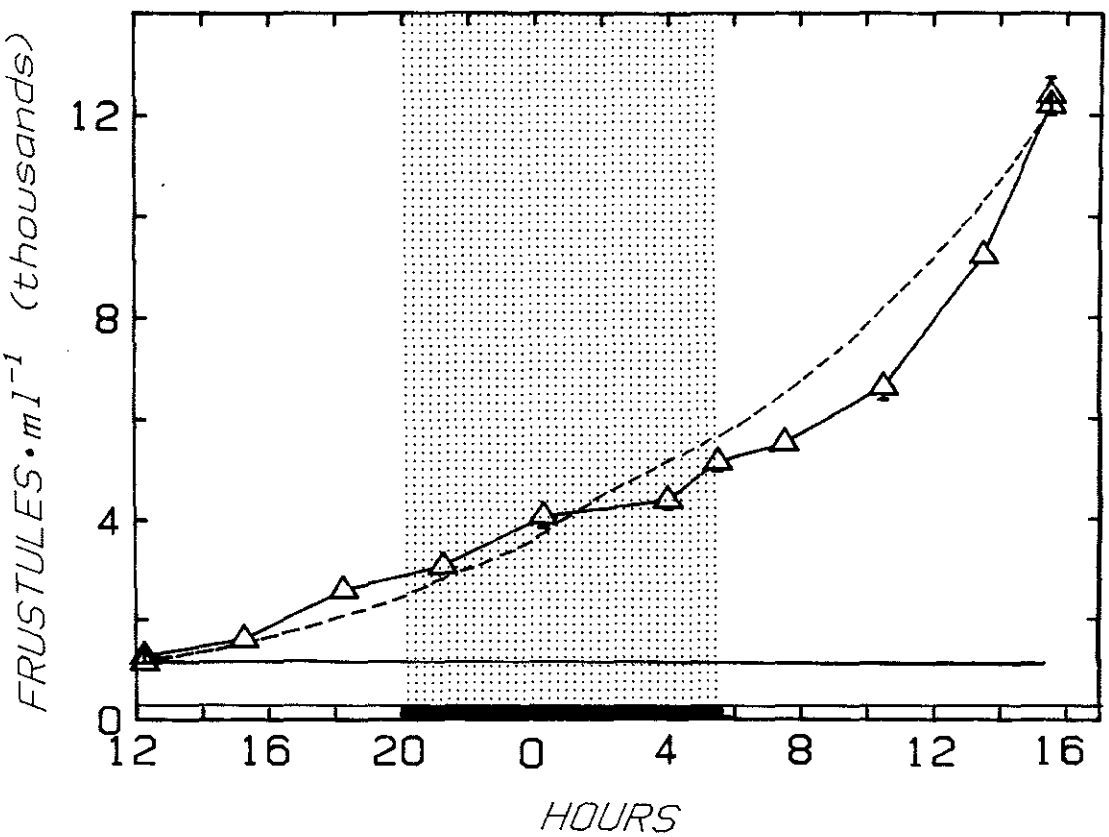

Fig. 7. Growth curves of Protoperidinium hirobis from the diel time Course experiment, L:D cycle as shown. Arrows denote multiples of inoculum cell concentration. Dotted line shows 24 hour interval over which growth rate was calculated.

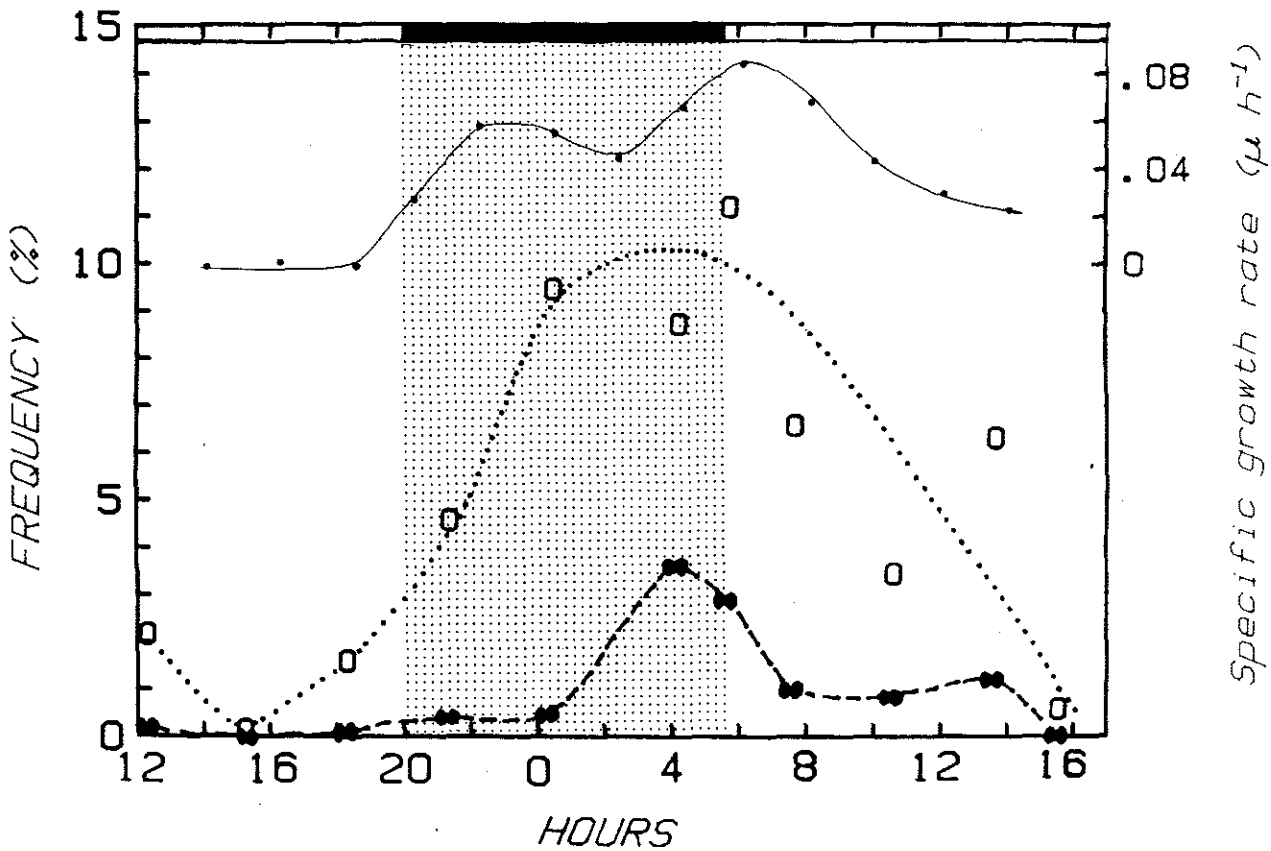

Fig. 8. Frequency of Protoperidinium hirobis elongated or dividing nuclei (O) and doublet cells (●●) and instantaneous growth rate (•) from the diel time course experiment.

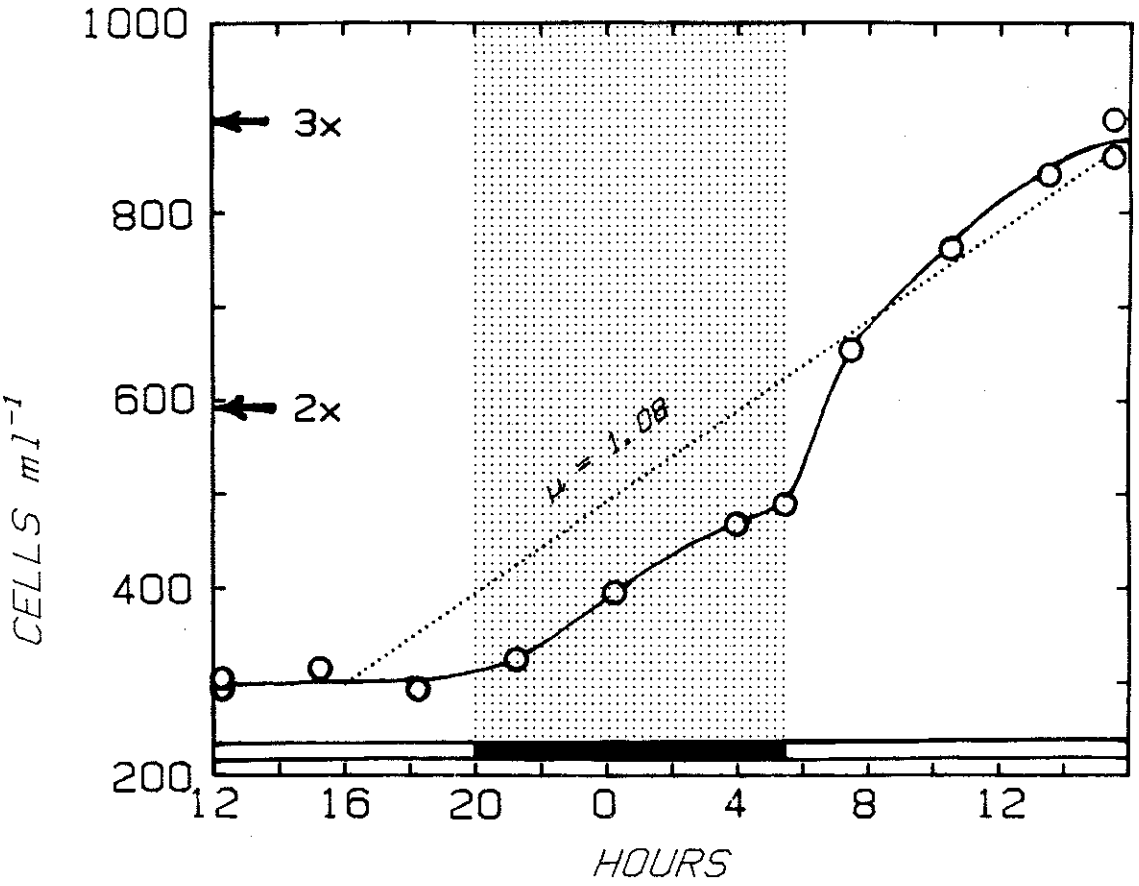

Fig. 9. Abundance of empty diatom frustules through time from the diel time course experiment. Dashed line = "predicted" frustule curve; the differences between the slopes of the two curves at a given time reflects the departure of the empirical curve from a hypothetical constant ingestion rate of 20.2 diatoms•grazer^{-1}•day^{-1}.

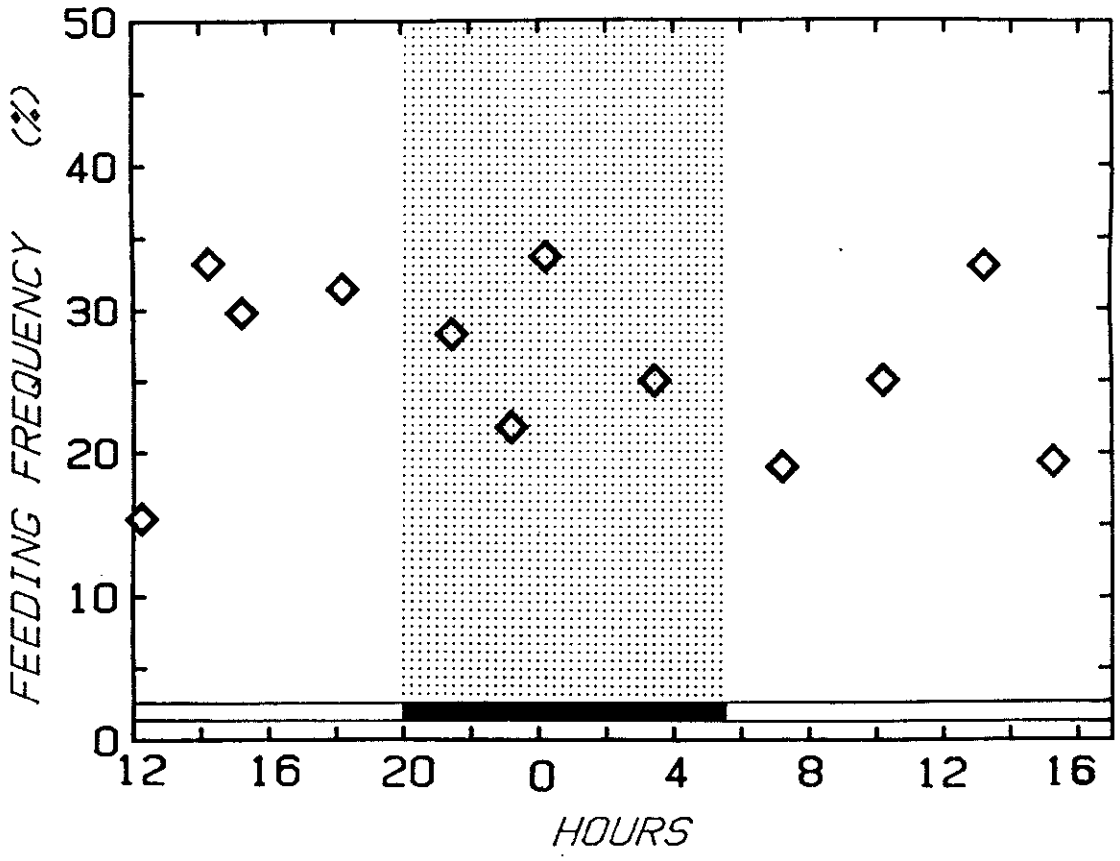

Fig. 10. Frequency of feeding Protoperidinium hirobis cells through time from the diel time course experiment.

CHAPTER 4

Ultrastructure of the Pseudopodal Feeding Apparatus of *Protoperidinium spinulosum* Schiller

Abstract

Serial ultra-thin sections of the thecate heterotrophic dinoflagellate Protoperidinium spinulosum Schiller were examined in order to describe the structures which comprise its pseudopodal feeding apparatus. The pseudopod or pallium consists of a complex array of membranous vesicles deployed within a membranous sac and includes arched, sometimes bifurcated microtubular ribbons. The pallium originates from a microtubular basket (which is located in the ventral region of the cytoplasm) and passes through an osmiophilic ring located inside the flagellar pore. This microtubular basket is distinct from the cytopharyngeal baskets found in some ciliates. The inward-directed apical end of this microtubular basket opens adjacent to the nucleus, becoming continuous with a central cytoplasmic region. In some feeding cells, large vesicles filled with a granular, electron-lucent substance, perhaps lysosomal enzymes, are clustered near the apical opening. This region is also distinguished from the denser, peripheral cytoplasm in feeding cells by the presence of numerous lipid droplets. Examination of a non-feeding cell has revealed a likely source of pseudopodal membrane: dense membranous whorls lie within the microtubular basket. A narrow pseudopodal appendage, also in this non-feeding cell, is strengthened with microtubular rows and may constitute the tow filament which serves to form an initial attachment between the dinoflagellate and its food. A complex myonemal system including osmiophilic ring, striated collars and connecting bands is described. Other thecate heterotrophic dinoflagellate species,

Protoperidinium hirobis, Protoperidinium punctulatum, and Oblea rotunda all possess structures resembling the microtubular basket and osmiophilic ring complex.

The structures that constitute the pallium and pallium precursors, described here for the first time, are unlike the feeding apparatus of other known protists, although some similarities with the dinoflagellate peduncle can be seen. The existence of this unique system of organelles may have important ramifications for the search for evolutionary relationships among protists.

INTRODUCTION

A novel pseudopodal feeding mechanism in thecate heterotrophic dinoflagellates of the genera Protoperidinium, Oblea and Zygabikodinium was described by Gaines and Taylor (1985) and by Jacobson and Anderson (1986). Although species of Protoperidinium have been the subject of ultrastructural investigations in the past (Dodge 1971, Neveux and Soyer 1976), no feeding structures have been identified. The only thecate heterotrophic species to have a feeding structure revealed, the freshwater dinoflagellate Peridiniopsis berolinense, has a peduncle with a complex multi-row microtubular array (Wedemayer and Wilcox 1984). Another thecate phagotroph, the photosynthetic Ceratium hirundinella has a microtubular strand or ribbon, but its involvement in feeding (if any) has not been determined (Dodge and Crawford 1970). The following study documents for the first time the ultrastructure of a novel feeding apparatus in both feeding and non-feeding cells of Protoperidinium spinulosum. This detailed morphological analysis is supplemented with brief examinations of three other thecate heterotrophs, Protoperidinium hirobis, Protoperidinium punctulatum and Oblea rotunda.

MATERIALS AND METHODS

All cells examined in this study, with the exception of Protoperidinium punctulatum, were selected from laboratory cultures. Feeding cells were selected by transferring cultures into petri dishes in which cells with deployed pseudopodia were readily visible.

Pre-feeding cells (one of which, termed cell F, is examined below) were obtained by selecting cells performing a characteristic spiralling pre-capture dance. This distinctive behavior usually persists for a minute or so prior to pseudopod deployment (Chapter 3). P. punctulatum, which was found in a net tow from Vineyard Sound, Massachusetts, was acclimatized by rotating the 80 μm size fraction of the tow plankton in a completely full centrifuge tube overnight, allowing immobilized dinoflagellates to resume full mobility.

Two fixation methods were used in TEM work. The first technique, used for all but two cells in this study, was developed as a result of the failure of conventional, sequential glutaraldehyde/OsO_4 fixation to preserve the pallium intact. Instead, cells were fixed by adding them via micropipette to an ice-cold mixture of glutaraldehyde and osmium tetroxide (2% and 1% final concentrations, respectively) that was buffered with 0.1 M cacodylic acid and osmotically augmented with NaCl (.43M final concentration); no calcium was added. This portion of the method was modeled after one of R. Triemer (pers. comm.). After rinsing in NaCl + buffer, the cells were transferred into drops of liquid 2% agar on glass slides and immersed in cold buffer. After 30,50 and 70% EtOH dehydration steps, the agar-embedded cells were exized as 1 mm blocks with a sharpened metal spatula while being viewed through a dissecting microscope. These blocks were then placed in centrifuge tubes for further dehydration and subsequent Epon/Araldite embedding. Resin-infiltrated cells were polymerized as flat mounts between slides and cover slips that had been treated with "T-fix" (Sunbeam Appliance Services Inc.; available through Polysciences Inc.),

a teflon spray (Spector, et al. 1981). Cured cells were exized from resin wafers and cemented onto blank resin cylinders for ultra microtomy with an Sorvall MT-2. Formation of ribbons of thin sections, critical for serial section analysis, was aided by application of a thin coat of Tackiwax (Boekel Industries, Inc.) to top and bottom faces of the specimen block (Knobler et al., 1978). Ultra-thin sections were collected onto Formvar-coated slot grids. As many as 50 sections could be positioned on two of the four slots on each grid. After post-staining with uranyl acetate and lead citrate (by immersing, not floating, grids in stain drops), the grids were lightly coated with evaporated carbon. Sections were examined on either a Zeiss 10CA or a Phillips 300 transmission electron microscope.

The second fixation protocol was designed using warm temperatures to stabilize microtubules and employing tannic acid to enhance membrane contrast (Simionescu and Simionescu, 1976). The addition of small amounts of Hg^{2+} to the initial fixative prevented detachment of the pallium from the feeding cell, and was used for both feeding and nonfeeding cells alike. An initial 30 min. fixation in cacodylate buffered 2% glutaraldehyde/1% tannic acid (Malinckrodt Inc.), including 1% saturated aqueous $HgCl_2$ at 20°C was followed by buffer rinse and a 30 min. cacodylate buffered 1% OsO_4 fixation also at 20°C. All solutions included NaCl as above. Cells were dehydrated in acetone after agar enrobement, and embedded as above in the low-viscosity medium of Spurr (1969). This second protocol was employed for both a feeding and non feeding cell. Those sections originating from these two cells are labeled in figure legends "+tannin".

Protoperidinium spinulosum was prepared for scanning electron microscopy by being washed sequentially with distilled water and 1% triton X detergent, rinsed in distilled water, fixed in formaldehyde, EtOH dehydrated and CO_2 Critical Point dried. Cells were imaged with a JEOL U-3 Scanning electron microscope.

Fluorescence observations were made on a Zeiss Inverted microscope with mercury illumination and Zeiss filter set 487706.

RESULTS

The following observations of P. spinulosum are derived chiefly from six cells, individually identified by the letters A through F: four feeding cells (A-D) including two serially sectioned cells (B=oblique cross sections, C=oblique longitudinal sections) and two non-feeding cells, E and F, the latter sectioned serially. Cells D and E (in which the pallium alone was documented) were tannin-fixed at 20°C. A fifth feeding cell (non-serially sectioned) was also examined, but is not illustrated. The ultrastructure of feeding cells will first be described, followed by non-feeding cells. Sections made from a given cell have been for the most part grouped together in plates; this organization has inevitably caused figure references in the text to be non-consecutive. A note should be made concerning lateral polarity; all sections are shown from a ventral, 'frontal' viewpoint (a natural way to view dinoflagellates), so that the cell's left is on the right side of the figure, and vice versa. All directions refer to the cell's polarity, not to the apparent "leftness"

or "rightness" of the figures themselves, which will be inversely related. Because of the complexity of the structures described herein, it is suggested that the reader review a diagrammatic overall view of feeding cell C (Fig. 1), the structure of which can be applied to other cells as well. As this cell is viewed dorsally, directions of lateral polarity are as shown in Fig. 1, and do not have to be reversed. The plates have been grouped either by cell series or by subject matter; this arrangement has resulted in a non-sequential presentation of figures in the text.

Extra-thecal morphology: the pallium

The pallium, or external pseudopod of five feeding Protoperidinium spinulosum cells, one fixed with tannic acid, all display a similar membranous morphology. This prominent structure which surrounds the prey is composed of a highly convoluted system of membranous channels and vesicles, the latter either empty or filled with electron-dense material (Fig. 2). Oddly, in some cases (involving both fixation protocols) the pallium sheet surrounding the diatom lacks an inner limiting membrane. Numerous vesicles seem to exist within a single-membrane "bubble" surrounding the diatom prey in cells preserved with either of the two fixation methods (Figs. 5,7,12). In places this outer membrane can be seen to be a single 7 nm unit membrane (Fig. 7 inset). In another specimen (cell B), an inner membrane is present; note also the degraded condition of the prey cytoplasm (Fig. 6). At high magnifications filamentous elements are visible within the pallium (Fig. 3). Note in this figure the very thin sheath (with a thickness of 150 nm) around the Chaetoceros spine. Some segments of the outer

membrane appear to be artifactually missing. In the midst of the membranous reticulum of the pallium, several microtubular ribbons radiate from the origin of the pallium at the flagellar pore. These ribbons may become bifurcate (Fig. 9) and are associated with filaments which seem to bind the individuals microtubules together (Fig. 10). In the proximal stalk-like region of the pallium of cell A, a filamentous fringe occurs on the outer membrane in association with periodic structures occurring every 200 nm on the inner surface of the membrane (Fig. 4). Periodic bands are visible in the stalk region of the pallium of cell C as well; a tangential section of the outer membrane (Fig. 11) reveals regularly-spaced transverse bands 30 nm wide separated by 220 nm intervals.

Intra-thecal morphology

Besides the pallium itself, the most conspicuous feature of feeding cells is the presence of a discrete, oblong cytoplasmic compartment continuous with the pallium at the flagellar pore (Figs. 2,14,35). The periphery of this compartment has the appearance in places of an electron dense wall; this wall is composed of an inner, parallel array of microtubules spaced every 45 nm and an outer, parallel array of membranous invaginations 30-40 nm wide and spaced every 60-80 nm apart. These two arrays are not parallel but are angled approximately 30° from each other, as can be seen in a tangential section of the compartment's dorsal face (Fig. 41). The microtubular array is oriented parallel to the long axis of the compartment which I shall call the microtubular basket (m.b.). The m.b. is surrounded by a membrane, but microtubules occur only on part of the inner surface of

this limiting membrane. Where microtubules do occur the outer membrane appears particularly dark and distinct (Fig. 24). The three-dimensional form of the m.b. has been reconstructed from serial sections of cells B and C. In cell B (Figs. 23-27) the posterior end of the m.b. has an oblong cross section with a tapered ventral edge. As it rises towards the cell apex it twists towards the nucleus, assuming the form of a right-handed helix (Figs. 26,27) and terminates adjacent to the nucleus, or to be precise, the dextro-lateral ventral face of the nucleus. At this point next to the nucleus, the electron-dense walls of the m.b. open and become a recurved flap (principally on the dorsal side) similar to a lily's corolla (Figs. 17,27,93a). The rows of microtubules continue into the flap, which appears as a slender amorphous band of intermediate electron density; the microtubules are rather indistinct. This morphology is also evident in cell C (Fig. 15), where two amorphous arcuate bands adjacent to the m.b. (which are united in sections ventral to this section) can be interpreted as a section like that indicated by the superimposed line in Fig. 17. Several mitochondria (or, more likely, a single anastomosing mitochondrion) reside in the region directly beneath the apical flap (Figs. 15, 17).

The distribution of microtubules is easily grasped when mapped on the three dimensional models (Fig. 92). In cell B the left face of the base of the m.b is encased in microtubules; at the apical opening, the flap originates from a dorsal continuation of these microtubules, near the sac pusule (Fig. 27). In cell C, the base of the m.b. is coated with microtubules on its dorsal side. The apical flap appears to arise

from microtubules situated on the right dorsal side, again on the side closest to the sac pusule (Fig. 43). The borders of the microtubule-bearing and lacking faces in cell C are situated along distinct 'corners' or ridges (Fig 93b).

Large non-pusule vacuoles are often associated with the m.b.. The m.b. in cells A and B are completely embedded in cytoplasm, with the small exception of cell A in which a vacuole is present adjacent to the anterior end of the m.b. (Fig. 16), while the anterior portion of the m.b. in cell C is surrounded by an extensive vacuole (Fig. 37). An even more extensive vacuole surrounds much of the m.b. of a second feeding cell (not illustrated).

The contents of the m.b. (which I term the "pallioplasm") of three feeding cells all show distinct differences compared to the bulk cytoplasm. For example, in no instances have such organelles as mitochondria, endoplasmic reticulum, trichocysts, etc. been found within the m.b., although numerous mitochondria (or, once again, an anastomosing mitochondrion) are situated at the basket's apical opening (Figs. 15,17). In cell A, numerous vesicles, some filled with osmiophilic material of a range of densities, give the pallioplasm a mottled appearance. (The darkest of these osmiophilic vesicles will be considered in depth later.)

At this point it is germane to note light microscopic auto-fluourescence observations of live P. spinulosum cells in which the cytoplasm fluoresces a brilliant, uniform green (with dark regions corresponding to sac pusule and nucleus). The extended pallium, however, has no detectible auto-fluorescence. In other words, the

auto-fluouresent material, though widely-distributed within the cytoplasm, is apparently not part of the pallium precursor. Parenthetically, this characteristic green fluorescence, which is observed without exception in P. spinulosum and the closely related species P. pellucidum, P. pallidum, and P. hirobis, is lipid soluble (i.e., disperses in acetone but not in water). Also, this green fluorescence is not to be confused with a rather dull green fluorescence seen in all heterotrophic and some phototrophic dinoflagellate species after fixation.

The pallioplasm varies somewhat in appearance from cell to cell. In cells B and C, which are attached to diatoms whose cytoplasm is in an advanced stage of degradation (i.e., lacking recognizable plastids), the pallioplasm appears to be less densely packed than that of cell A, whose diatom cytoplasm was still relatively intact (compare Fig. 24,31 with Fig. 14).

Some characteristic features of the pallioplasm include microtubules situated in arched ribbons separate from the peripheral microtubules (Fig. 24). The ribbons appear to be continuous with those seen in the pallium. Perhaps the most striking feature of the feeding apparatus is an osmiophilic ring through which the m.b. inserts. Several sections taken longitudinally (Fig. 15,36) and transversely (Fig. 22) show the torus-like form of this very electron-dense structure. Regular corrugations sometimes occur on its outer surface (Fig. 21). However, little distinctive structural organization is discernible in a glancing, tangential section (Fig. 32) apart from barely-discernible bands, unlike those of striated collars (Figs.

36,40). An electron-lucent fibrillar region surrounds the osmiophilic ring (Figs. 14,21,35). This feature has been seen in all four feeding cells whose osmiophilic ring was examined.

The osmiophilic ring is located at the center of a complex system of electron-dense interconnecting bands. This is best exemplified by cell C (Figs. 31-39) in which the ring is connected to two striated collars situated about the ducts of the two pusules. The band associated with the collecting pusule is actually only indirectly connected with the striated collar; the osmiophilic ring is directly connected first to a thecal structure that forms part of the wall of the collecting pusule duct via a thick (.4 μm) electron-dense band, in which cross-striations are barely visible (inset, Fig. 33). This band is then connected via a slender band to the striated collar itself. This arrangement is especially clear in cell B (Fig. 23) in which the thick band (b) is connected to the striated collar of the collecting pusule by a relatively delicate strand. However, the connection between sac pusule striated collar and osmiophilic ring is not certain in this cell, since some relevant sections are missing. Note the manner in which each of the two flagella pass through their respective striated collars; the longitudinal flagellar is associated with the sac pusule (Fig. 39) and the transverse flagellum with the collecting pusule (Fig. 34). This arrangement holds true also for P. hirobis and Oblea rotunda (see below). The striated collar of the sac pusule in cell C appears to interact with the basal body microtubular root (Fig. 39). Note the amorphous electron-dense substance which coats the upper portion of this root. A second thick (.3 μm) band is

anchored to the thecal structure referred to above adjacent to the first thick band and is continuous with a dark layer of the pore plate (Fig. 31). This plate, also referred to as the median sulcal plate, has a unique, fibrous composition with a pale outer layer and an electron-dense inner layer (Figs. 28,50).

The positioning of the electron-dense band, pusular, pallioplasmic systems are intimately related to the rigid, exoskeletal morphology of the theca. In particular, a protuberance extends from the inner surface of the sulcus and terminates with a distinctive orthogonal strut (Fig. 37); this protuberance is composed of three minute internal sulcal plates. The arrangement of these sulcal plates was determined from a reconstruction of the posterior sulcal region of the theca (Fig. 94) made from ten sections including Figs. 36 and 37. The inner protuberance formed by these sulcal plates lies on the right side of the posterior flagellar pore (Fig. 95). A schematic diagram helps relate these structures to the sulcus as a whole. The osmiophilic ring along with the striated collar of the sac pusule is anchored to the orthogonal strut, and the duct of the sac pusule runs immediately below the strut. A second, less-pronounced protuberance rises at the point where the collecting pusule duct exits through the anterior flagellar pore (Fig. 31) and is composed of portions of the right and anterior sulcal plates. As described above, several electron-dense bands are anchored to this protuberance. The transverse flagellum, running along this duct, can be traced in its entirety through this series of sections; however, this is not the case with the longitudinal flagellum. It apparently became detached at the point where it enters

the duct of the sac pusule (Fig. 38) and does not appear again until Fig. 35; thus, its passage through the flagellar pore is not explicitly apparent. Despite this uncertainty, it seems clear that the longitudinal flagellum, sac pusular duct and the pallium share the same orifice, the posterior flagellar pore.

In addition to the m.b., there exist several less conspicuous cytoplasmic structures related to the feeding apparatus. The central region of the cytoplasm near the apex of the m.b., between the sac pusule and nucleus appears slightly less dense than peripheral cytoplasm (Figs. 13,44). In cell A, several large vesicles filled with an electron-lucent granular substance are located near the apex of the m.b. (Fig. 13); these vesicles are not found, however, in cells B or C but are present in cell F (see below). In cell B, this region also contains numerous small (0.1 μm) osmiophilic droplets. These droplets are identical to those found in the pallium and pallioplasm (Figs. 6 and 23, respectively) and appear in Fig. 27 to be streaming out of the opening of the m.b.. This interpretation may also be applied to cell C, in which lipid droplets surround the apical end of the m.b. (Fig. 14,42). These droplets appear to be situated within small vesicles, as must be the case if they had been transported form the pallium since digestive enzymes liberated in the pallium could damage the dinoflagellate cytoplasm if not properly contained. In sections made between the m.b. and nucleus (Fig. 43,44) these droplets abound in the central region of the cell, but are absent in the peripheral cytoplasm. Dichtyosomes are lined up along the interface between these central and the denser peripheral cytoplasmic regions (Fig. 45).

Nonfeeding cells

Structures found in feeding cells of Protoperidinium spinulosum, such as the microtubular basket, are also present in nonfeeding cell E (Fig. 53). Only a single section of the m.b. has been obtained from this cell; peripheral rows of microtubules are present, along with a central microtubular structure, and, unlike the m.b. of feeding cells, an oblong osmiophilic body 0.3x1 μm in size is present in the otherwise featureless pallioplasm. The m.b. is conspicuously located in a very large vacuole, a condition similar to that in several feeding cells. A convoluted membranous structure, perhaps continuous with the pallioplasm, is found in the flagellar pore (Fig. 50) and has a conspicuous glycocalyx. No osmiophilic ring is found, but it may easily have been missed due to the incomplete sampling of thin sections. Cell E is highly vacuolated, especially in the region surrounding the sac pusule (Fig. 53). An unidentified flagella-like structure with a barely discernible peripheral row of microtubules and an elaborate outer glycocalyx (Fig. 52) exists in addition to the longitudinal flagellum, the latter of which appears in Fig. 46.

A second non-feeder named cell F was fixed while the cell was engaged in a spiralling pre-capture "dance" (indicating that the cell was prepared to deploy its pallium: Chapter 3). It has a distinct ultrastructural appearance which is apparently due to the warm, tannic acid/glutaraldehyde preservation method. A m.b. and osmiophilic ring is present, with an electron-lucent region (smaller than that seen in feeding cells) adjacent to the latter (Figs. 61,62). The sulcus is filled with an electron dense substance (perhaps a stain-induced

artifact) in which the embedding plastic was soft, resulting in uneven sectioning (Figs. 53,59). A partially-obscured system of very regularly spaced (5.5 nm from line to line) membranous whorls resembling a myelin sheath can be seen in the sulcus (Figs. 70,73) and has been reconstructed by use of a mosaic of differentially exposed prints (Fig. 71). Similar formations are also located within the m.b., but have a less-ordered structure (Figs. 56-58) with 9 nm membrane spacings. Adjacent to this system of membranes, the pallioplasm has a very fine, smooth texture, with microtubular rows in the peripheral pallioplasm (Figs. 58,64). The only other cytoplasmic region with such a homogenous texture is located adjacent to the posterior face of the nucleus (Figs. 55,59). No continuity between the perinuclear region, populated with large vesicles filled with a granular, electron-lucent material, and the pallioplasm has been detected. However, some relevant sections may be missing; a complete series of m.b. sections is not yet available. The osmiophilic ring does not appear as electron-dense as those fixed with the cold glutaraldehyde/ OsO_4 mixture, but is similar in its featureless internal composition (Fig. 64). In contrast to feeding cells, no regularly-spaced membranous channels have been seen adjacent to the m.b. in cell F.

A small lobate pseudopodal structure containing one to several rows of microtubules emerges from the congested sulcus (Fig. 65-67). This pseudopod was not detected in this cell with light microscopy. The granular matrix of this small pseudopod resembles that of the transverse flagellum (Fig. 68) (this matrix has apparently become extracted in cold-fixed cells: see transverse flagellum in Fig. 13) but

the pseudopod clearly lacks an axonemal strand, so it cannot be the longitudinal flagellum. The latter, however, was not located. The outer membrane of the pseudopod has a thin glycocalyx; inside this membrane the microtubules, spaced 20 nm apart, are embedded in an amorphous electron-dense substance and appear to be composed of 13 tubulin subunits per revolution.

The sac pusule of cell F holds copious amounts of membranous bodies. In one section an inclusion filled with granular material is present (Fig. 76) while in another section multi-layered concentric membranous whorls are encountered (Figs. 74,75). All feeding cells, however, appear to have empty sac pusules (Figs. 13,27,45). Returning to cell F, the pusule is lined in places by a 50 nm layer of cytoplasm sandwiched by a system of membranes (Fig. 60). This cytoplasmic layer is continuous with the featureless groundplasm surrounding the basal bodies (Fig. 63) but seems somewhat distinct from the cytoplasm surrounding the large perinuclear vesicles.

Miscellaneous organelles

Several distinctive structures (though not necessarily involved in feeding) were encountered. A radially arranged cluster of mucocysts was found in cell C on the left ventral face of the hypotheca near the sulcus (Fig. 77). This location corresponds to the ventral pore (Fig. 47) in the center of the first postcingular plate. The mucocysts terminate in a hexagonally arranged cluster of pores with 100 nm diameters (Fig. 78). In the same region of cell F a cluster of mucocysts has openings which converge on a thecal pit and which are releasing a darkly-stained substance (Fig. 80). The ventral pore is

visible as an ordered cluster of mucocyst pores in cell B as well (Fig. 18).

Scattered throughout the periphery of the cytoplasm, just inside the amphiesma (the system of thecal plates enclosed within flattened membrane vesicles), are lamellar structures composed of up to two dozen stacked, planar lamellae with spacings of 10 nm (Fig. 79). Each lamella is divided in half by a thin, central band; the thick bands are probably two adjacent, closely appressed membranes. The lamellae appear to separate along either 'thick' or 'thin' membranes. These structures are often associated with lipid droplets (Fig. 82) and have been seen in each of five specimens of P. spinulosum and also in P. hirobis and Oblea rotunda.

Another peripherally located organelle, the trichocyst (which is an ejectile structure found in most dinoflagellates), has a distinctive, banded appearance (Fig. 82). Groups of trichocysts line up with the margins of the cingulum in cell A. A cross-sectioned trichocyst from cell F shows the characteristic paracrystalline structure with a 7 nm periodicity (Fig. 83).

Lastly, the apical pore of cell G is figured (Fig. 81), revealing no conspicuous cytoplasmic specializations.

Additional species

The feeding apparatus of three additional species has been examined. Protoperidinium hirobis, whose thecal plate arrangement is very similar to that of P. spinulosum, also has two distinctive pusules, both of which have striated collars surrounding their outlet ducts. One of these, on the sac pusule, is illustrated (Fig. 84); the

longitudinal flagellum enters the pusule just inside the striated collar. The m.b.-like structure includes microtubular bands (Fig. 86) and large oblong osmiophilic bodies up to 0.5x1.5 μm in size. The pallioplasm of P. hirobis is continuous with a light-toned central cytoplasmic region surrounded by the nucleus and a darker, electron-dense cytoplasmic region (Fig. 85). An osmiophilic structure similar to an osmiophilic ring but lacking a surrounding electron-lucent region is attached to the m.b. near the flagellar pore (Fig. 85). Note the fibrous composition of the pore plate (Fig. 84).

A single section of the m.b. of a non-feeding P. punctulatum cell reveals a structure quite similar to that of P. spinulosum (Fig. 91). An osmiophilic ring situated at the posterior end of the m.b., a microtubular lining of the pallioplasm and elongate osmiophilic bodies 0.2x1-2 μm in size lie in the upper pallioplasm are evident. In addition, a striated root-like structure is attached to the lower surface of the m.b..

A fourth species, Oblea rotunda is represented by a cell feeding on the dinoflagellate Heterocapsa triquetra. The pallium passes though an osmiophilic ring (which has a small electron-lucent core) in the wide flagellar depression (Figs. 87,88). Two regions of the pallium itself are evident: a proximal non-vesicular stalk within which microtubules are located, and a multi-vesicular region adjacent to the prey cell (Fig. 83). The theca of the prey seems to have been dissolved; a very thin pseudopodal film with a very distinct, electron-dense outer surface encapsulates the captured dinoflagellate. Perhaps the myriad vesicles of the pallium have been derived in part from its prey, which

appears to be considerably degraded; only the thyllakoid membranes remain intact. The inner continuation of the pallium adjacent to the basal bodies and between the two pusules (Fig. 90) has a rather inconspicuous appearance compared with the m.b. of P. spinulosum; a row of tightly arranged microtubules exist without an outer membranous complex (Fig. 89).

DISCUSSION

A coherent picture of the feeding apparatus of Protoperidinium spinulosum has emerged from the seven cells examined here, six of which have been figured. The overall organization of relevant organelles in Cell C is illustrated by a cut-away illustration (Fig. 1). This dorsal view reveals the arrangement of the m.b. and its osmiophilic ring adjacent to the inner thecal protuberance. Also shown are the connections between osmiophilic ring and striated collars, and the location of the basal bodies between the sac and collecting pusules. I will now discuss the structure of these organelles and compare them to similar structures in other cell systems.

The terms used in this report can at times be confusing. The pseudopod which envelopes the prey outside the thecal wall of the dinoflagellate is termed the pallium. Inside the cell this pseudopodal material is termed the pallioplasm, especially where it is confined within the microtubular basket. A small lobate pseudopod seen in cell F and perhaps cell E as well is provisionally regarded as being distinct from the pallium, as will be discussed below.

The microtubular basket

The microtubular basket, at least in feeding cells, is clearly an open-ended conduit which funnels the pallioplasm down through the flagellar pore. The single peripheral row of microtubules in the m.b. distinguishes it from the peduncle seen in Gymnodinium lebouriae (Lee 1977) and Katodinium glandulum (Dodge, 1971) which are multi-row microtubular structures. While the peduncle is primarily an ingestion organ, able to pierce prey organisms and transport organelles such as plastids and mitochondria through its microtubular basket intact, the m.b. of P. spinulosum serves both to transport out through the flagellar pore large quantities of cytoplasmic material that form the pallium (membranes, lysosomes, microtubular ribbons) and to endocytose the liquified components of the prey (which must diffuse out of the diatom through minute pores within the frustule wall into the pallium). It is possible that the "suction" force which draws material up through the peduncle of certain naked dinoflagellates and the microtubular basket of Protoperidinium may have a common (and as yet unknown) mechanism. Endocytosis through the microtubular basket seems to be illustrated by the distribution of small lipid-like election dense droplets which appear to well up out of the m.b. through its apical opening and into the surrounding central cytoplasm. This process may have been witnessed when a living cell observed during pseudopod retraction exhibited cytoplasmic streaming in a region between to the sac pusule and nucleus (unpubl. obs.). Spasmodic motion has also been seen in in the ventral cytoplasm of a non-feeding Protoperidinium depressum cell (Cachon et al., 1983). During this

endocytotic process, the digestive enzymes that had been released within the pallium must be contained within endocytotic vesicles.

The discovery of a m.b. in each of four species of thecate heterotrophic dinoflagellates strongly suggests that this structure is a constant feature among species of Protoperidinium and the allied diplopsaloid dinoflagellate, and possibly among Podolampus and Blepharocysta as well. Besides the microtubular rows that line the basket, elongate osmiophilic bodies have been found in Protoperidinium spinulosum (cell E), P. hirobis and P. punctulatum. These structures are similar to the rod-shaped bodies seen within the peduncular microtubular basket of Gymnodinium lebouriae (Lee, 1977), Katodinium fungiforme (Spero 1982), and of Peridiniopsis berolinense (Wedemayer and Wilcox, 1984) and may be contain digestive enzymes.

Microtubular oral structures are found in a number of protists, but none closely resemble the microtubular basket of Protoperdinium. The dinoflagellate peduncle has microtubules arranged in multiple, overlapping rows of microtubules, unlike the single row found in Protoperidinium. Elaborate microtubular structures are also present in trichomonads, a group of endoparasitic flagellates. Like Protoperidinium, there exists a cytoplasmic region partially bound by a single row of microtubules, the latter which are termed the pelta-axostyle complex (Honigberg et al., 1971; Brugerole, 1980). Whether these structures are evolutionarily related to the dinoflagellate microtubular basket remains to be seen. A weaker resemblance exists in the case of euglenoid flagellates in which a row of microtubules lines part of the euglenoid resevoir, through which

food particles are ingested (Walne, 1980). A complex microtubular oral structure found in some ciliates, the cytopharyngeal baskets or cyrtos, (Fig. 84 of Small and Lynn, 1985) bears few similarities with the microtubular basket of Protoperidinium.

Returning to the pseudopodal deployment phase, it is tempting to speculate that the large electron-lucent vesicles found near the nucleus and the apical opening of the m.b. constitute primary lysosomes, some of which are transported into the pallium to effect the liquification of the prey cytoplasm. In fact, a vesicle of similar appearance to the large perinuclear vesicles is present in the pallium of cell D alone, adjacent to a recently-captured diatom; this diatom is the least degraded of all those examined, so it might be inferred that the diatom had been captured soon before the cell was fixed. Many small electron-dense droplets are found in the pallia of cells A,B and C, which appear to have been allowed a relatively long time interval to degrade the enclosed diatom prey, but not in the pallium of cell D, in which electron-dense droplets are very few in number.

A notable feature of the complex structure of the m.b is its outer membrane, which has a particularly bold appearance adjacent to microtubular rows and which, in places, takes the form of regularly spaced pillar-like channels. These channels resemble those seen adjacent to food vacuoles of the phagocytic flagellate Gyromitus disomatus (Swale and Belcher, 1974) which were interpreted to be endocytotic vesicles. The m.b. channels also have a beaded appearance similar to that seen in G. disomatus, but do not form the discrete, regularly spaced cylindrical tubules seen in tangential section.

Instead, tangential sections of the channels which surround the m.b. of P. spinulosum appear as continuous, parallel rows. The diameter of the channels in both G. disomatus and P. spinulosum measure 40 nm in diameter. The presence of such an extensive array of channels of possibly endocytotic function suggests that this constitutes, together with the large apical opening of the m.b., a second route for the inward transport of ingested material. These membranous channels were not seen in cell F, but additional non-feeding cells need to be examined.

The question of the source of the enormous quantities of membranes needed to form a pallium (enough, in some cases, to envelope a chain of diatoms several hundred micrometers in length) can now be at least partially answered. In cell F, which was preparing to feed, two membranous complexes have been found. The first is located in the posterior face of the m.b. and takes the form of a multi-laminate mass of membranes with a periodicity of 9 to 14 nm. The second is found in the poorly-sectioned sulcal region both immediately within or outside of the flagellar pore. This complex takes the form of tightly-packed fingerprint-like membranous whorls called myelin figures with a periodicity of only 5 nm. The uneven sectioning of the sulcal region in which these myelin figures are found, which is clearly the result of a localized lack of rigidity in the embedding plastic, may, in concert with the myelin figures, indicate the presence of lipid-rich structures. Apparently, a great store of membranes is accumulated near the flagellar pore prior to feeding. However, the precise organization of this complex of membranes is not certain, since myelin figures can

be produced as an artifact of suboptimal fixation (Rogers and Perkins 1968). The membranous complex seen within the m.b., which does not have the distinctive myelin appearance, is similar to the electron dense "rhoptry" structures observed in Plasmodium berghi by Steward et al. (1985). The periodicity of the rhoptry structures is 5 nm, and are thought to be the storage site for membranes to be discharged outside the cell. Non-feeding cells in various stages of readiness to deploy their pallia need to be examined in order to reveal the membrane dynamics of the feeding apparatus in P. spinulosum.

The conspicuous presence of the osmiophilic ring (which surrounds the posterior end of the m.b.) has been repeatedly detected in P. spinulosum and in P. hirobis, P. punctulatum and Oblea rotunda as well. Such a structure has been seen in several phagotrophic dinoflagellates including the parasitic Protoodinium chattoni (Cachon and Cachon, 1971) and the peduncle-bearing Gyrodinium lebouriae (Lee, 1977). In all these cells the osmiophilic ring is situated where the peduncle or pseudopod leaves the cell, forming a valve or sphincter-like structure. Without exception an electron-lucent, fibrillar region has been found in P. spinulosum to surround the osmiophilic ring. This juxtaposed arrangement is somewhat reminiscent of the "fine fibrillar deposit" adjacent to the ring-shaped osmiophilic collars in the fusules of nassellarian radiolaria (Anderson, 1977). However, no suchfibrillar zone was found in the other dinoflagellates examined in this study, and its function is not known.

The myonemal system

Cachon et al. (1983) described a "myonemal" system in the

dinoflagellate Kofoidinium pavillardi composed of the striated root of the transverse flagellum. The term myoneme refers to protozoan structures that may be contractile, somewhat analogous to the muscles of metazoans. The myoneme of K. pavillardi, which has a diameter of 1 μm, is very similar to the electron-dense bands found in Protoperidinium spinulosum. In K. pavillardi, the myoneme begins at the basal body, runs around the duct of the collecting pusule, and then splits into four branches which wind around a pusule. These investigators also reported the periodic sudden contraction of the collecting pusule of Protoperidinium depressum, and suggest that a myonemal structure like that in K. pavillardi may be able to exert a squeezing force upon the collecting pusule, resulting in forceful expulsion of its contents. However, no ultrastructural data for P. depressum was presented. (Parenthetically, the enormous sac pusule of P. depressum was regarded by Cachon et al. as a "large vacuole", not a pusule at all, and the small collecting pusule, 6 μm in diameter, was considered as having a similarly-sized companion.) Since Protoperidinium and Kofoidinium are relatively distantly related dinoflagellates, it would not be surprising should they have dissimilar myonemal structures.

The situation in P. spinulosum is quite different than that in K. pavillardi. The structures that might pass as myonemes in P. spinulosum are discrete and multiple, not a single continuous structure as in K. pavillardi. Three distinct myonemal bands are present; one connecting osmiophilic ring to sac pusule striated collar (and orthogonal strut), another connecting osmiophilic ring to the duct of

the collecting pusule and thence to the adjacent striated collar, and a third connecting this latter duct with the pore plate. These myonemal bands typically appear to be amorphous, but regular striations are faintly discernible in places; they may be composed of the same material that constitutes the osmiophilic ring, but at present it can only be said that these diverse structures have identical, nearly featureless electron-dense appearances.

The existence of striated collars, which were not mentioned by Cachon et al., have also been noted in Peridiniopsis berolinense by Wedemayer and Wilcox (1984) and in Gymnodinium sp. by Roberts (1986). The striated collars in P. spinulosum are rather robust, with a thickness of 0.3 μm as opposed to 0.1 μm in Gymnodinium sp.. The existence of a striated root associated with the basal bodies (a common situation among protists) cannot yet be confirmed in P. spinulosum. However, an amorphous electron-dense material surrounds the proximal part of the microtubular root in cell C; this may be related to the striated root. Such an amorphous structure is present in cell F as well. Further, the microtubular root in cell C is associated with a striated collar; recall that the striated root which constitutes a myoneme in K. pavillardi wrapped around the duct of a pusule in a location similar to that of the striated collars. Interestingly, a distinctly striated structure is attached to the outer wall of the m.b. in P. punctulatum, but little can be inferred from this one section. The myonemal system in Protoperidinium needs to be examined further to determine whether there is ever any involvement of the flagellar striated root (where it exists) with other myonemal structures, and to

examine the nature of such striated structures as the one found in P. punctulatum. Since flagellar root structures may be contractile (Sleigh, 1979), one must be mindful of the potential for the generation of forces within the myonemal system.

The pallium

Several details of the pallium deserve comment. The commonly encountered lack of an inner membrane adjacent to the diatom frustule is startling. Certainly, the contents of the pallium must be continuously bounded by a plasma membrane, but it seems that what must have been an inner plasma membrane adjacent to the prey diatom (and is in fact found in the pallium of cell B) is absent in cells A, and C. Only a single outer membrane is found, enclosing a multitude of empty vesicles (many of which are closely appressed to the outer membrane) next to the frustule. This situation is diagrammatically presented in Fig. 96. Either the putative inner membrane has been destroyed during fixation, perhaps becoming artifactually reorganized as a series of small vesicles, or the inner membrane so reorganize in life. Such a single outer membrane seems structurely weak and vulnerable to lysis; this situation needs further investigation, utilizing carefully adjusted fixation techniques that would prevent any extraction of cytoplasmic components.

Additional interesting features of the pallium include a filamentous fringe covering the stalk or sulcal region of the pallium, and a series of transverse bands spaced 200 nm apart. These bands are similar to those seen lining the sulcus of Peridiniopsis berolinense (Wedemayer and Wilcox, 1984) in Fig. 14, which are spaced only 50 nm

apart. The filamentous fringe is similar to that seen in the cytoplasmic appendage in cell E (Fig. 52) but not seen on the pseudopod in pre-feeding cell F (which was preserved by a different method). It is possible that the fringe seen in Figs. 4 and 52 have the same origin, according to the following reasoning: the small pseudopod of cell F is very possibly the tow filament observed during the capture of prey organisms by several species of Protoperidinium, including P. spinulosum (chapter 3). The presence of microtubular rows may explain the gradual contraction of this tow filament prior to the envelopment of the prey by the pallium. Perhaps this filament, trailing outside the sulcus of a cell searching for food, adheres to a successfully encountered diatom (assisted by a sticky glycocalyx) and remains in place, while shortening, as additional pseudopodal structures either follow the outer surface of the tow filament to reach the attached prey or stream through the center of the filament, incorporating the components of the tow filament into the pallium itself. For example, perhaps the filamentous fringe seen in Fig. 4 was derived from the elaborate glycocalyx of the tow filament (Fig. 52). These scenarios are depicted diagrammatically in Fig. 96.

Thecal structures

The manner in which the osmiophilic and the striated collar of the sac pusule are anchored to the inner thecal protuberance near the posterior flagellar pore is intriguing. Analysis of the cell C serial section sequence shows that this protuberance is composed of three minute thecal plates only a few micrometers in size that are attached to the right sulcal plate, as shown in Figure 93. This protuberance

has been documented with scanning electron microscopy in an isolated hypotheca of Protoperidinium grande by Gocht and Netzel (1974). Their Fig. 5 clearly depicts the inner surface of the pore plate and what appear as a long narrow slit (the flagellar pores) just anterior to the posterior protuberance. The three diminutive sulcal plates seen in Fig. 93 correspond to the single "posterior accessory sulcal plate" described by Balech (1974). Either Balech did not investigate P. spinulosum or the three minute plates cannot be readily disarticulated by conventional bleach techniques. Also, Balech (1974) stated that the accessory sulcal plate is connected to the left sulcal plate, not the right sulcal plate as shown in Fig. 93. A second, shallow inner protuberance associated with the anterior flagellar pore serves as an anchor point for thick bands connecting the osmiophilic ring, collecting pusule striated collar, and the pore plate.

The pore plate or the median sulcal plate, which has been described by Balech (1974) as a "membranous" (i.e., very thin) ovoid structure, has a characteristic fibrous structure in both P. spinulosum and P. hirobis. In P. spinulosum the pore plate has a conspicuous outer osmiophilic layer which is connected to a myonemal element. It would be remarkable if this apparently non-rigid plate was able to deform from forces applied by the myonemal band, thereby modulating the diameter of the posterior flagellar pore. Such an adaptation may be advantageous to a dinoflagellate endeavoring to reduce the duration of pallium deployment or retraction. However, the diameter of the flagellar pore in cell F is not significantly wider than that of other cells, even though the pallium was soon to be deployed. This idea may

deserve additional study.

This study is the first to reveal the complex ultrastructure of the pallium and the inner microtubular basket/pallioplasmic complex in Protoperidinium. These structures are apparently unique among dinoflagellates and other protists, but their existence in Protoperidinium and perhaps other thecate heterotrophic dinoflagellates may be of use in establishing or confirming evolutionary relationships among protists. A greater understanding of the functionings of the pallium requires further morphological analysis as well as experimental cytochemical studies such as the determination of acid phosphatase distributions throughout the dinoflagellate's feeding cycle. Although the delicacy of the pallium and the difficulty with which thecate heterotrophic dinoflagellates are cultured combine to make their study challenging, these protists represent an exciting opportunity to address some basic questions in cell biology.

REFERENCES

Anderson, O.R. 1977. Cytoplasmic fine structure of Nassellarian radiolaria. Mar. Micropaleon. 2:251-264.

Balech, E. 1974. El genero "Protoperidinium" Bergh, 1881 ("Peridinium" Ehrenberg, 1831, Partim). Rev. Mus. Arg. C. Nat. "B. Rivadivia" 4:1-79.

Brugerole, G. 1980. Etude ultrastructurale du flagellé Protrichomonas legeri (Léger 1905), Parasite de l'estomac des Bogues (Box boops). Protistologica 16:353-358.

Cachon, J. and M. Cachon 1971. Protoodinium chattoni Hovasse. Manifestations ultrastructurales des rapports entre le Peridinien et la Meduse-hote: fixation, phagocytose. Arch. Protistenk. Bd. 113:293-305.

Cachon, J., M. Cachon and A. Boillot 1983. Flagellar rootlets as myonemal elements for pusule contractility in dinoflagellates. Cell Motility 3:61-77.

Dodge, J.D. and R.M. Crawford 1970. The morphology and fine structure of Ceratium hirundinella (Dinophyceae). J. Phycol. 6:137-149.

Dodge, J.D. 1971. Fine structure of the Pyrrophyta. Bot. Rev 37:481-507.

Gaines, G, and F.J.R. Taylor 1984. Extracellular feeding in marine dinoflagellates. J. Plank. Res. 6:1057-1061.

Gocht, H. and H. Netzel 1974. Rasterelektronenmikroskopische Untersuchungen am Panzer von Peridinium (Dinoflagellata). Arch. Protistenk. Bd. 116:381-410.

Honigberg, B.M., C.F.T. Mattern, and W.A. Daniel 1971. Fine structure of the mastigont system in Tritrichomonas foetus (Riedmüller). J. Protozool. 18:183-198.

Jacobson, D.M. and D.M. Anderson 1986. Thecate heterotrophic dinoflagellates: feeding behavior and mechanisms. J.Phycol. 22:258-269.

Knobler, R.L., J.G. Stempak and M. Laurenein 1978. Preparation and Analysis of serial sections in electron microscopy. In Principles and Techniques of Electron Microscopy, Vol. 8, M.A. Hayat, ed.. Van Nostrand Reinhild Co., New York. pp. 113-155.

Lee, R.E. 1977. Saprophytic and phagocytic isolates of the colourless heterotrophic dinoflagellate Gyrodinium lebouriae Herdman. J. mar. biol. Ass. U.K. 57:303-315.

Mizuhira, V. and Y. Futaesaku 1972. New fixation for biological membranes using tannic acids. Acta. Histochem. Cytochem. 5:233-236.

Neveux, J. and M.O. Soyer 1976. Characterization des pigments et structure fine de Protoperidinium ovatum Pouchet (Dinoflagellata). Vie Milieu 26:175-199.

Roberts, K.P. 1986. The flagellar apparatus of Gymnodinium sp. (Dinophyceae). J. Phycol. 22:456-466.

Rogers, H.J. and H.R. Perkins 1968. Cell Walls and Membranes. ed. E & FN Spon Ltd. London. 435pp.

Simionescu, N. and M. Simionescu 1976. Galloylglucoses of low molecular weight as mordant in electron microscopy. J. Cell Biol. 70:608-621.

Sleigh, M. 1979. Contractility of the roots of flagella and cilia. Nature 277:263-264.

Small, E.B. and D.H. Lynn 1985. Phylum Ciliophora Doflein, 1901. In Lee, J.J., S.H. Hutner, and E.C. Bovee (eds), An Illustrated Guide to the Protozoa, Society of Protozoologists, Lawrence, KS. pp.393-575.

Spector, D.L., L.A. Pfiester and R.E. Triemer 1981. Ultrastructure of the dinoflagellate Peridinium cinctum f. ovoplanum. II. Light and electron microscopic observations on fertilization. Amer. J. Bot. 68:34-43.

Spero, H.J. 1982. Phagotrophy in Gymnodinium fungiforme (Pyrrophyta): The peduncle as an organelle of ingestion. J. Phycol. 18:356-360.

Spurr, A.R. 1969. A low viscosity epoxy embedding medium for electron microscopy. J. Ultrastruct. Res. 26:31-43.

Stewart, M.J., S. Schulman and J.P. Vanderberg 1985. Rhoptry secretion of membranous whorls by Plasmodium berghi sporozoites. J. Protozool. 32:280-283.

Swale, E.M.F. and J.H. Belcher 1974. Gyromitus disomatus Skuja- a free-living colourless flagellate. Arch. Protistenk. Bd. 116:211-220.

Walne, P.L. 1980. Euglenoid flagellates. In Cox, E.R. [ed.] Phytoflagellates, Elsevier North-Holland, Inc., New York, pp.165-212.

Wedemayer, G.J., and L.W. Wilcox 1984. The ultrastructure of the freshwater, colorless dinoflagellate Peridiniopsis berolinense (Lemm) Bourrelly (Mastigophora, Dinoflagellida). J. Protozool. 31:444-453.

Figure 1. Schematic cut-away illustration of cell C (dorsal view) showing arrangement of relevant organelles. Nucleus (brown) has been mostly cut away to reveal (pink) pusules and (gold) microtubular basket. Basal bodies and flagella (magenta) enter pusule ducts inside of small black striated collars which encircle the ducts. The outline of the pore plate is indicate behind collecting pusule duct; the transverse flagellum passes through this duct and exits through the anterior flagellar pore (not shown) bordering pore plate. Note the thecal protuberance (grey) adjacent to the relatively large, black osmiophilic ring at base of the microtubular basket..

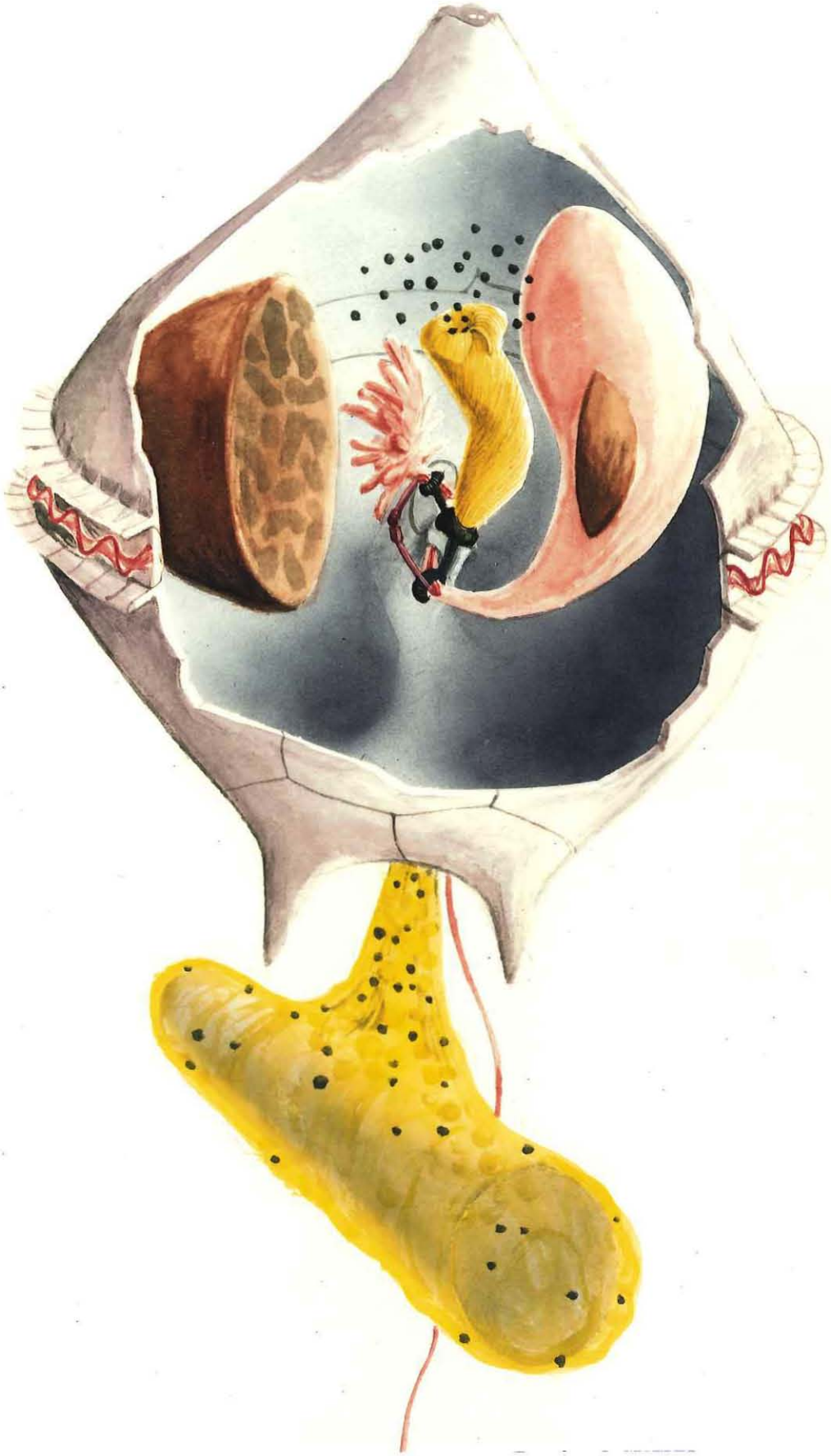

Abbreviations:

b, osmiophilic band
bb, basal body
cp, collecting pusule
er, endoplasmic reticulum
ga, golgi apparatus
lf, longitudinal flagellum
m, mitochondria
N, nucleus
os, orthogonal strut
p, posterior flagellar pore
pp, flagellar pore plate
sp, sac pusule
tf, transverse flagellum

Plate I. Pallium of Protoperidinium spinulosum. Scale bars = 1 μm unless otherwise indicated.

Figure 2. Longitudinal section of cell A (antapex) with pallium which surrounds the diatom Eucampia zoodiacus (frustule wall, thin arrow) emerging through flagellar pore (p). Note electron-dense droplets (thick arrow) and microtubules (curved arrow).

Figure 3. Pallium extension of cell C surrounding hollow spine of Chaetoceros sp.. Note microfilaments (arrow) which are enlarged in inset at bottom of figure.

Figure 4. Proximal stalk region of pallium of cell A showing periodic thickenings (thin arrows) of membrane and outer fringe of filaments (thick arrow).

Figure 5. Pallium envelope of cell A surrounding Eucampia zoodiacus prey. Note lack of inner limiting membrane.


2
P
3
4
5

Plate II. Pallium of *Protoperidinium spinulosum* (cont'd).

Figure 6. Pallium of cell B, with transverse section of antapical horn of *P. spinulosum*. An inner membrane (thin arrows) surrounds *Eucampia zoodiacus* frustules. Note electron-dense droplets (thick arrow), arched microtubular ribbons (curved arrow) and the highly degraded condition of the diatom cytoplasm.

Figure 7. Pallium of cell A surrounding *Eucampia zoodiacus* with degraded cytoplasm. Note electron-dense droplets (thick arrow) and delicate outer pallium membrane (thin arrow). Inset shows high magnification of outer membrane, which appears as a single 7 nm lipid bilayer (arrow); scale bar = 100nm.

Figure 8. Microtubular ribbons of cell B (see Fig. 6).

Figure 9. Bifurcated microtubular ribbon in pallium of cell C, also visible in Figs. 28,29.

Figure 10. Microtubular ribbon as in Fig. 8 featuring filamentous connections between tubules (arrow).

Figure 11. Glancing tangential section of outer pallium membrane of cell C showing regularly spaced transverse bands.

Figure 12. Pallium envelope of cell D surrounding recently captured *Ditylum brightwellii* cell. Note vesicle filled with granular material (arrow). (+ tannin).

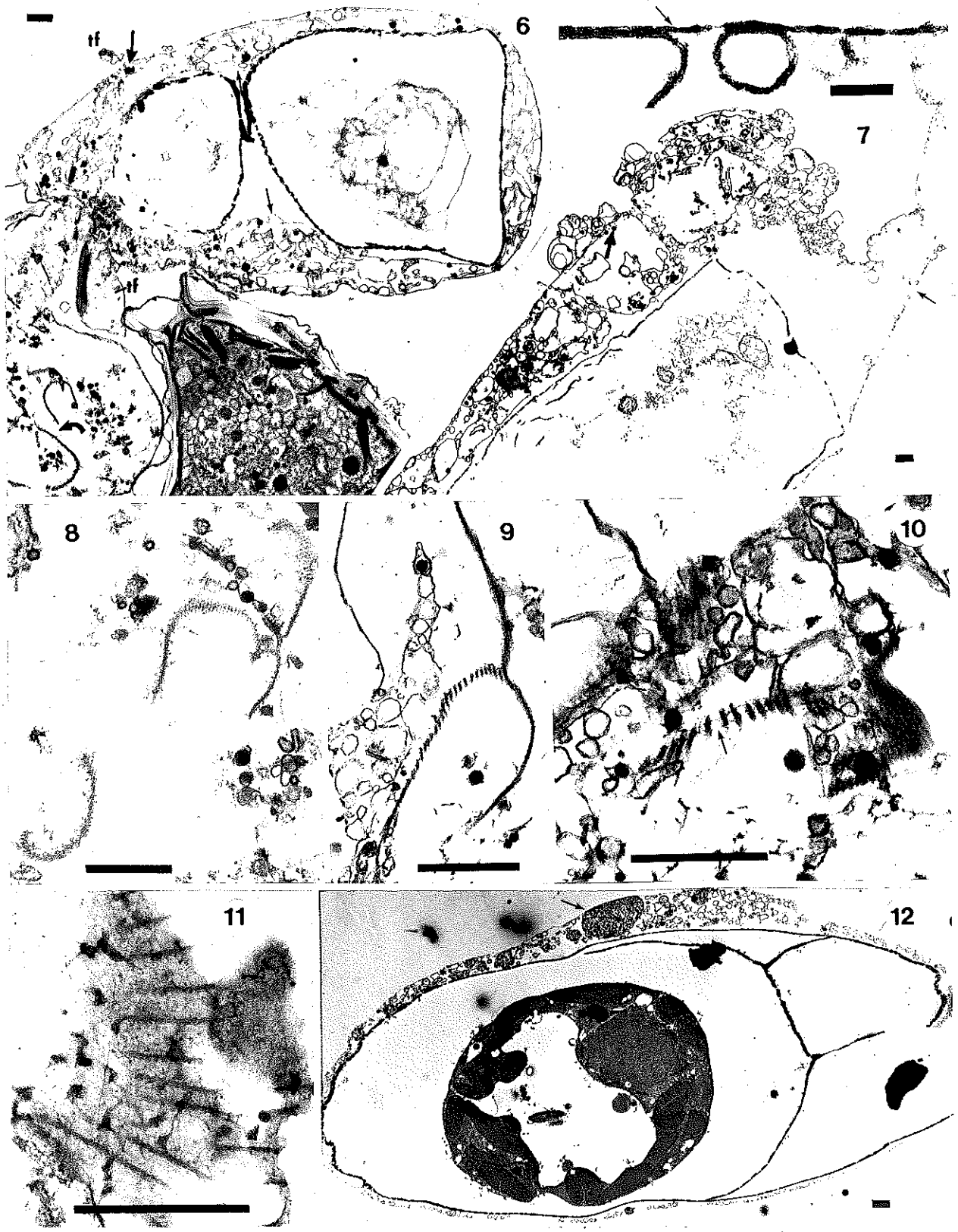
6
tf
tf
7
8
9
10
11
12

Plate III. Microtubular basket (m.b.) of Protoperidinium spinulosum.

Figure 13. Cell A with large sac pusule, nucleus and two portions of m.b.: posterior (thick arrow) and anterior (curved arrow). Note cluster of spherical vesicles (thin arrows) which lie in a relatively non-dense central cytoplasmic region and the 'empty' appearance of the transverse flagellum (tf).

Figure 14. Posterior end of m.b. (near flagellar pore of cell A) with electron-dense droplets. Note osmiophilic ring (thick arrow) with surrounding electron-lucent zone and row of microtubules (thin arrow).

Figure 15. Anterior end of m.b. of cell C. Note several rows of microtubules (thin arrows), arched bands (thick arrows) and mitochondria (m) between. The arched bands appear to be recurved apical flap of the m.b., as may be seen by noting the similarity of the arrangement along the dashed line in Fig. 17. Note lack of electron-dense droplets in the region directly between m.b. and arched bands.

Figure 16. Anterior end of m.b. (near nucleus of cell A) with a row of microtubules (thin arrows) which terminate (curved arrows), regular membranous channels (thick arrow) and large granular vesicles (asterisk). Note invagination of nuclear envelope (open arrow).

Figure 17. Anterior end of m.b. of cell B showing opening adjacent nucleus. Note regularly space membranous channels (arrows) on dorsal face of m.b. adjacent to cluster of mitochondria. Electron-dense droplets are absent from region in 'crook' of recurved m.b. wall. Dashed line indicates the likely orientation which resulted in Fig. 15.

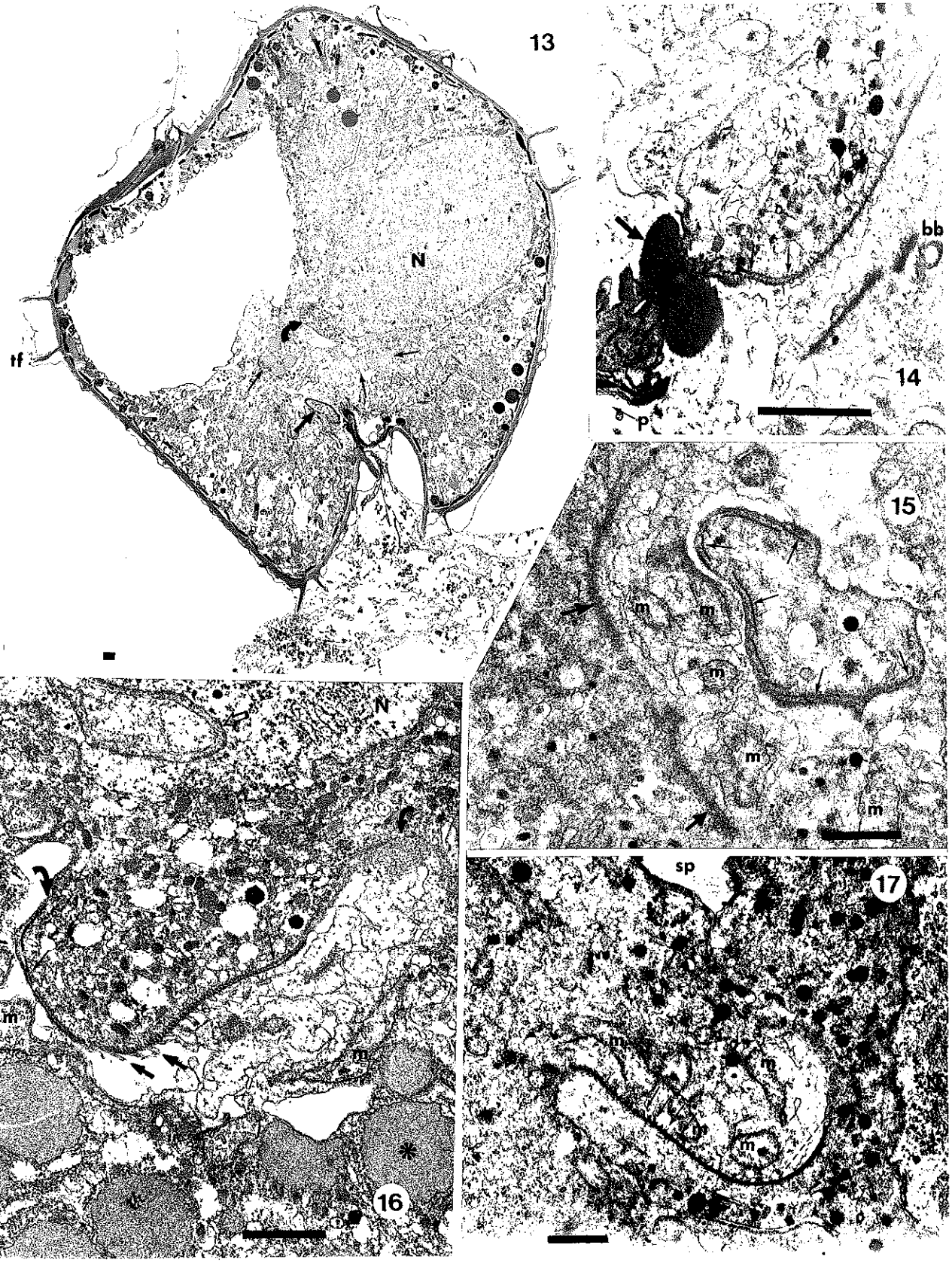
13
N
tf
bb
14
p
15
m
m
m
m
m
m
N
m
m
m
16
*
sp
17
m
m
m
m
p

Plate IV. Serial oblique-transverse sections of feeding Protoperidinium spinulosum, cell B, from antapex to mid-cell.

Figure 18. Section posterior to flagellar pore, showing stalk of pallium (thick arrow) and cluster of mucocysts with converging apertures on left ventral hypotheca (thin arrow).

Figure 19. Section through flagellar pore (thin arrow) with pore plate (=median sulcal plate) shaped like the curve side of a reversed "B"(thick arrow). Pallium (arrow) and longitudinal flagellum (lf) in sac pusule duct are juxtaposed. See Fig. 95 for diagram of pore plate.

Figure 20. Section anterior to flagellar pore. Note corrugations (thin arrow) within electron-lucent zone. Transverse flagellum (tf) has exited cell through anterior flagellar pore (not shown).

Figure 21. Osmiophilic ring with surrounding electron-lucent zone.

Figure 22. Central lumen of osmiophilic ring (white arrows), barely discernible, filled with pallioplasm. Regular ridges occur on osmiophilic ring (black arrows).

Figures 23-27: These four section were included in the three-dimensional reconstruction of the m.b. (Fig. 93a). Note the elongation and reorientation of the m.b. (thick arrows).

Figure 23. M.b. indicated by thick arrow. Both striated collars (that of sac pusule, sp, and collecting pusule, cp) are section off-center and appear "closed". Electron-dense band (b), which joins osmiophilic ring in lower sections, is joined to striated collar of collecting pusule by thin strand. Note microtubular root (arrow) of basal bodies (not shown) which seems to join striated collar of sac pusule within a electron-lucent cytoplasmic region between the pusules.

Figure 24. See Fig. 23; note "open" collars (thin arrows) around each pusule. Note electron-dense droplets within m.b. (thick arrow). Trichocyst (t) resembles electron-dense band at low magnification.

Figure 25. M.b., showing discontinuous peripheral microtubules (thin arrows), distinct, electron-dense outer membrane outside of microtubular row (paired arrows) and central microtubular row (thick arrow).

Figure 26. M.b. curving toward nucleus, with electron lucent zone persisting between pusules. Collecting pusule has long radiating tubules (arrows).

Figure 27. M.b. opening (arrow) adjacent to nucleus, anterior to collecting pusule. See Fig. 16 for enlargement.

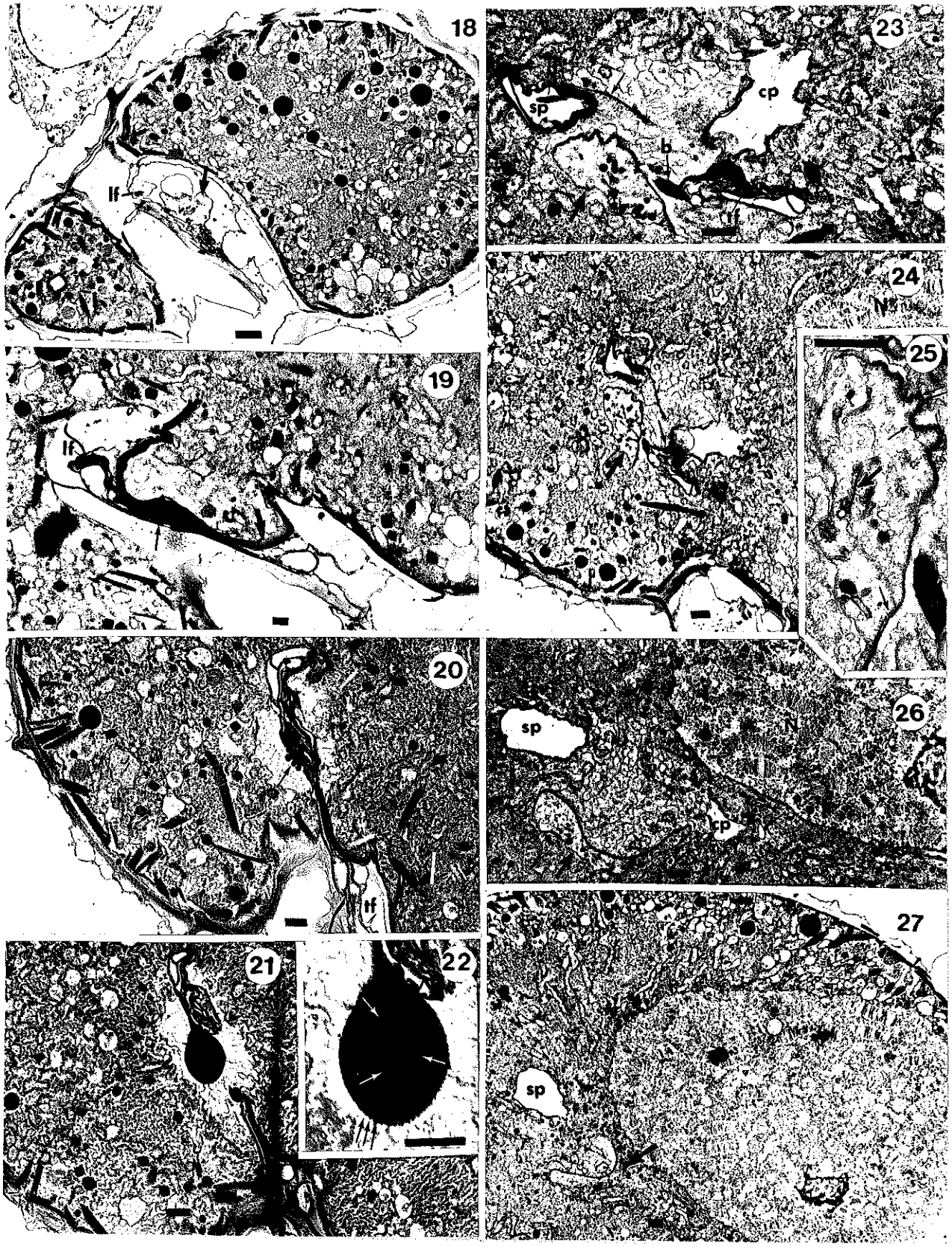
18
lf
23
sp
cp
b
lf
24
N
25
19
lf
20
lf
26
sp
N
cp
21
22
27
sp

Plate V. Serial oblique-longitudinal sections of feeding Protoperidinium spinulosum (cell C). Section angle parallels ventral face of hypotheca.

Figure 28. Sulcus with protruding pore plate (thick arrow) and bifurcated microtubular ribbon (thin arrow) within pallium.

Figure 29. Section dorsal to above; glancing section of m.b. (thin arrow) and beginning of electron-lucent zone (thick arrow) adjacent to osmiophilic ring. Note emergence of transverse flagellum (curved arrow).

Figure 30. M.b. with microtubules along inside edge (thin arrows). Note bundles of microfilaments (thick arrow) and anterior flagellar pore (curved arrow) and anterior thecal protuberance (paired arrows).

Figure 31. M.b. and ventral face of osmiophilic ring (thin arrow). Note concavity of m.b. and associated parallel network of membranous channels (thick arrow). Osmiophilic band (b) connects thecal structure (paire arrows) in duct of collecting pusule (cp) with dark band within pore plate (pp).

Figure 32. Osmiophilic ring, tangential section of ventral face. Banded structure (arrows) marginally discernible. Scale bar=100 nm.

Figure 33. See Fig. 31 legend. Note tubules from collecting pusule (thick arrows) and electron-dense band approaching osmiophilic ring (thin arrow). Inset detail this band, in which cross striations are marginally discernible (arrows).

Figure 34. See Fig. 31 legend. Note parallel membranous channels (thin arrows) and thick (striated) band (thick arrow) connecting osmiophilic ring and thecal elements (curved arrow) within collecting pusule.

Figure 35. Pallioplasm passing through osmiophilic ring into pallium. Transverse flagellum on inner side of striated collar of collecting pusule duct.

Figure 36. Detail of striated collar enclosing transverse flagellum, with several striations indicated (arrows).

Figure 37. Wide-angle view of m.b. (curved arrows), whose anterior portion is surrounded by a large vacuolar space, basal bodies (bb) and sac pusular duct (thick arrow) next to accessory sulcal plates (thin arrows). Orthogonal strut (os) of the anterior ancillary sulcal plate adjacent to the electron-dense band which connects striated collar of sac pusule to osmiophilic ring. Note ring of golgi apparatus (white arrows).

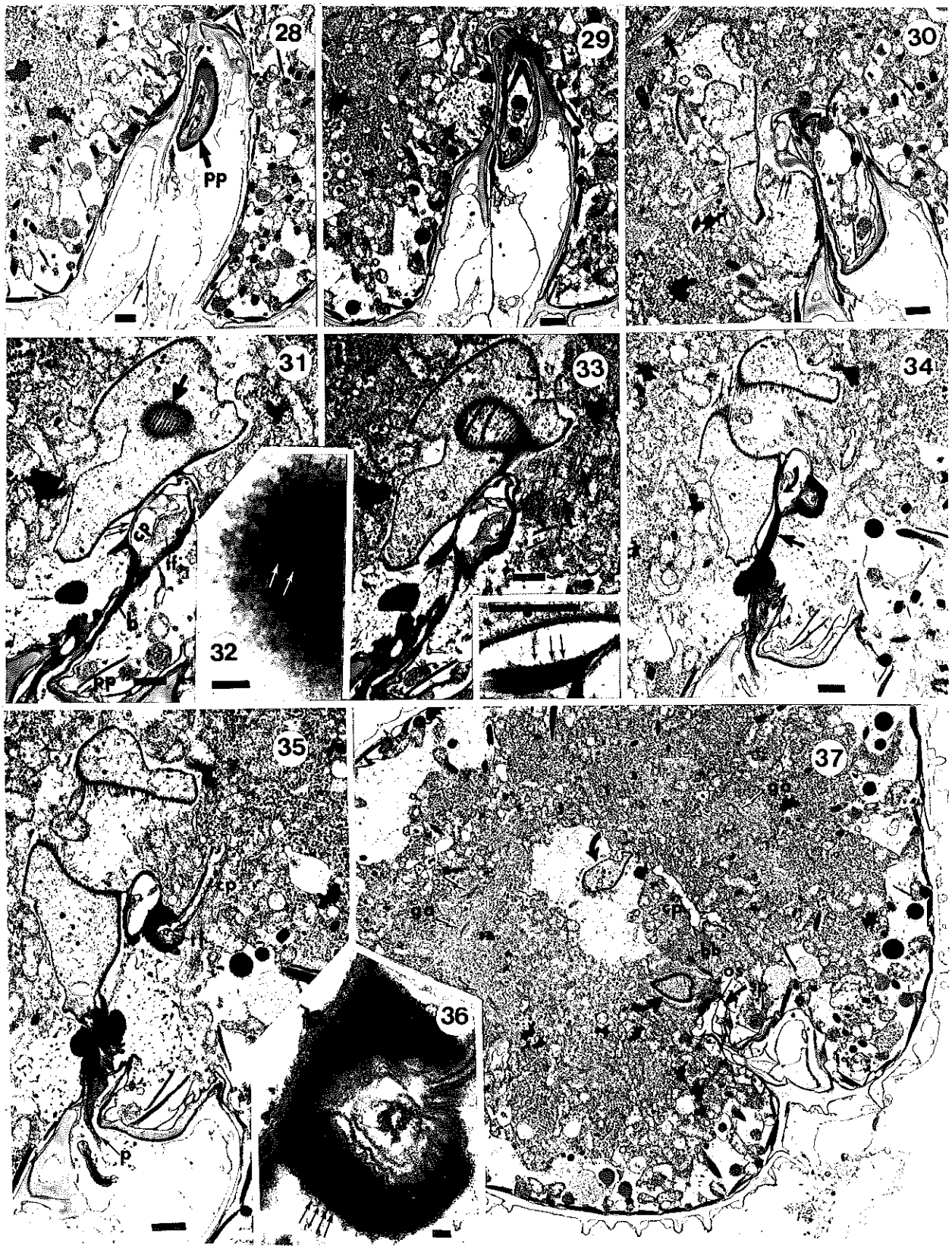
28
PP
29
30
31
cp
if
b
PP
32
33
34
35
cp
p
36
37
cp
pb

Plate VI. Serial oblique-longitudinal sections of Protoperidinium spinulosum (cell C), cont'd.

Figure. 38. Glancing, tangential section of dorsal face of m.b., showing parallel membranous channels (thick arrow). Note striated collar (double arrow) about duct of sac pusule with stub of (detached) longitudinal flagellum (white arrow) and dense cytoplasm around basal body of transverse flagellum (tf). Black diagonal line is artifact in formvar support film.

Figure 39. Detail of base of flagella (note chevron-shaped structure within longitudinal flagellum, arrow) and associated microtubular root (thick arrow) with electron-dense substance adhering to upper portion of root and striated collar of sac pusule. Note apparent connection between microtubules and striated collar.

Figure 40. Detail of striated collar of sac pusule (striation bands indicated). Scale bar = 100nm.

Figure 41. Tangential section of m.b. slightly deeper that that of Fig. 38. Note membranous channels (thick arrows) which are angled 30° from the microtubular rows (thin arrows). The membranous channels have somewhat of a beaded appearance (arrow). Scale bar = 100nm,

Figure 42. Joined basal bodies and microtubular root (arrow).

Figure 43. Anterior end of m.b. (thick arrow) and two bands = recurved segments of m.b. (thin arrows). Golgi apparatus indicated by white arrows. Peripheral dark curved lines are wrinkle-artifacts.

Figure 44. Section between anterior end of m.b. and nucleus. Note dozens of electron-dense droplets (thin arrows) and ring of golgi apparatus (white arrows).

Figure 45. Detail of central cytoplasmic region rich in electron-dense droplets (left) and denser, peripheral cytoplasm (right) with golgi apparatus (white arrows) between. Note filament bundles (black arrows).

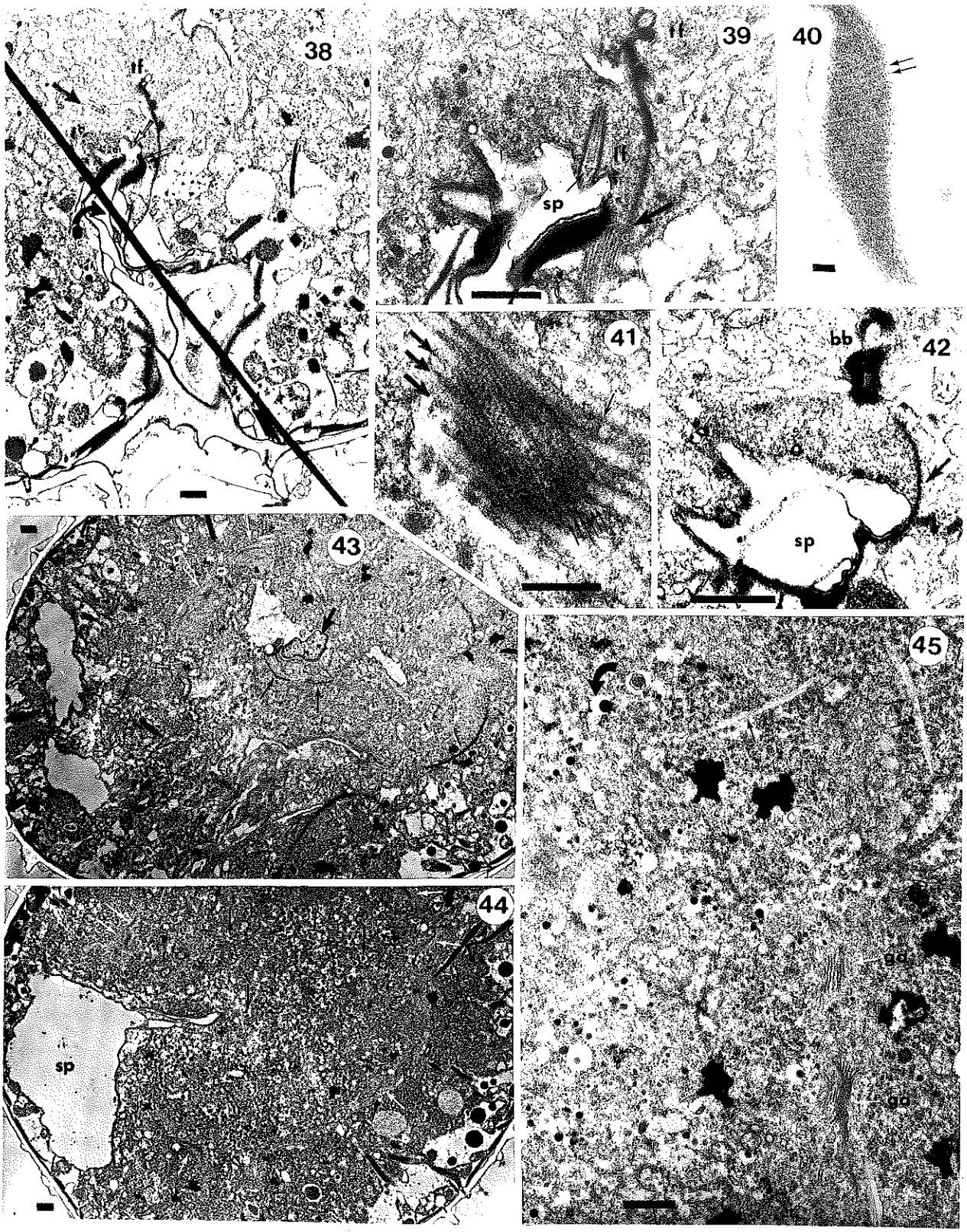
38
tf
39
tf
tf
sp
40
41
42
bb
sp
43
44
sp
45
gg
gg

Figure VII. Non-feeding Protoperidinium spinulosum, cell E.

Figure 46. Mid-cell longitudinal section through flagellar pore (thick arrow). Longitudinal encountered thrice (thin arrows). Note myriad peripheral vesicles.

Figure 47. Scanning election micrograph of non-feeding Protoperidinium spinulosum (transverse diameter = 50μm) Note dimple-like ventral pore to (cell's) left of sulcus.

Figure 48. Antapical view of sulcus as above showing groove in which the flagellar pores lie enclosed between large left sulcal list (thin arrow) and right sulcal list (thick arrow). Longitudinal flagellum present (curved arrow).

Figure 49. M.b. from section situated ventral to that of Fig. 46 (see Fig. 52). Note peripheral rows of microtubules (thin arrows) and inner microtubules (thick arrow).

Figure 50. Upper elongation of m.b. detailing microtubular row.

Figure 51. Detail of flagellar pore (see Fig. 46). "Residual" pseudopodal mass present with glycocalyx (thin arrows). Note three-layered composition of pore plate (pp) and normal, homogeneous structure of accessory sulcal plate (arrowhead).

Figure 52. Detail of flagella-like cytoplasmic appendage (see Fig. 53). Note conspicuous filamentous fringe and inconspicuous inner row of microtubules (arrows).

Figure 53. Section ventral to that of Fig. 46, showing m.b. within large vacuole and a fringed appendage (arrow).

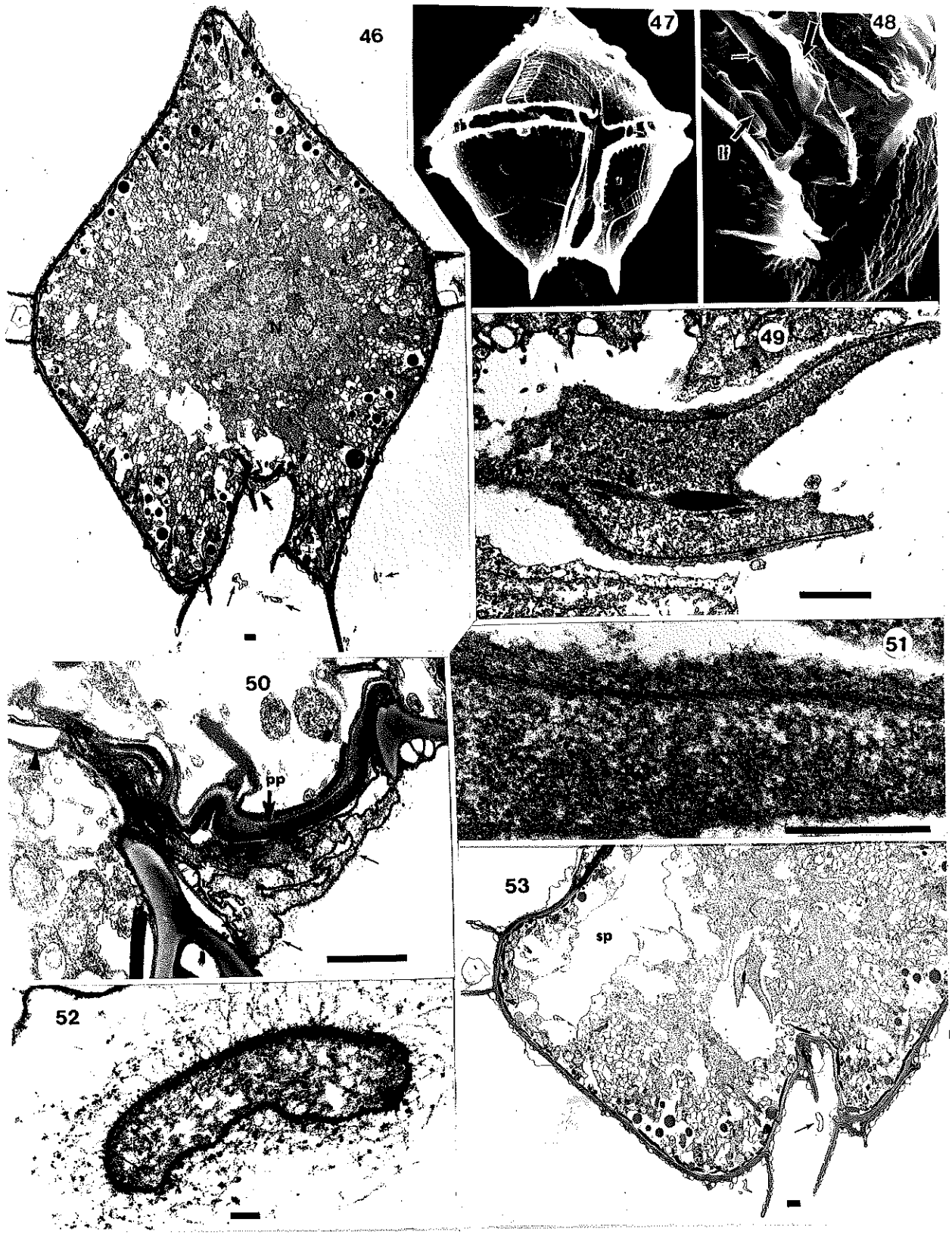
46
N
47
48
49
50
pp
51
52
53
sp

Plate VIII. Serial oblique-longitudinal sections of non-feeding P. spinulosum cell F (+ tannin).

Figure 54. Mid-cell section with large electron-lucent vesicles (thin arrows) lying within smooth cytoplasmic region adjacent to concavity in nucleus (note glancing section of right lobe of nucleus (thick arrow), and row of golgi apparatus (white arrows). Outer membranes of mitochondria are prominently stained.

Figure 55. Section ventral Fig. 53 showing electron lucent vesicles (thin arrows) and elongate m.b. (thick arrow).

Figure 56. Region surrounding m.b. (thick arrow). Note smooth cytoplasm between sac pusule and nucleus, cluster of electron-dense bodies (thin arrow) and golgi apparatus (white arrow).

Figure 57. Detail of clustered bodies.

Figure 58. M.b. (thick arrow) adjacent to sulcus with three rows of microtubules (thin arrows). Pore plate (curved arrow) has very wide electron lucent layer.

Figure 59. M.b. in close proximity to region of smooth cytoplasm between sac pusule and nucleus. Detail of electron dense regions of m.b. in Fig. 71.

Figure 60. Detail of electron-lucent vesicle and sac pusule wall with thin cytoplasmic lining (thin arrow).

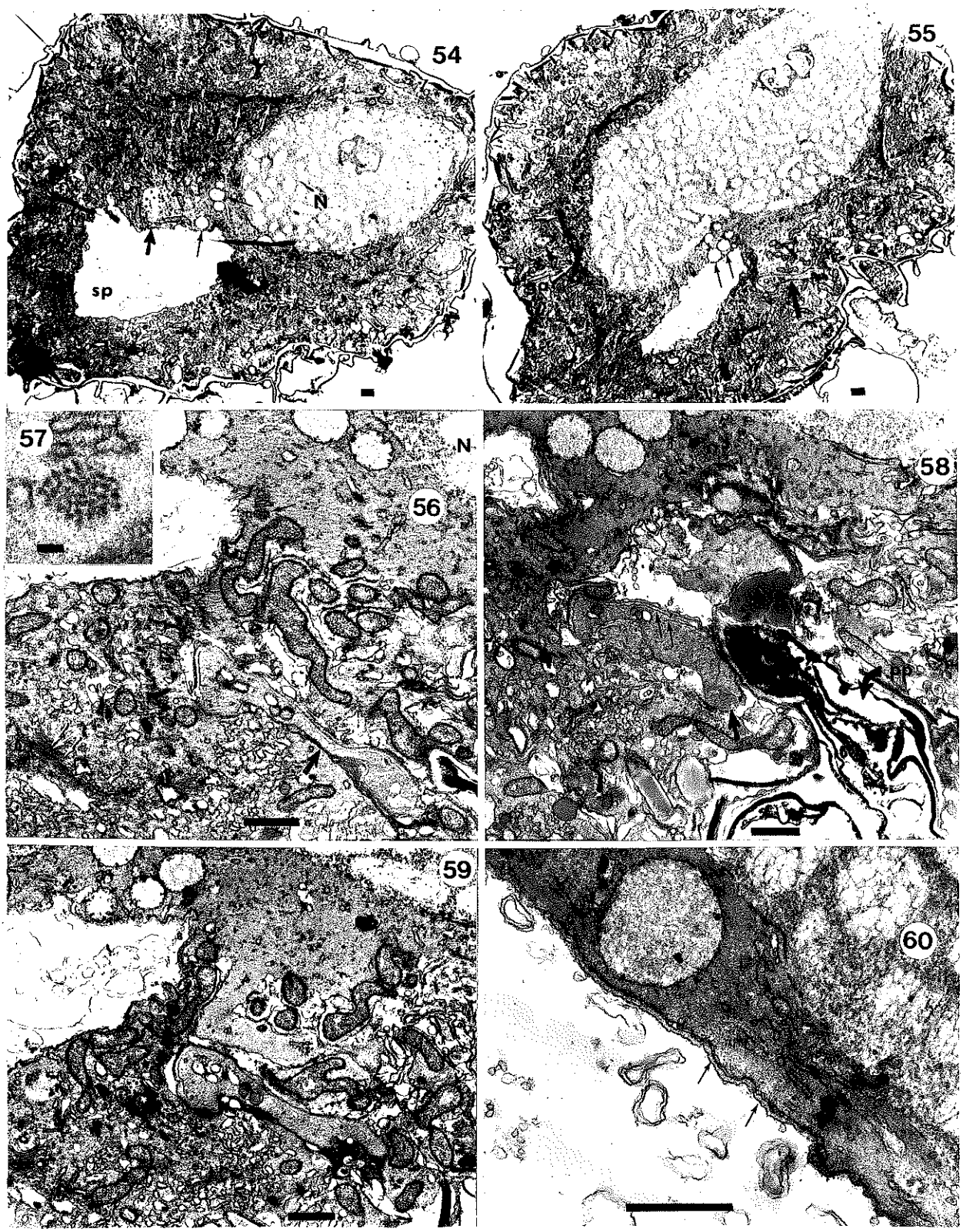
54
N
sp
55
57
N
56
58
PP
59
60

Plate IX. Serial oblique-longitudinal sections of non-feeding P. spinulosum cell F (+ tannin), cont'd.

Figure 61. M.b. adjacent to part of osmiophilic ring (thick arrow) and electron lucent zone (asterisk). Note m.b. microtubular rows (thin arrows), basal body (bb) and smooth endoplasmic reticulum (er).

Figure 62. Pallioplasm of m.b. passing out through osmiophilic ring (thick arrow) which appears to be continuous with a small pseudopod containing microtubules (curved arrow). Note amorphous material surrounding microtubular root of basal body (thin arrows).

Figure 63. Ventral side of osmiophilic ring (thick arrow) and basal body with microtubular root (thin arrows). Cytoplasm surrounding basal body appears continuous with that of the sac pusule lining (see cytoplasmic discontinuity, white arrows).

Figure 64. Detail of m.b and osmiophilic ring showing microtubular rows (arrows).

Figure 65, 66. pseudopod emerging from congested sulcus. Note peripheral microtubular row (arrows).

Figure 67. Pseudopod, as in Fig. 63, showing microtubules crossing over from right edge to left (arrows).

Figure 68. Transverse flagellum with matrix similar to that of pseudopod; scale bar = 100nm.

Figure 69. Detail of microtubules in pseudopod; scale bar = 100nm.

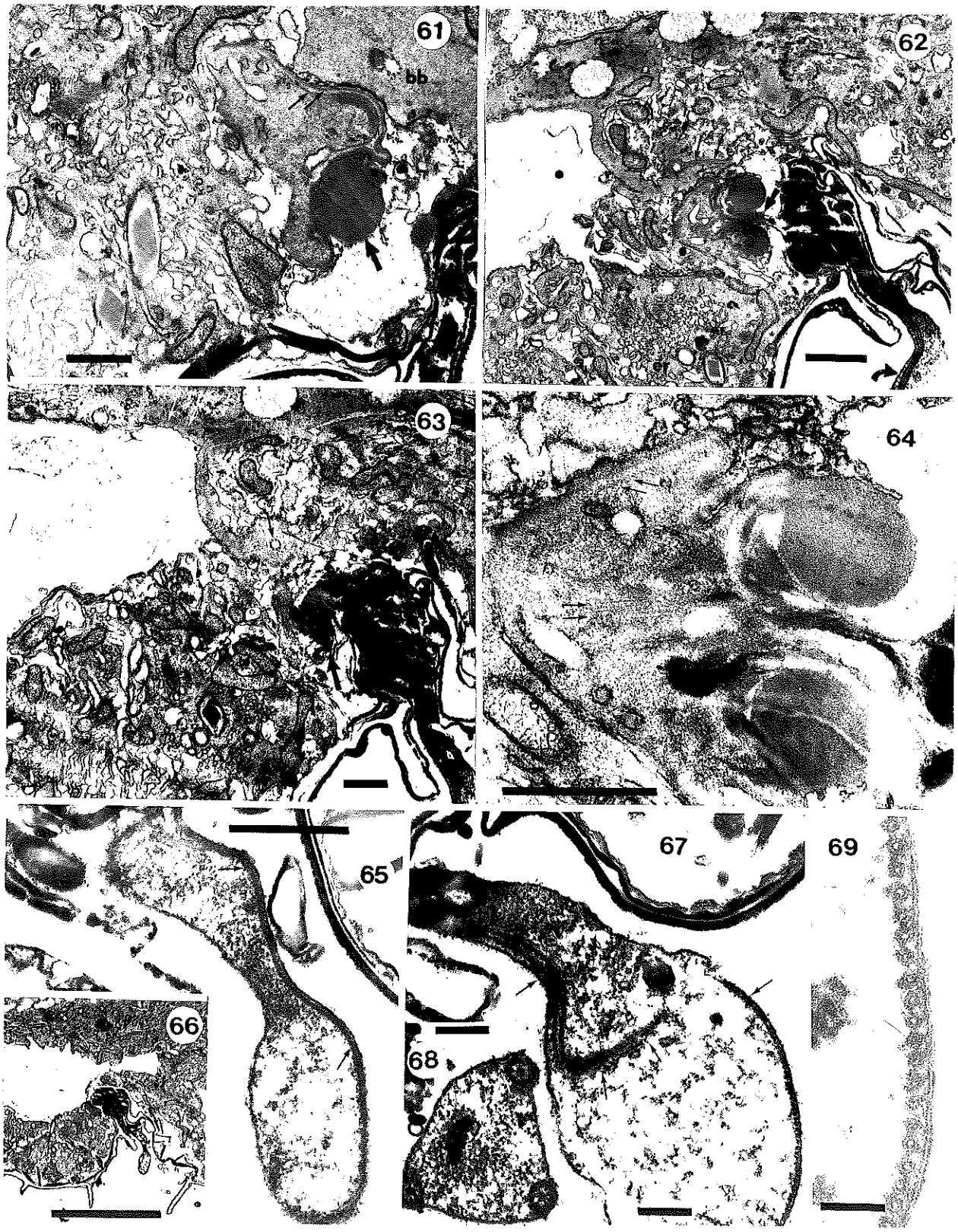
61
bb
62
63
64
65
66
67
68
69

Plate X. Serial oblique-longitudinal sections of non-feeding P. spinulosum cell F (+ tannin), cont'd.

Figure 70. Poorly sectioned sulcal region; fingerprint-like patterns (arrows) barely discernible within dark "chatter" bands.

Figure 71. Detail of fingerprint patterns, including portion of mosaic of longer exposures revealing continuation of concentric bands; scale bar = 100nm.

Figure 72. System of whorled membranes at posterior end of m.b. (seen also in Fig. 59) whose lateral walls are indicated by arrows..

Figure 73. Tracing of Fig. 71 mosaic (employing additional mosaic elements) showing three systems of membranous whorls; scale bar = 100nm.

Figure 74. Sac pusule containing concentric membranous whorls (arrows).

Figure 75. Detail of whorl; scale bar = 100nm.

Figure 76. Non-membranous contents of sac pusule.


70

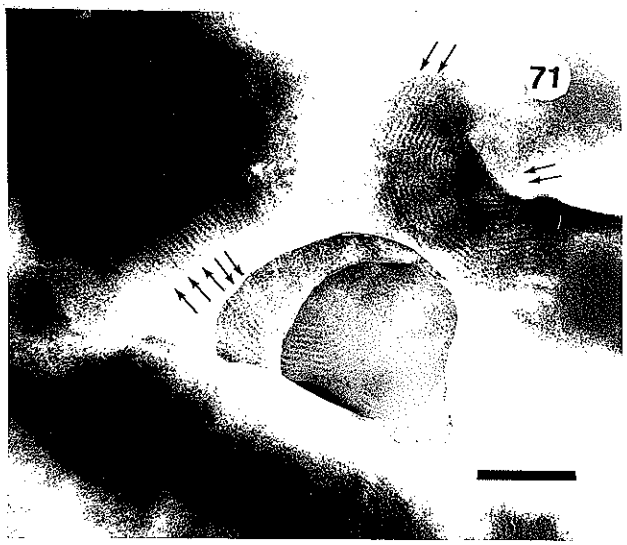
71

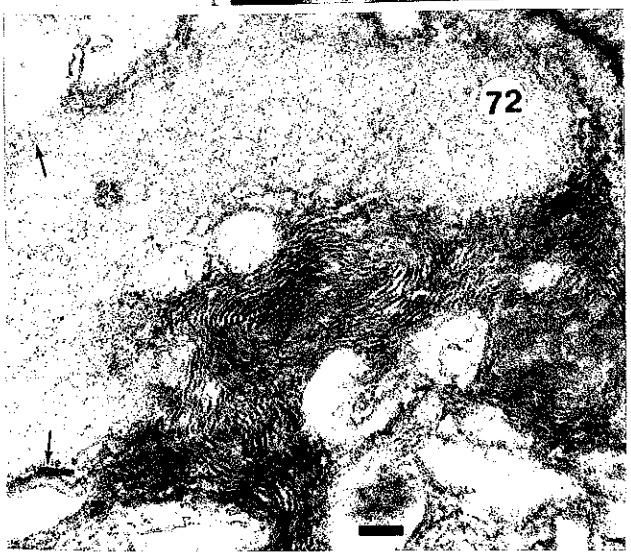
72


73

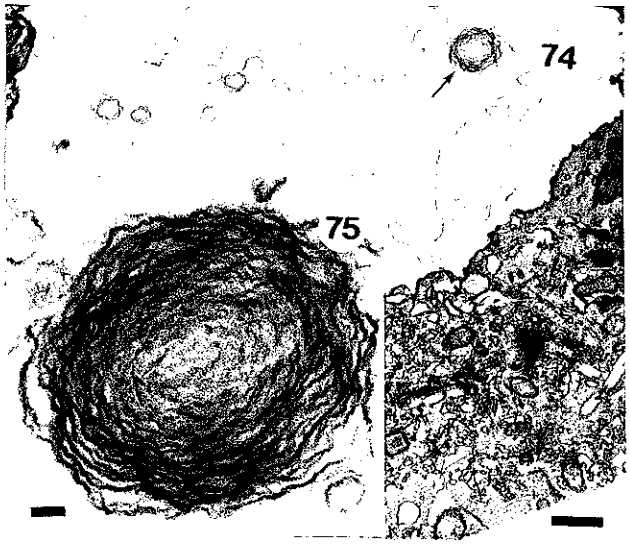
74
75

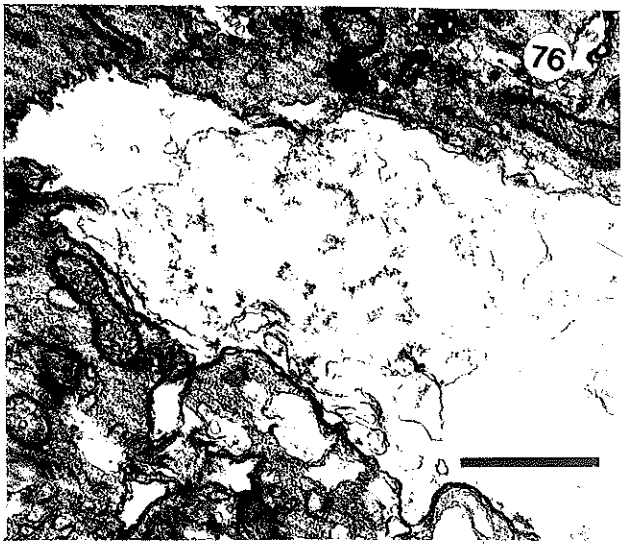
76

Plate XI. Miscellaneous organelles of Protoperidinium spinulosum.

Figure 77. Ventral oblique-longitudinal section of cell C hypotheca showing cluster of mucocyst vesicles (arrow).

Figure 78. Detail of mucocyst cluster with a glancing section through thecal apertures (white arrows) of mucocysts. Transverse flagellum also shown.

Figure 79. Sub-thecal lamellar bodies of cell A showing alternation of thin and thick bands (arrows); scale bar = 100nm.

Figure 80. Cluster of mucocysts (arrows) located on left ventral hypotheca of cell F (+ tannin) with converging apertures ejecting dense substance (mucus?).

Figure 81. Apical pore of cell C. No conspicuous organelles apparent.

Figure 82. Banded trichocysts (thick arrows) arranged parallel to top and bottom cingular margins of cell A. Note lamellar bodies oriented against theca (white arrows).

Figure 83. Transverse section of trichocyst (cell F, + tannin) showing paracrystalline structure (arrows).

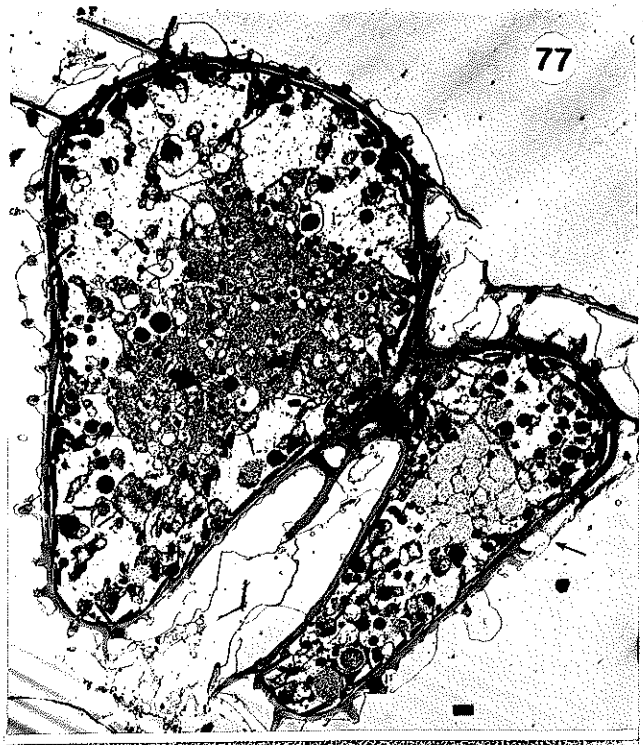
77

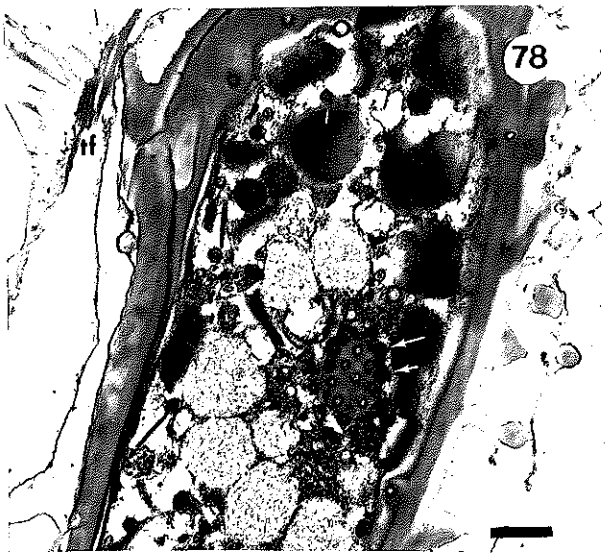
78
ff

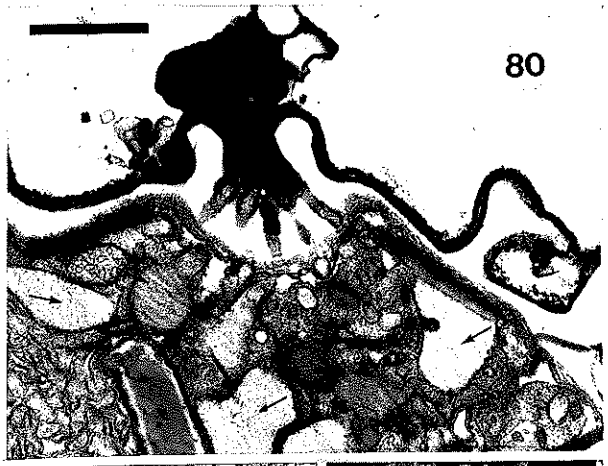
80

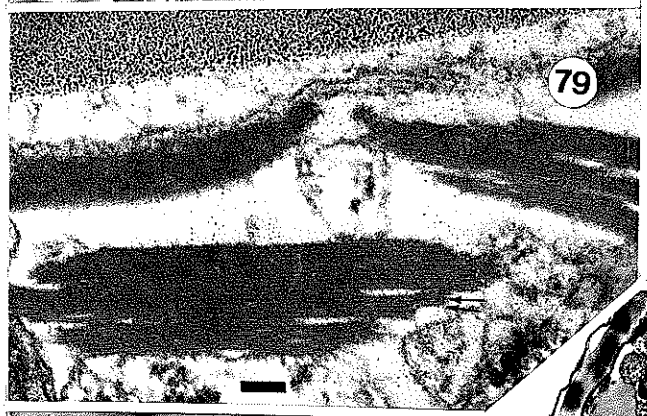
79

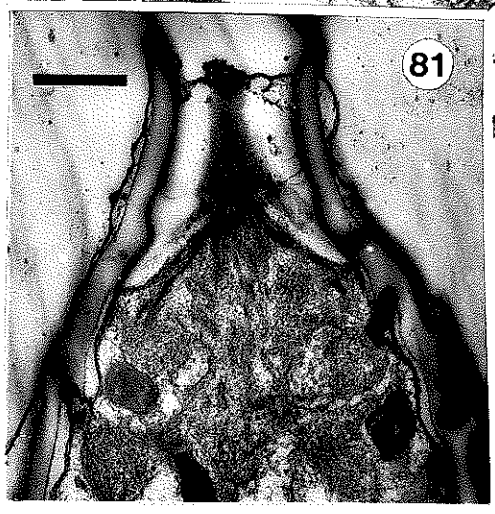
81

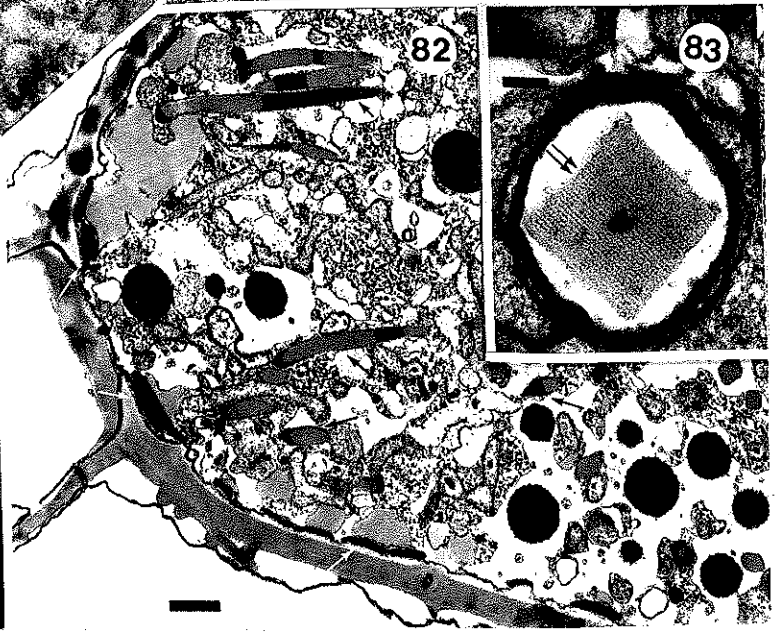
82
83

Plate XII. Feeding apparatus in additional species.

Figures 84-86. Protoperidinium hirobis, longitudinal sections.

Figure 84. Sac and collecting pusules and basal bodies, with stub of longitudinal flagellum entering sac pusule (thick arrow). Note collar about mouth of sac pusule (thin arrows) and thick pore plate (pp).

Figure 85. M.b. (thick arrow) with osmiophilic ring at posterior tip (thin arrow). Note ovoid osmiophilic structures (curved arrows) and central region of relatively electron-lucent cytoplasm bordered by dense cytoplasm (white arrows).

Figure 86. Detail of m.b. with rows of microtubules (white arrows) and osmiophilic bodies (black arrows).

Figure 87-89, 91. Oblea rotunda, oblique sections.

Figure 87. Hypothecal section revealing osmiophilic ring (thick arrow) and pallium (thin arrow) entering wide flagellar pit.

Figure 88. Detail of osmiophilic ring with symmetrical electron lucent cores and indistinct m.b. structure (arrows).

Figure 89. Detail of m.b . showing microtubular row (black arrows); opposite face of m.b. not as distinct (white arrows); scale bar = 100nm.

Figure 90. Basal bodies and m.b. (arrow) between two pusules.

Figure 91. M.b. of Protoperidinium punctulatum showing microtubular rows (thin arrows), osmiophilic ring (thick arrow) slender osmiophilic bodies and striated stand (curved arrow).

Figure 92. Pallium of Oblea rotunda surrounding remains of Heterocapsa triquetra. Note anterior stalk of pallium with microtubules (arrow) and posterior vesicular zone next to prey.

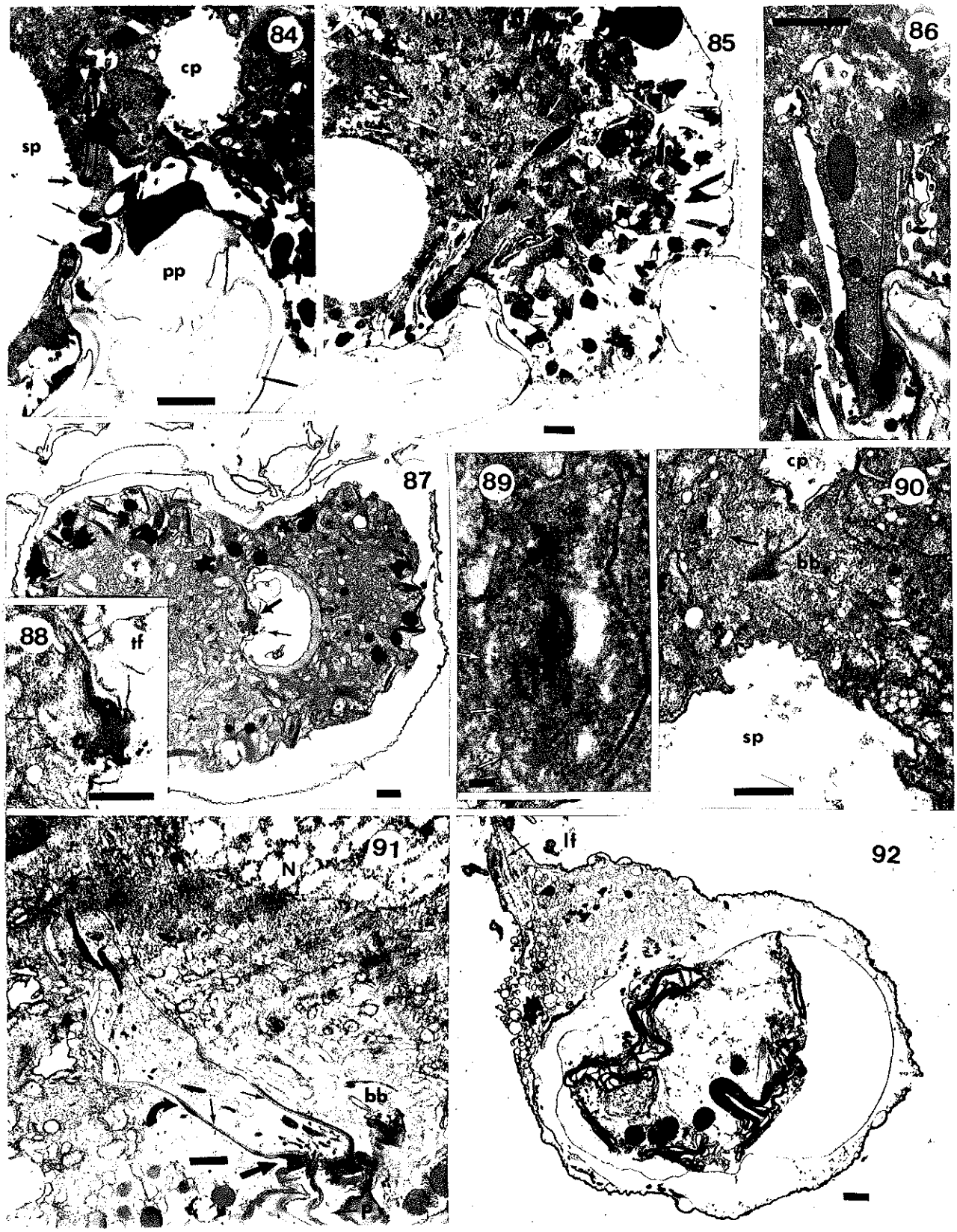
84
cp
sp
pp
85
86
87
88
tf
89
90
cp
bb
sp
91
N
bb
P
92
tf

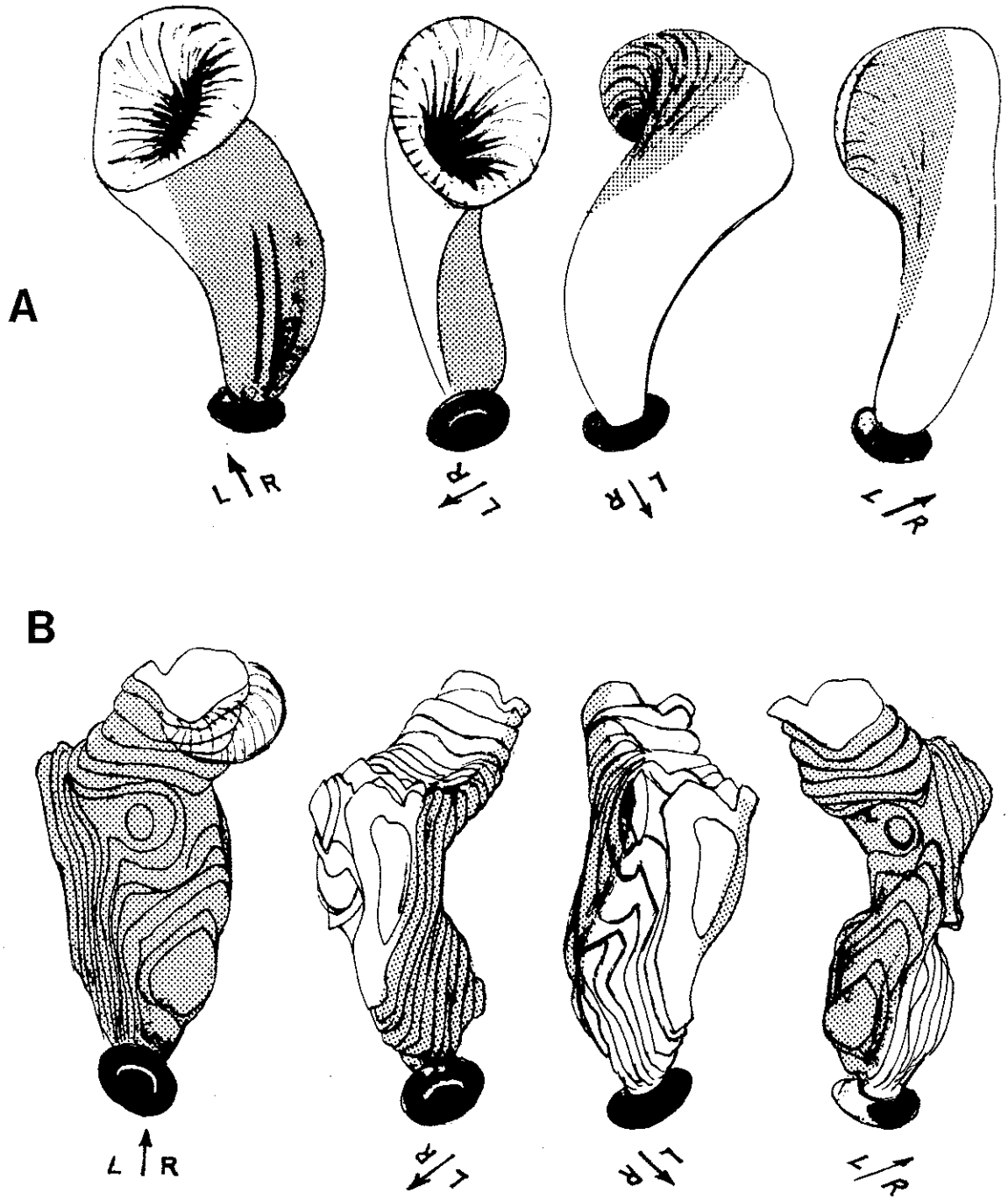

Figure 93. Three-dimensional models of the microtubular basket of Protoperidinium spinulosum. Shaded areas indicate presence of microtubules on inner surface of m.b. membrane. Orientation within cell is provided by arrows which point to ventral face of cell.

A. M.b. of cell B: the trumpet-like anterior region has been freely interpreted from limited sections like Fig. 17; the oblong posterior portion of the m.b. is documented more thoroughly.

B. M.b. of cell C: apical end has been omitted due to incomplete section record. However, an indication of the morphology of the "apical flap" is included in first view.

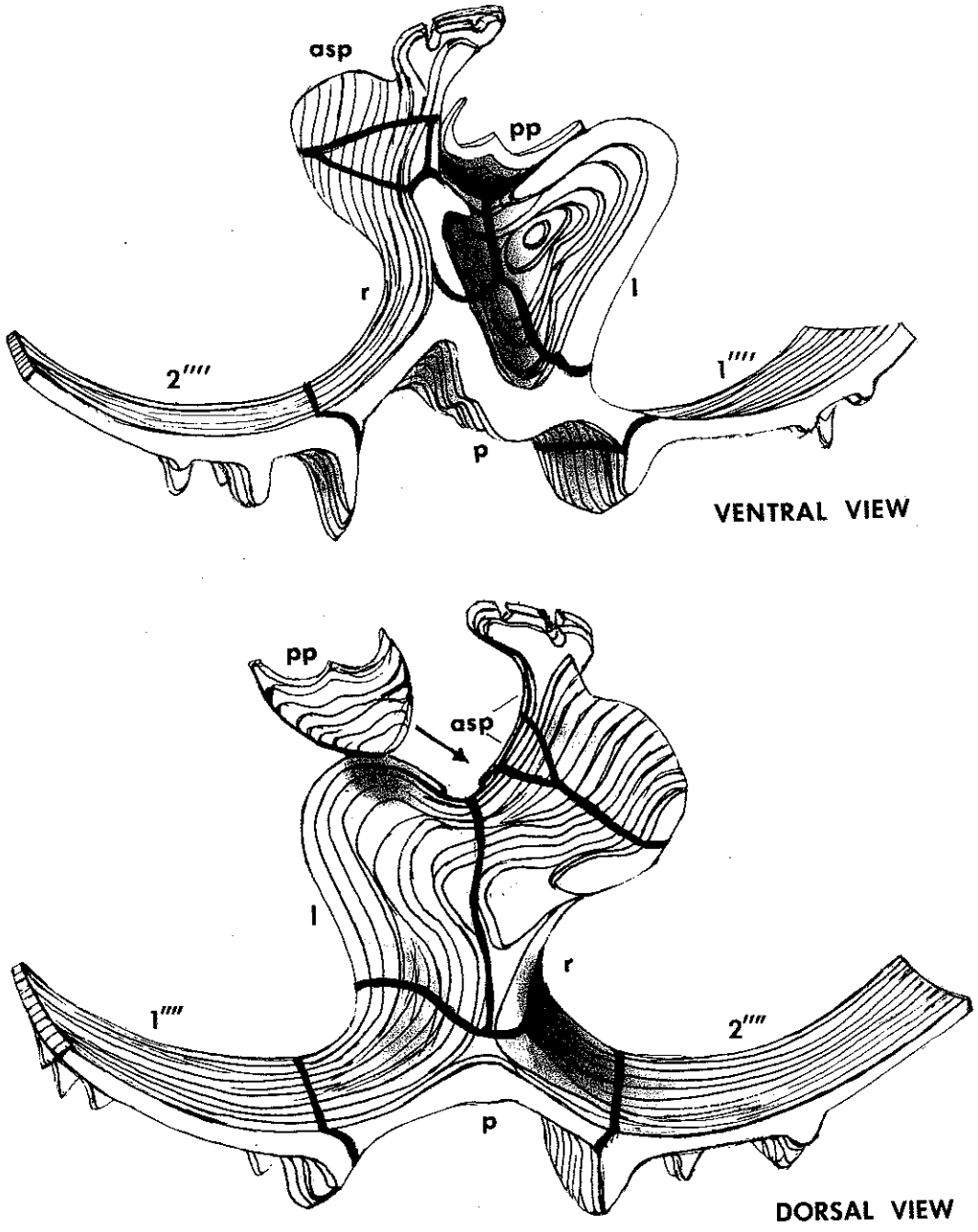

Figure 94. Three-dimensional model of posterior region of sulcus in cell C, including three accessory sulcal plates which form posterior protuberance capped by the distinctive orthogonal strut. Sutures between plates as shown by wide bands. Note posterior ventral concavity, which serves to orient this structure within Fig. 95.

Abbreviations:

r	right sulcal plate	pp	pore plate
l	left " "	asp	accessory sulcal plates
p	posterior " "	1,2''''	antapical plates

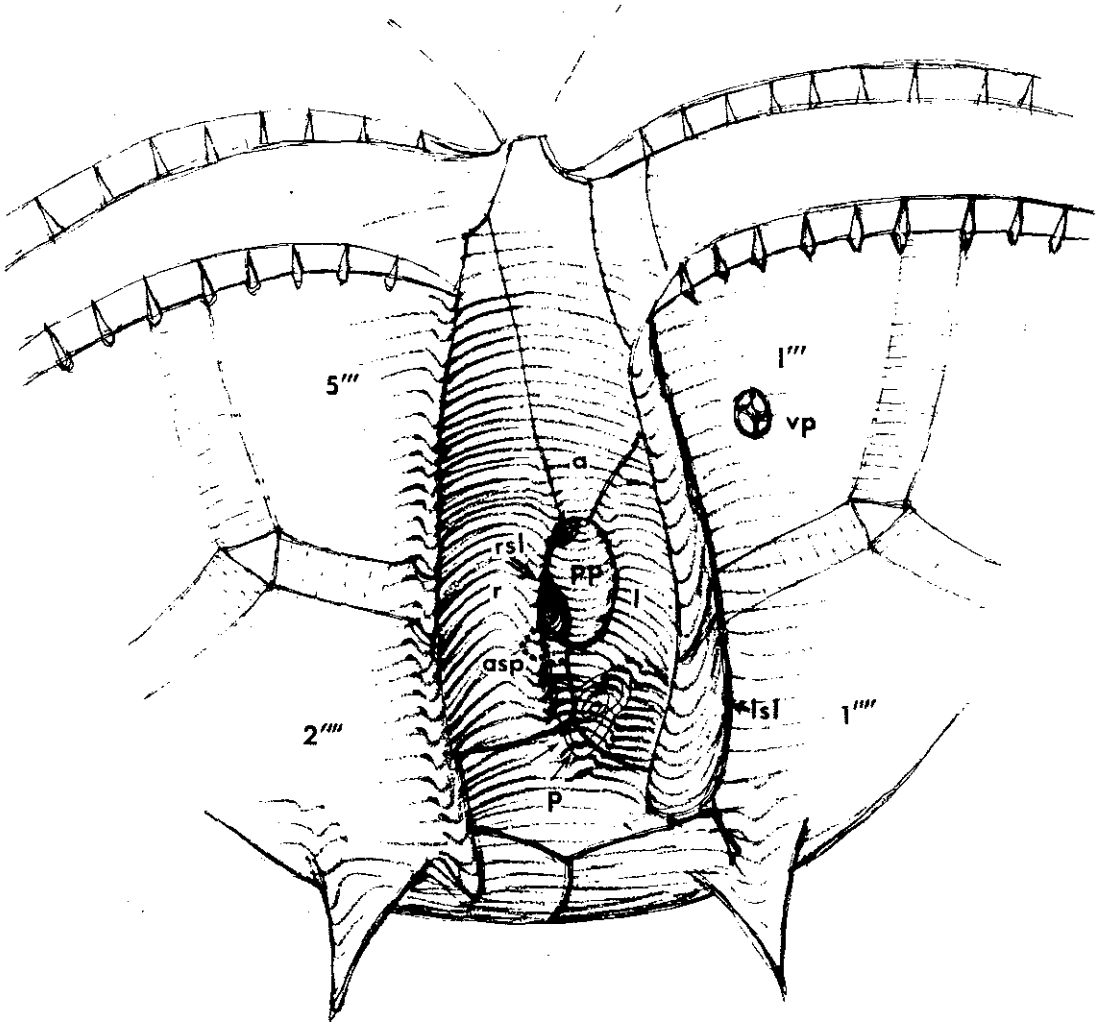

Figure 95. Contoured schematic drawing of sulcus of Protoperidinium spinulosum, with sulcus "opened" somewhat to reveal flagellar pores which are normally hidden behind right sulcal lists (i.e. Fig. 48). Several concentric contours representing the concavity featured in Fig. 94a serve to orient the protuberance (formed by the accessory sulcal plates), which is situated on the (cell's) inner right side of the posterior flagellar pore.

Abbreviations:

a	anterior sulcal plate	rsl	right sulcal list
r	right " "	lsl	left sulcalt list
l	left " "	asp	accessory sulcal plates
p	posterior " "	vp	ventral pore
pp	pore plate	1,5'''	1st and 5th post-cingular plates
		1,2''''	Antapical plates

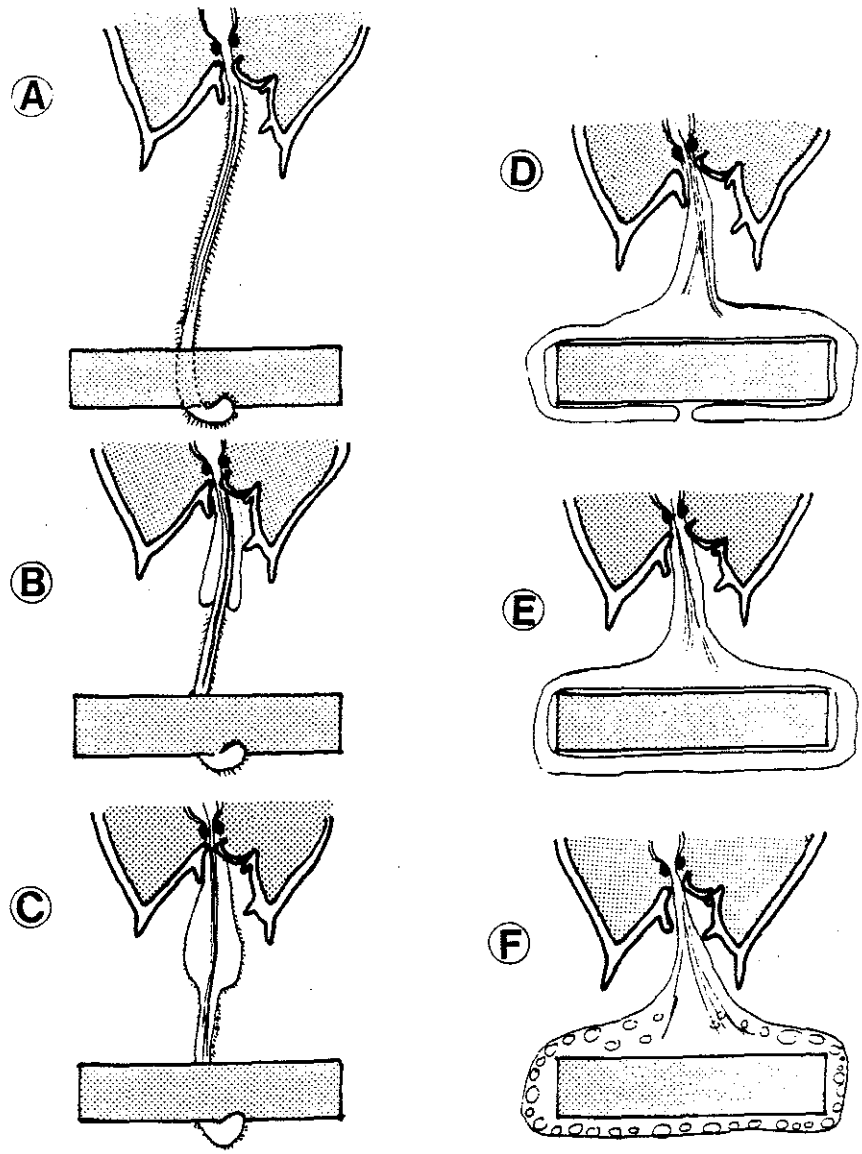

Figure 96. Schematic diagrams of deployment of tow filament and pallium in Protoperidinium spinulosum, including antapex of dinoflagellate and rectangular diatom.

A. Tow filament (= lobate pseudopod), with internal microtubules and "sticky" glycocalyx, attaches to diatom.

B,C. As tow filament shortens, pallium streams either around (B) or through (C) tow filament.

D. Pallium spreads across surface of diatom.

E. Membranes fusion results in complete envelope around diatom.

F. The situation usually encounter in sectioned feeding cells: inner membrane has evidently disintegrated, either in life or as an artifact of fixation.

CONCLUSIONS

This thesis has done much to characterize the previously unknown function of thecate heterotrophic dinoflagellates in the marine food web. In Chapter 1 the abundance patterns of these microheterotrophs in a coastal embayment are described; highlights include a bloom composed of several Protoperidinium species with cell densities exceeding $6 \cdot 10^4 \cdot l^{-1}$, and a clear covariation between these dinoflagellates and diatoms, their likely food source. Small-scale vertical distributions of several thecate heterotrophic dinoflagellates (Appendix III) is characterized by the lack of diel migratory behavior, although such behavior is evident in two co-occuring phototrophic dinoflagellates.

Feeding behavior of thecate heterotrophic dinoflagellates on diatoms (and, in some cases, dinoflagellates) is documented in Chapter 2. The elaborate pseudopod or pallium which envelops and digests large chains of diatoms was an unexpected discovery. Such large food items, which support the growth of large zooplankters such as copepods, was previously thought to be unavailable to protists.

Ingestion and growth rates have been measured in laboratory cultures using Protoperidinium hirobis feeding on the diatom Leptocylindrus danicus, revealing surprisingly high growth rates (1.7 divisions$\cdot d^{-1}$ and individual ingestion rates of 23 diatoms$\cdot d^{-1}$. These data suggest that a P. hirobis bloom population of $10^4 \cdot l^{-1}$ may be capable of grazing a significant portion (10%) of large ($2 \cdot 10^6 \cdot l^{-1}$) diatom blooms each day. More typically, populations ranging from 10^2

to $10^3 \cdot 1^{-1}$ would not be expected to have a substantial impact on diatom population dynamics. Cell division on a light/dark cycle is periodic, but division occurs during a wide interval of 16 hr., principally at night.

The structural basis for the pallium feeding system is described in Chapter 4. During deployment the pallium passes through an elaborate microtubular basket (and a large osmiophilic ring situated at the posterior end of the basket) before reaching the flagellar pore. In the course of a meal, catabolized food material, including small lipid droplets, are transported from the pallium back into the microtubular basket and thence, through a large trumpet-shaped apical opening near the nucleus, into the central cytoplasmic region of the cell. A source of the great quantities of membrane that makes up the pallium has been tenatively identified in the microtubular basket where, in a pre-feeding cell, dense membranous whorls were discovered. Such whorls are situated in a cytoplasmic mass in the sulcus as well.

Many additional questions have been raised as as a result of these investigations. The ecology of these microheterotrophs needs further study in order to understand, for example, what these dinoflagellates are preying upon in the diatom-poor central oceanic gyres, how food quality influences growth, and the nature of food selectivity (and associated chemosensory mechanisms) in thecate heterotrophic dinoflagellates.

Much study is needed to further elucidate how the ultrastructure of these dinoflagellates relates to cell function. This system may be a good one in which to study membrane dynamics, as most pallium membrane

storage, deployment, and recycling would likely be restricted to the microtubular basket region. The dynamics of lysosomes in the course of feeding should also be studied, using cytochemical assays for acid phosphatase or other enzymes. Finally, the unique cell structures described here may provide new insights into the evolutionary relationships between dinoflagellates and other protists such as euglenoids and trichomonads.

APPENDIX I

Cell counts of dinoflagellates of Perch Pond, Massachusetts, 1983-4

APPENDIX 1: Cell counts (ml^{-1}) of dinoflagellates in Perch Pond, 1983-4. + = $1-49 \cdot 1^{-1}$, ++ = $50-99 \cdot 1^{-1}$. Asterisks denote heterotrophs.

SPECIES	DATES (month/day) 2/18	2/24	3/2	3/10	3/16	3/23	3/30	4/6
Amphidiniopsis kofoidii*			+			+		
Amphidinium crassum*						+		
Dinophysis acuminata	+	+	+	+		+	++	++
D. norvegica		+	+	+			+	+
Glenodinium oblique								
Gonyaulax longicornu			+				+	
G. polyedra								
G. rugosa								
G. spinifera								
G. tamarensis				+	+	+	.1	.1
G. verior						+	+	
Gonyaulax sp. A								
Gonyaulax sp. B*				+	+	+	+	
Gymnodinium abbreviatum*								
G. estuariale								
G. sanginium								
G. lazulum*								
Gyrodinium dominans								
G. uncatenum								
G. spirale*		+			+		+	+
Heterocapsa triquetra	1.3	.4	.3	.2	1.8	6.9	6.7	25.0
Katodinium rotundatum	.2	2.1	17.0	2.4		.5		
Kryptoperidinium foleaceum								
Nematodinium armatum						+		
Oblea rotunda*	.1	+	.1	+	.2	.2	.2	.1
Peridinium asciculiferum								
Peridinium sp A.								
Phaeopolykrikos hartmanni								
Polykrikos schwartzii*								
Prorocentrum gracile								
P. micans	+	+	+	+		+	+	
P. minimum								
P. scutellum								
Protoperidinium** bipes	++	.1	++	+		.1	+	
P. cerasus								
P. claudicans								
P. conicoides					+	+	+	+
P. conicum								
P. cf. leonis (sp. A)								
P. minutum								
P. oblongum								
P. pellucidum		.1	.2	.4	1.1	.8	1.1	1.3
P. punctulatum	+	+	++	+			+	+
P. pyriforme			.1			++	+	
P. spinulosum								
Protoperidinium sp. B	+			+	+			.8
Protoperidinium sp. C		+	+	+			+	+
Scrippsiella cf.trochoidea						++	++	.2
Scrippsiella sp. A								
Zygabikodinium lenticulatum*		+	+	++	+	+	+	+
Ebria tripartata*	.8	.4	.3	.1	.1	.1	++	+

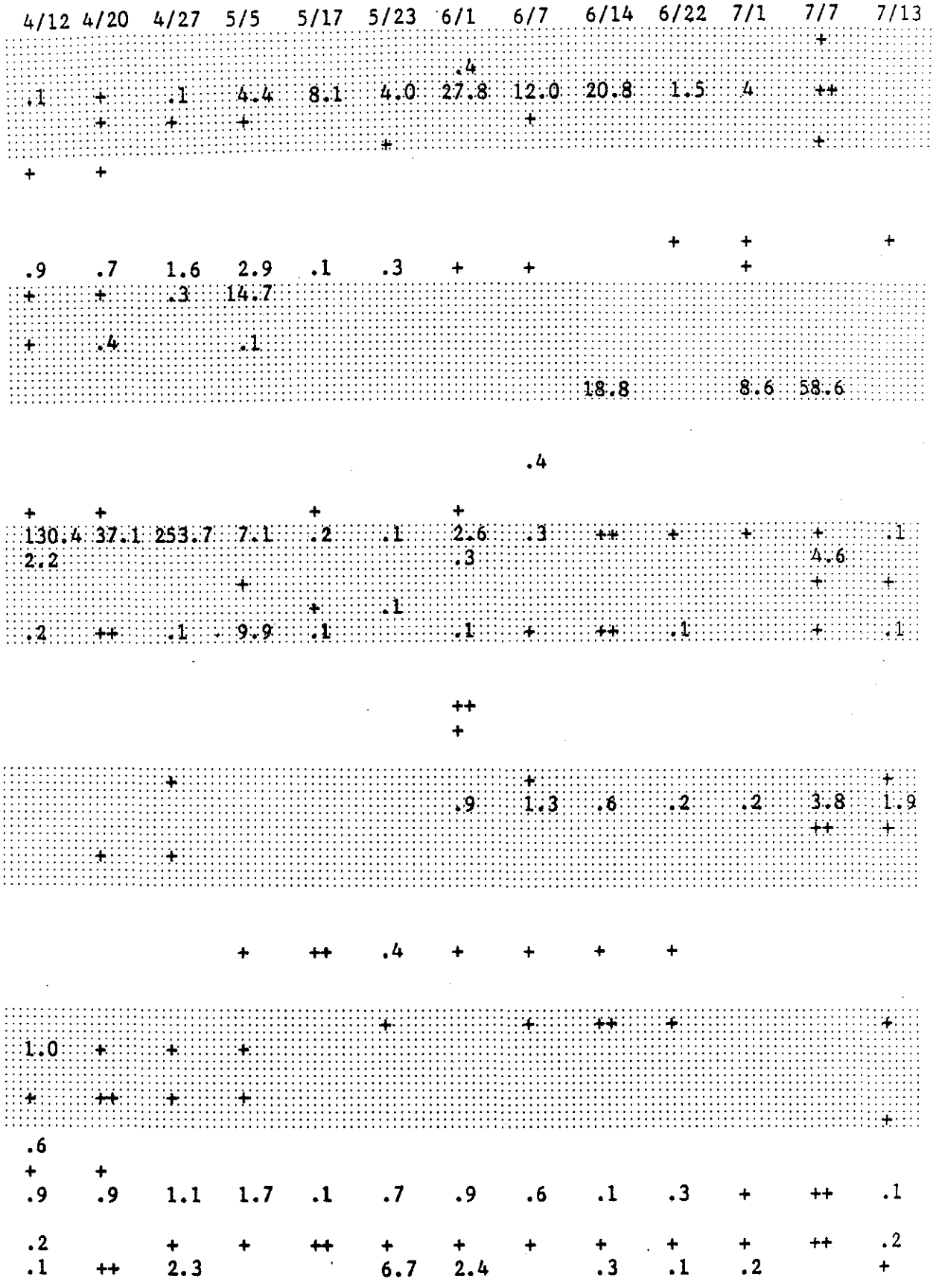
4/12 4/20 4/27 5/5 5/17 5/23 6/1 6/7 6/14 6/22 7/1 7/7 7/13

	7/25	8/3	8/16	8/25	9/1	9/7	9/15	9/23
Amphidiniopsis kofoidii*				.1				
Amphidinium crassum*								
Dinophysis acuminata		.1	.1	.3	.1	+	.7	2.7
D. norvegica								
Glenodinium oblique					.3		+	59.8
Gonyaulax longicornu				.8				
G. polyedra				3.1	16.6	15.5	14.3	.2
G. rugosa			+	.1	.3		38.3	
G. spinifera		2.1						
G. tamarensis				+	+	+	.1	.1
G. verior	.8			.4	.1	.1		.9
Gonyaulax sp. A	.2		.2	2.1	2.7	4.8		.6
Gonyaulax sp. B*							.1	.5
Gymnodinium abbreviatum*								+
G. estuariale		34.6						1.2
G. sanginium								.8
G. lazulum*								
Gyrodinium dominans*					.6			
G. uncatenum	1.1	12.6					.6	4.4
G. spirale*								
Heterocapsa triquetra				.7	.3			.1
Katodinium rotundatum	1.3	15..	17.0	2.4		.5		
Kryptoperidinium foleaceum			.2					
Nematodinium armatum		+					1.8	.2
Oblea rotunda*	.6	.2	1.0	+	1.1	.8	.6	1.0
Peridinium asciculiferum			++	6.9	.2	4.4		.2
Peridinium sp A.			++	14.0	9.3	21.0		3.1
Phaeopolykrikos hartmanni							++	
Polykrikos schwartzii*			.4		1.2	.2	.6	+
Prorocentrum gracile	4.2		.1	1.1	+			4.3
P. micans	+	+	+	+		.2		.1
P. minimum	1.5			.8		1.5		.6
P. scutellum	.4	.1						
Protoperidinium** bipes		+						
P. cerasus								
P. claudicans								
P. conicoides								
P. conicum								
P. cf. leonis (sp. A)		2.9	1.8	26.4	2.8	4.1	.7	.9
P. minutum			2.2	18.4	.2	.1	++	
P. oblongum	.2	.2	.1	10.1	.8	1.4	+	.3
P. pellucidum								
P. punctulatum								
P. pyriforme								
P. spinulosum	.8	2.7	2.1	5.7	.1	.6	.1	
Protoperidinium sp. B								
Protoperidinium sp. C								
Scrippsiella cf.trochoidea	3.2	29.0	10.6	12.2	14.9	2.9	37.9	105.8
Scrippsiella sp. A						.3	++	.6
Zygabikodinium lenticulatum*	.5	.1		.1			+	.1
Ebria tripartata*							.6	.8

9/29	10/5	10/11	10/19	10/29	11/5	11/15	11/22	11/30	12/8	12/16
					++					
13.8	37.4	4.9	3.9	4.8	3.1	15.3	5.8	4.6	1.6	2.2
6.6									+	
+										
.2										
971	7.9	155.5	.5	3.0						
.1										
						.3	+			
		.1								
2.7	.1	.1								
+	.2	+								
	+	+				+				
34.7		1.5								
2.6	15.5	1.0	2.1	++	+	+				
	7.1	4.5								
				+	1.4	.3	1.6	.2	+	+
.1	++	.2	.3	7.1	337.3	534.6	934.1	1011	7.8	2.1
				21.1						
	.2	.1							.2	
.3	.4	.6	.5	.9	.2		+	+		
.3	.7	.4	.3		.6	.3	1.5	.2	+	
	.8									
1.1	.1	.7								
	++									
++	.1	+			.1	.8	9.6	25.4	11.4	1.1
.1		.6	.7							
		.1	++		.2					
		.1	.1		++	+				
2.1	++	1.1						+	+	+
+										
						+	+	+		+
.6	++	.2	.2	+			+			
.1		.1				+				
.4	.8	.7	.6	+	*					
.2	++	+								
									.2	.1
325	.2	1.2	2.5	8.6		19.9	10.3	7.3	1.1	.2
.9										
		.1	++	.4	.1	+	+		+	
		.3	1.2	1.3	.1	++	.2	.6		.6

	12/21	1/16	2/2	2/14	2/21	2/29	3/8	3/19
Amphidiniopsis kofoidii*							+	
Amphidinium crassum*								
Dinophysis acuminata			++	+	++	.1	2.9	.1
D. norvegica				+				
Glenodinium oblique								
Gonyaulax longicornu					+		+	
G. polyedra								
G. rugosa								
G. spinifera								
G. tamarensis				+	+	+	+	+
G. verior								
Gonyaulax sp. A								
Gonyaulax sp. B*							+	
Gymnodinium abbreviatum*								+
G. estuariale		1.7	198.0	11.8	31.7	25.9	43.2	22.1
G. sanginium								
G. lazulum*								
Gyrodinium dominans*								1.1
G. uncatenum								
G. spirale								
Heterocapsa triquetra	128.2	145.6	407.4	74.9	233.5	238.3	578.5	1015
Katodinium rotundatum	1.5	50.0	139.4	106.7	146.1	25.0	35.6	18.3
Kryptoperidinium foleaceum								
Nematodinium armatum								
Oblea rotunda*	.1	.2	.4	.1	.2	.9	2.6	1.9
Peridinium asciculiferum								
Peridinium sp A.								
Phaeopolykrikos hartmanni								
Polykrikos schwartzii*								
Prorocentrum gracile								
P. micans								
P. minimum		*	.2					++
P. scutellum								
Protoperidinium** bipes				*		+	.1	
P. cerasus						+	.1	+
P. claudicans				+	+	+	+	+
P. conicoides		+		+	+	+	.1	+
P. conicum								
P. cf. leonis (sp. A)								
P. minutum								
P. oblongum								
P. pellucidum								+
P. punctulatum								
P. pyriforme								
P. spinulosum								
Protoperidinium sp. B	.2	+	++		+	+	.2	1.3
Protoperidinium sp. C					+	+	.1	+
Scrippsiella cf.trochoidea				+		+		+
Scrippsiella sp. A								
Zygabikodinium lenticulatum*	+	++	+	+	.1	+	+	+
Ebria tripartata*			83.6	7.7	2.1	1.7	2.5	1.5

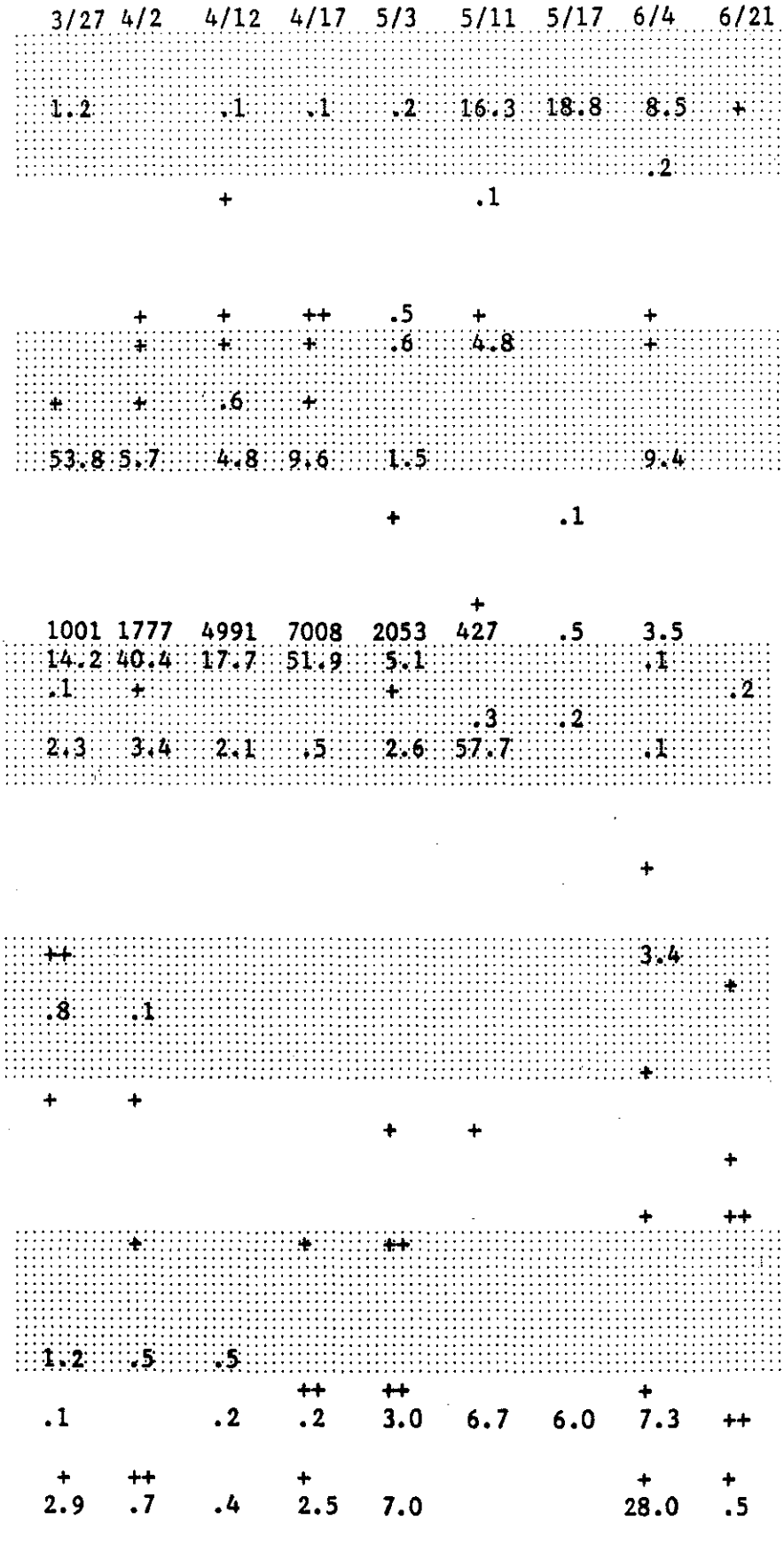
3/27 4/2 4/12 4/17 5/3 5/11 5/17 6/4 6/21
1.2 .1 .1 .2 16.3 18.8 8.5 +
.2
+ .1
+ + ++ .5 + +
+ + + .6 4.8 +
+ + .6 +
53.8 5.7 4.8 9.6 1.5 9.4
+ .1
+
1001 1777 4991 7008 2053 427 .5 3.5
14.2 40.4 17.7 51.9 5.1 .1
.1 + + .2
.3 .2
2.3 3.4 2.1 .5 2.6 57.7 .1
+
++ 3.4
.8 .1 +
+ +
+ +
+
+ ++
+ ++
1.2 .5 .5
++ ++ +
.1 .2 .2 3.0 6.7 6.0 7.3 ++
+ ++ + + +
2.9 .7 .4 2.5 7.0 28.0 .5

APPENDIX II

Taxonomic drawings of three unidentified dinoflagellates encountered during the study of Perch Pond, Massachusetts

(see Chapter 1)

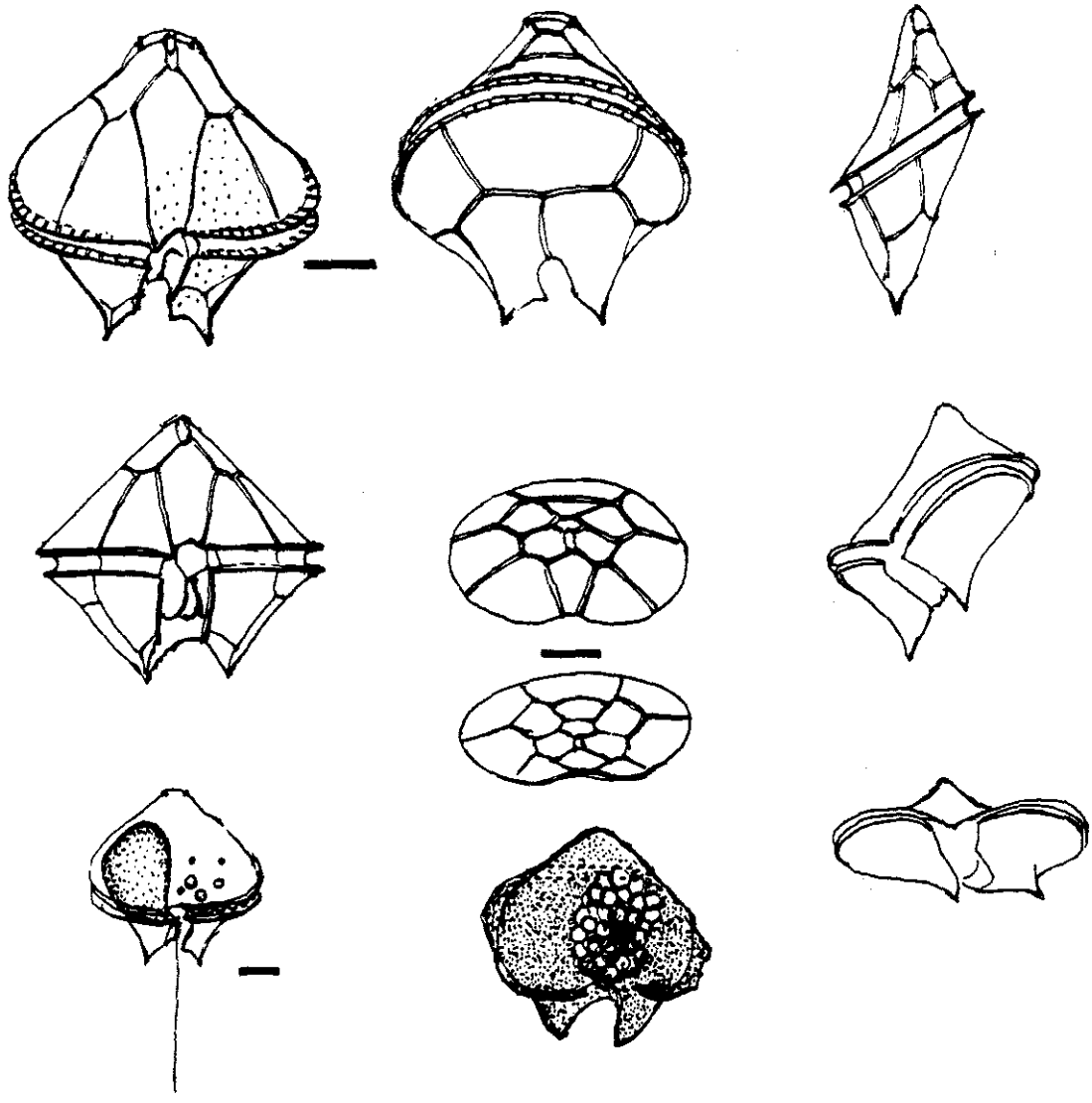

Figure 1. Protoperidinium sp. A. This species is similar in tabulation and morphology to P. leonis, but differs in being dorso-ventrally flattened. Included are views from various angles; the morphology of the sac pusule is featured at lower left, and, at lower center, the cyst stage is shown. All scale bars = 10μm.

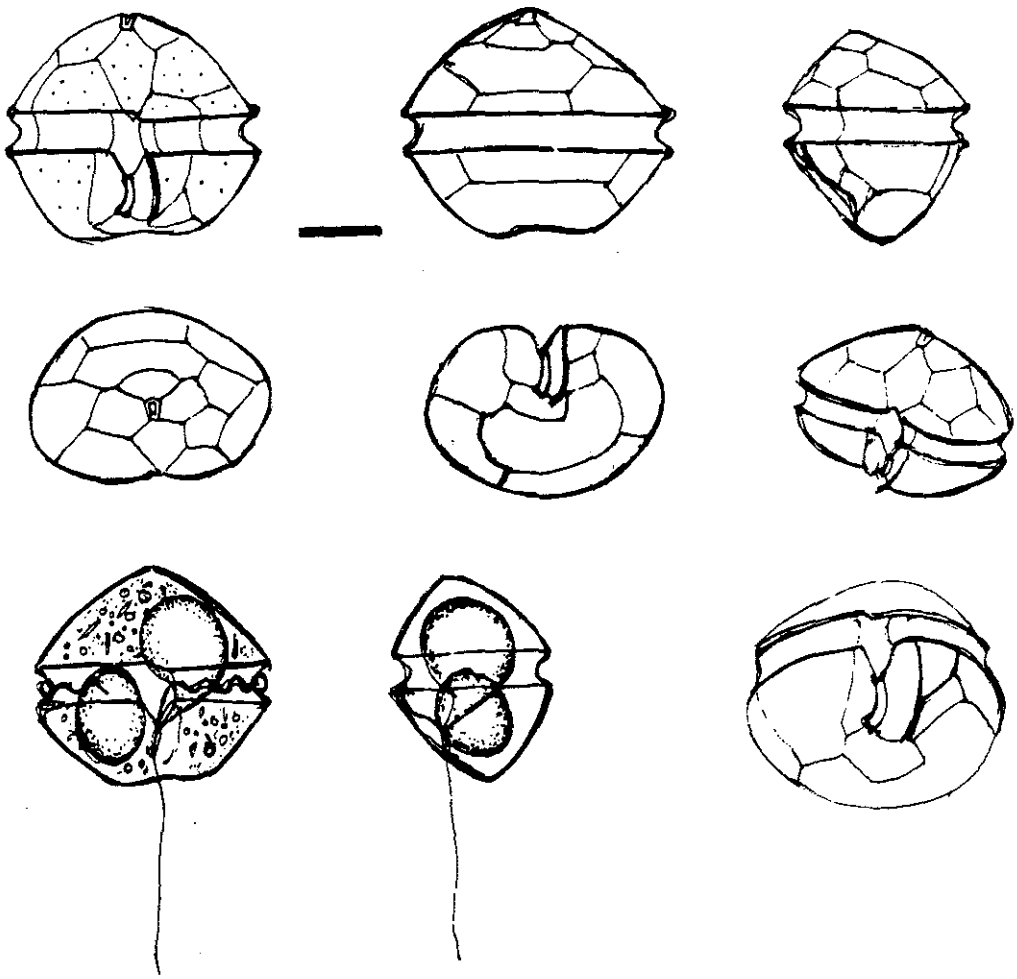

Figure 2. Protoperidinium sp. C. A small cold water species witha unique epithecal tabulation (note quadralateral 1st precingular plate) and additional hypothecal plate bordering the left side of the sulcus. Note two large, similarly shaped pusules at lower left. Scale bar = 10μm.

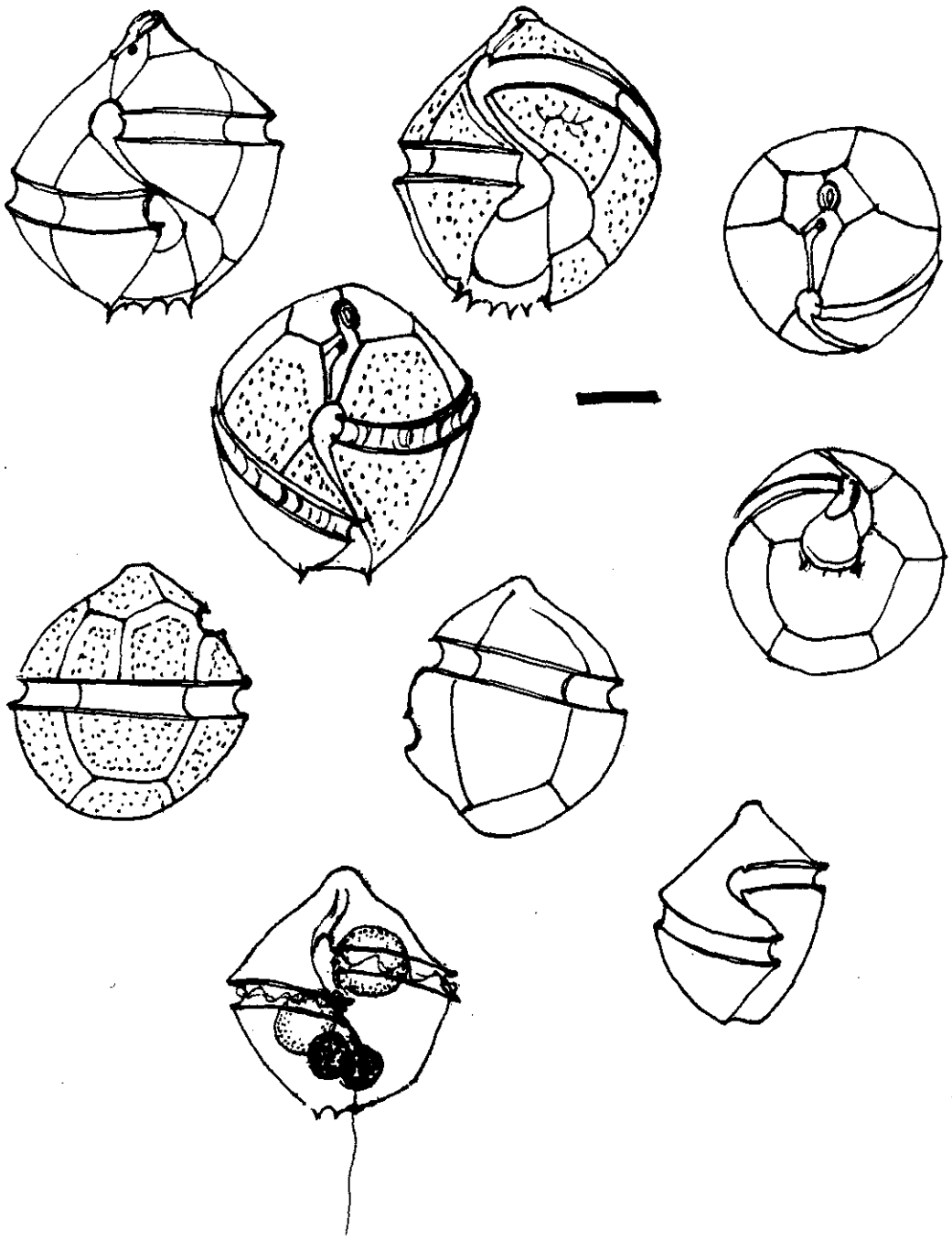

Figure 3. Gonyaulax sp. B. A colorless species resembling G. kofoidii with weakly reticulate thecal ornamentation. Lower drawing depicts two pigmented inclusions (ranging in hue from green to orange) and two large pusules. Lower right drawing shows a small, dorso-ventrally compressed specimen, perhaps a young cell. Scale bar = 10μm.

APPENDIX III

Small Scale Vertical Distribution Patterns of Heterotrophic Dinoflagellates Over a Diel Cycle

Abstract

Diel small-scale vertical distribution patterns of eight dinoflagellate species (two phototrophic, six heterotrophic) were monitored in an estuarine embayment. Both phototrophic species (Gonyaulax tamarensis and Heterocapsa triquetra) displayed strong vertical migratory patterns, but no diel migration pattern was detectable in Protoperidinium conicum, P. claudicans, P. pellucidum, Zygabikodinium lenticulatum (all thecate species) and Gyrodinium spirale (a naked species). Oblea rotunda showed weak shifts in depth distributions. Depth distributions are shown for several species of diatoms, on which most or all of the heterotrophs are known to feed, but no correlations between dinoflagellates and diatoms were detected. This is the first study to demonstrate diel vertical distribution patterns (characterized by lack of vertical migration) in heterotrophic dinoflagellates.

INTRODUCTION

Daily vertical migration in photosynthetic dinoflagellates is a well-studied phenomenon (Hasle 1950, Eppley et al. 1968, Kamykowski and Zentara 1977). A common scenario is that of dinoflagellates moving from their night time location in nutrient-rich subsurface waters into the bright surface layer during the day, and then sinking into the subsurface layer at the day's end (Heaney and Eppley, 1981). The migratory habits of nonphotosynthetic dinoflagellates, however, have not yet been examined. The present study, run in conjunction with the latter part of that of Anderson and Stolzenbach (1985) describes for the first time the small-scale vertical distribution patterns of thecate and naked dinoflagellates over a diel cycle.

METHODS

Study Site. Salt Pond (Eastham, Massachusetts) is an circular estuarine embayment 82,200 m^2 in area connected by a long, narrow tidal channel to a salt marsh system adjacent to the ocean at Nauset. Mean and maximum depths are 3.4 and 7 m, respectively, at slack low tide; the depth of the sampling site near the center of the pond ranged from 4.5 to 5.5 m.

Vertical Cell Distributions. Samples were collected at 0.5 m depth intervals with a system composed of separate, weighted, lengths of Tygon tubing that were suspended from a floating rubber tire tube. At 3 hr intervals the tygon tubes were connected in succession to a DC pump

(Fluid Metering, Inc., Model RP); after a period of flushing, 500 ml samples were collected into bottles except for the last time point where 50 ml were collected; therefore the least abundant species were not counted for the final 1200 hr sample. These samples were then transported to the shore and transferred to bottles holding glutaraldehyde, resulting in a final fixative concentration of 2%. At a later date the fixed samples were sieved on a 15 μ Nitex screen immediately prior to counting in order to reduce the total volume from 500 to 50 ml, and subsequently left overnight in a 50 ml settling chamber. Samples were counted on a Zeiss Inverted microscope at 160x by scanning one half slide in its entirety. Typical counts for common species ranged between 100-200 cells. The 4.5 m sample at the final collection (1200 hr) was lost.

RESULTS AND DISCUSSION

The vertical profiles of the two phototrophic species, Gonyaulax tamarensis and Heterocapsa triquetra both show a strong vertical migratory pattern (Fig. 1). Both populations reached their deepest distribution shortly after midnight and rose into the surface waters during the morning: G. tamarensis avoided the upper meter of water, while H. triquetra ranged into this upper layer only on the second morning when clouds reduced surface irradiance.

The heterotrophic species (5 thecate, 1 naked) displayed no strong vertical migrations. Populations of Protoperidinium conicum, P. claudicans, Zygabikodinium lenticulatum and Gyrodinium spirale were characterized by deep distributions, their peak cell densities ranging

from 2 to 5 meters in depth (Fig. 3,4). The depth distribution (kite) diagrams are plotted with the surface held constant. Consequently, the tidal cycling (Fig. 5) gives an artifactual impression of periodic migration. P. conicum is replotted with the pond floor held constant to illustrate this point (Fig. 1); note how the temporal distribution patterns of this heterotroph contrasts with the two phototrophs. Of these heterotrophic species, all but P. claudicans and P. pellucidum were abundant, with maximal abundances > 100 cells/liter.

The two remaining heterotrophs, both thecate, show peculiar distributional patterns. P. pellucidum was not an abundant species but clearly displayed a near-surface distribution throughout the study. Maximal numbers usually occurred in the upper half-meter layer of the water column. Oblea rotunda, a more abundant species, had a variable depth distribution, ranging from uniform (i.e. 0830 and 1200 hr) to near surface-weighted (2300 hr - 1200' hr) to bottom-weighted (1600 hr). A subtle, coherent pattern seems to exist from 1600 hr to 1100 hr, with an upward shift in depth distribution followed by a downwind shift; this pattern is the reverse of that of the phototrophic dinoflagellates.

In summary, the heterotrophic dinoflagellates of Salt Pond, which co-occurred with dinoflagellates exhibiting strong diel vertical migrations, did not display any strong migratory patterns with the possible exception of Oblea rotunda. With the exception of the surface-dwelling Protoperidinium pellucidum, all abundant heterotrophs maintained a relatively deep distribution pattern.

REFERENCES

Anderson, D.M., and K.D. Stolzenbach 1985. Selective retention of two dinoflagellates in a well-mixed esturaine embayment: the importance of diel vertical migration and surface avoidance. Mar. Ecol. Prog. Ser. 25: 39-50.

Eppley, R.W., Holm-Hansen, O., Strickland, J.D.H. (1968). Some observations on the vertical migration of dinoflagellates. J. Phycol. 4: 333-340.

Hasle, G.R. 1950. Phototactic vertical migration in marine dinoflagellates. Oikos 2:162-175.

Heaney, S.I. and R.W. Eppley 1981. Light, temperature and nitrogen as interacting factors affecting diel vertical migrations of dinoflagellates in cultrue. J. Plankton Res. 3:331-344.

Figures 1-3. Diel vertical distributions of 8 dinoflagellate species. Heterotrophs are denoted by asterisks. Protoperidinium conicum is plotted twice, once with the surface held constant as are the balance of the figures and once with the pond floor held constant (Fig. 1); this last plot removes the tidal oscillation from the data.

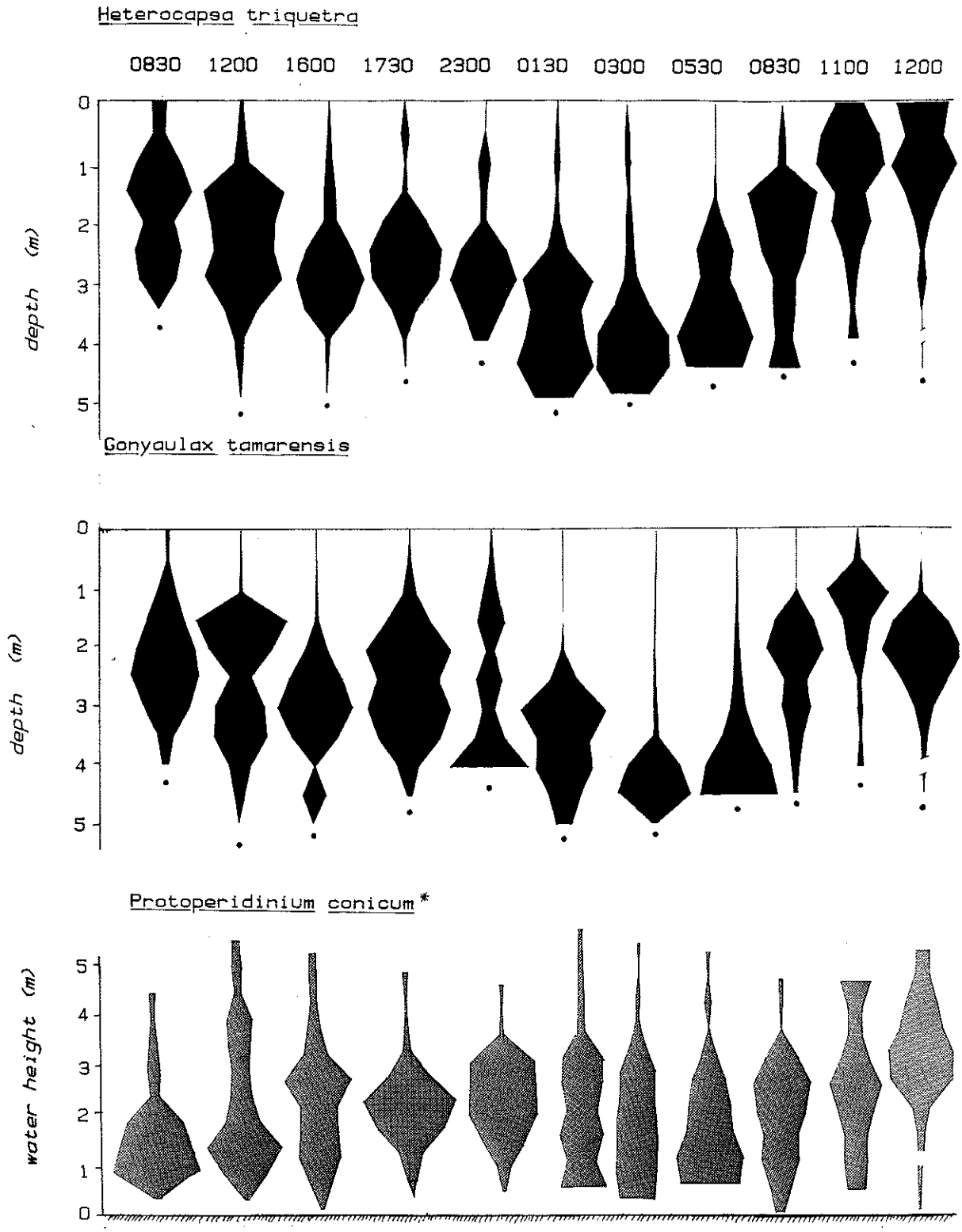
Heterocapsa triquetra
0830 1200 1600 1730 2300 0130 0300 0530 0830 1100 1200
depth (m)
0
1
2
3
4
5
Gonyaulax tamarensis
depth (m)
Protoperidinium conicum*
water height (m)

Figure 1.

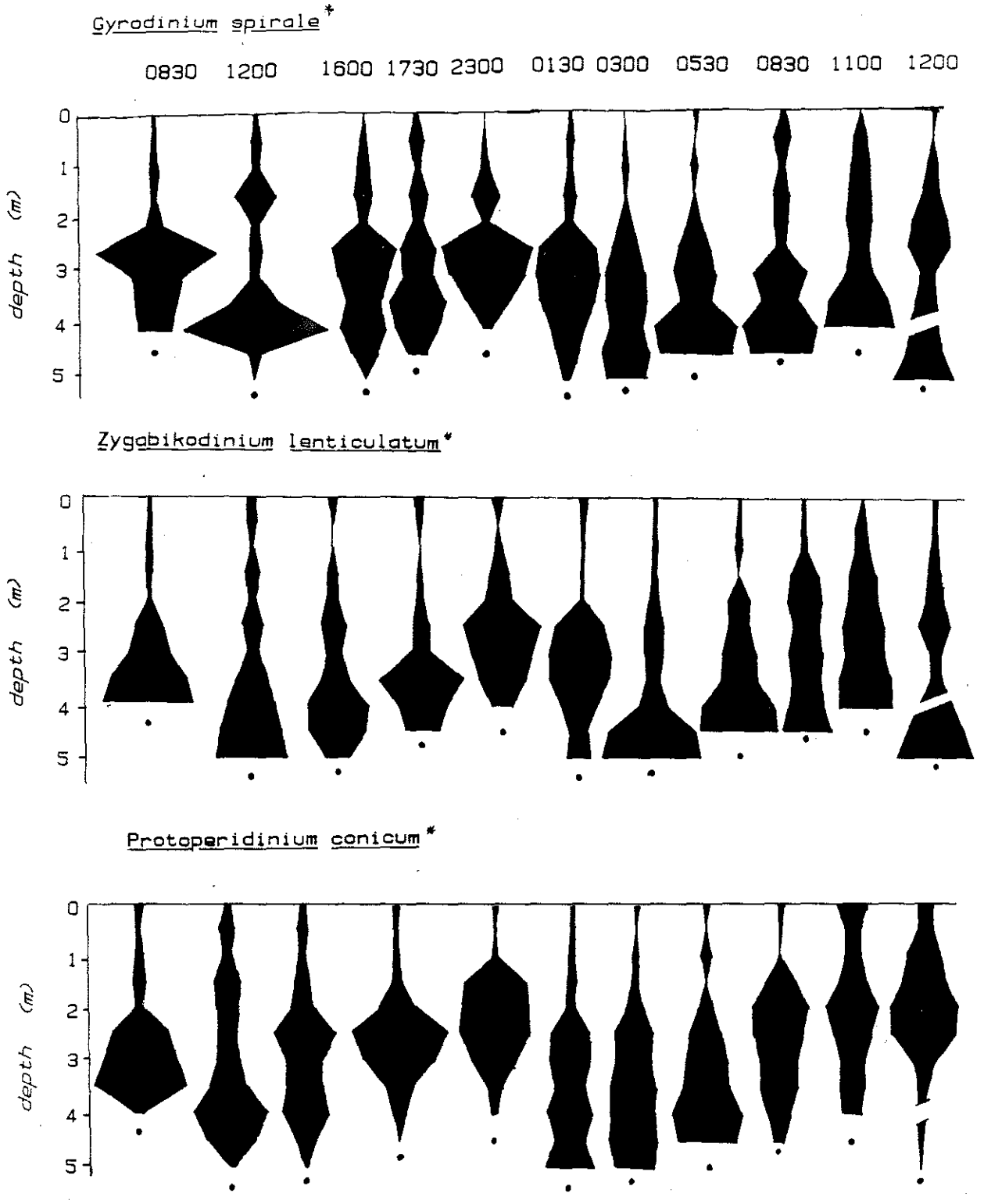
Gyrodinium spirale*
0830 1200 1600 1730 2300 0130 0300 0530 0830 1100 1200
depth (m)
0
1
2
3
4
5
Zygabikodinium lenticulatum*
depth (m)
0
1
2
3
4
5
Protoperidinium conicum*
depth (m)
0
1
2
3
4
5

Figure 2.

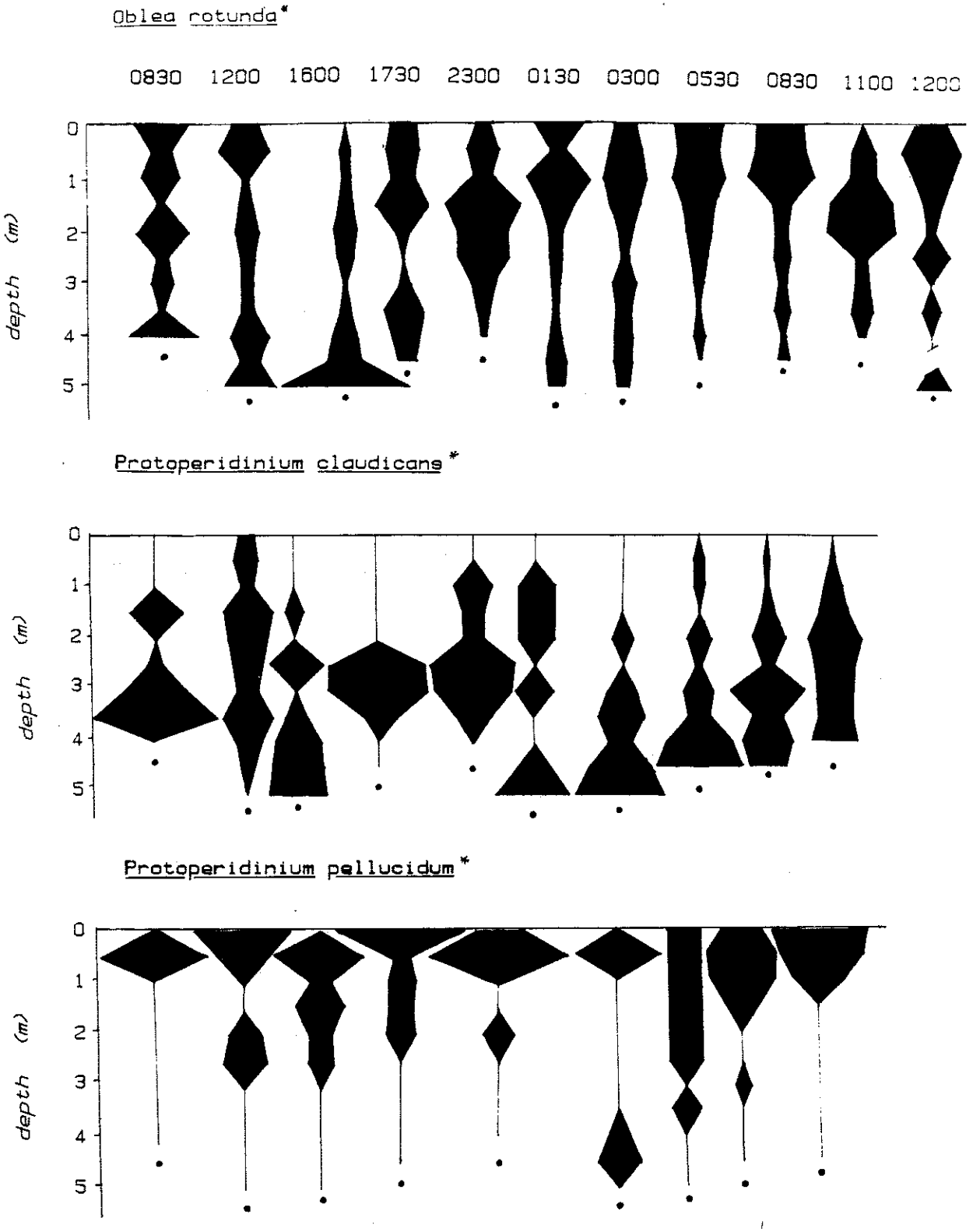
Oblea rotunda*
0830 1200 1600 1730 2300 0130 0300 0530 0830 1100 1200
depth (m)
0
1
2
3
4
5
Protoperidinium claudicans*
depth (m)
0
1
2
3
4
5
Protoperidinium pellucidum*
depth (m)
0
1
2
3
4
5

Figure 3.